

## INFORMATION TO USERS

This manuscript has been reproduced from the microfilm master. UMI films the text directly from the original or copy submitted. Thus, some thesis and dissertation copies are in typewriter face, while others may be from any type of computer printer.

**The quality of this reproduction is dependent upon the quality of the copy submitted.** Broken or indistinct print, colored or poor quality illustrations and photographs, print bleedthrough, substandard margins, and improper alignment can adversely affect reproduction.

In the unlikely event that the author did not send UMI a complete manuscript and there are missing pages, these will be noted. Also, if unauthorized copyright material had to be removed, a note will indicate the deletion.

Oversize materials (e.g., maps, drawings, charts) are reproduced by sectioning the original, beginning at the upper left-hand corner and continuing from left to right in equal sections with small overlaps. Each original is also photographed in one exposure and is included in reduced form at the back of the book.

Photographs included in the original manuscript have been reproduced xerographically in this copy. Higher quality 6" x 9" black and white photographic prints are available for any photographs or illustrations appearing in this copy for an additional charge. Contact UMI directly to order.

**UMI<sup>®</sup>**

Bell & Howell Information and Learning  
300 North Zeeb Road, Ann Arbor, MI 48106-1346 USA  
800-521-0600



UNIVERSITY OF ALBERTA

CATALYTIC OXIDATION OF METHANE OVER SUPPORTED PALLADIUM  
CATALYSTS

BY

Wei Ye 

A THESIS

SUBMITTED TO THE FACULTY OF GRADUATE STUDIES AND  
RESEARCH IN PARTIAL FULFILLMENT OF THE REQUIREMENT FOR  
THE DEGREE OF MASTER OF SCIENCE

IN

CHEMICAL ENGINEERING

DEPARTMENT OF CHEMICAL AND MATERIALS ENGINEERING

EDMONTON, ALBERTA

SPRING 1999



National Library  
of Canada

Acquisitions and  
Bibliographic Services

395 Wellington Street  
Ottawa ON K1A 0N4  
Canada

Bibliothèque nationale  
du Canada

Acquisitions et  
services bibliographiques

395, rue Wellington  
Ottawa ON K1A 0N4  
Canada

*Your file* *Votre référence*

*Our file* *Notre référence*

The author has granted a non-exclusive licence allowing the National Library of Canada to reproduce, loan, distribute or sell copies of this thesis in microform, paper or electronic formats.

The author retains ownership of the copyright in this thesis. Neither the thesis nor substantial extracts from it may be printed or otherwise reproduced without the author's permission.

L'auteur a accordé une licence non exclusive permettant à la Bibliothèque nationale du Canada de reproduire, prêter, distribuer ou vendre des copies de cette thèse sous la forme de microfiche/film, de reproduction sur papier ou sur format électronique.

L'auteur conserve la propriété du droit d'auteur qui protège cette thèse. Ni la thèse ni des extraits substantiels de celle-ci ne doivent être imprimés ou autrement reproduits sans son autorisation.

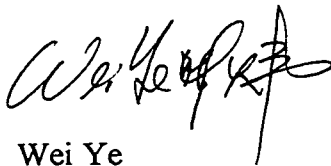
0-612-40128-6

UNIVERSITY OF ALBERTA  
RELEASE FORM

NAME OF THE AUTHOR	Wei Ye
TITLE OF THESIS	Catalytic Oxidation of Methane Over Supported Palladium Catalysts
DEGREE	Master of Science
YEAR THIS DEGREE GRANTED	1999

Permission is hereby granted to the University of Alberta to reproduce single copies of this thesis and to lend or sell such copies for private, scholarly or scientific research purpose only.

The author reserves all other publication right in association with the copyright in the thesis, and except as herein before provided neither the thesis nor any substantial portion thereof may be printed or otherwise reproduced in any material form whatever without the author's prior written permission.



Wei Ye

Box 106

11012 - 82 Ave

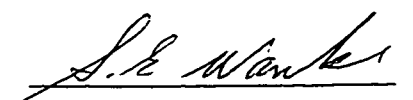
Edmonton, Alberta, Canada

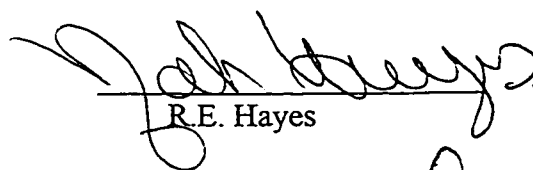
T6G 2P6

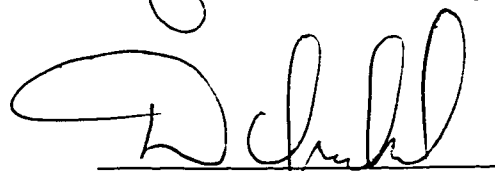
Date: January 26, 1999

## FACULTY OF GRADUATE STUDIES AND RESEARCH

The undersigned certify that they have read, and recommend to the Faculty of Graduate Studies and Research for acceptance, a thesis entitled **Catalytic Oxidation of Methane Over Supported Palladium Catalysts** submitted by **Wei Ye** in partial fulfillment of the degree of **Master of Science in Chemical Engineering**.

  
S.E. Wanke (supervisor)

  
R.E. Hayes

  
M.D. Checkel

Date: January 26, 1999

**To my dearest parents**

**Your love, understanding, and encouragement have always  
been the driving force behind my accomplishments**

## ABSTRACT

Methane is a component in the exhaust of most combustion processes, and the increased use of methane as a fuel will increase the methane emissions unless more effective exhaust clean-up catalysts are developed. Methane is the most difficult of all hydrocarbons to oxidize and catalyst with increased activity at low temperature are required to effectively decrease methane emissions from exhaust, especially during start-up of engines. In the current study the methane oxidation activity of various supported metal catalysts has been measured.

It is generally accepted that supported palladium is the most active catalyst for complete methane oxidation. Various supported Pd catalysts and supported Pd-Fe and Pd-Cu catalysts were examined in preliminary studies. Integral fixed-bed reactors, using feeds containing methane, oxygen and helium, were used to study the rates of methane oxidation over temperature ranges from 200 to 600°C. It was observed that Pd supported on silica prepared from palladium chloride precursor was the most active catalyst for methane combustion. Most of the studies were done with 5% Pd/Al<sub>2</sub>O<sub>3</sub> catalysts, because these catalysts showed the largest changes in activities with use.

It was observed, as had been by other investigators, that the activity of Pd/Al<sub>2</sub>O<sub>3</sub> is a strong function of the treatment history; exposure of the catalyst to high temperatures (325 to 525°C) in the presence of methane and oxygen resulted in large increases in catalytic activity at lower temperatures. Such increases in activity occurred in spite of decreases in Pd surface areas.



Studies were conducted to determine the effects of various pretreatment on activities. Catalysts were also characterized by x-ray diffraction, hydrogen chemisorption and low-temperature nitrogen adsorption (BET) after various treatments in an attempt to discover catalyst structure – activity relationships. It was found that Pd and PdO crystal sizes are not correlated with catalytic activities. The catalytic activities were found to be very dependent on the support (silica supported catalyst had the highest activities) and on the Pd precursor. Catalysts made with PdCl<sub>2</sub> had higher activities than those made with Pd(C<sub>5</sub>H<sub>7</sub>O<sub>2</sub>)<sub>2</sub>. The oxidation-reduction behavior of Pd appears to be correlated with catalytic activities. The Pd/SiO<sub>2</sub> catalyst made with PdCl<sub>2</sub> was difficult to reduce after use, while the Pd/SiO<sub>2</sub> catalyst made with Pd(C<sub>5</sub>H<sub>7</sub>O<sub>2</sub>)<sub>2</sub> was difficult to oxidize. It is recommend that the reduction and oxidation behavior of supported Pd catalyst be investigated in detail.

## ACKNOWLEDGMENTS

I am grateful to my supervisor Dr. Sieghard Wanke for his support and valuable guidance during the course of my research. Thanks are due to his tremendous efforts in guiding me to write this thesis. I would also like to thank Dr. Ah-Dong Leu for measuring the x-ray profiles and the BET surface areas. Many thanks are due to Ms. Andree Koenig, who provided assistance with the gas chromatographic analyses, and Mr. Walter Boddez and Mr. Richard Cooper for keeping all the electronic equipment functioning.

I express gratitude to my dearest Karen whose understanding and care made my life more enjoyable. Thanks are due to my colleague Ms. Bu who made my life at office and in the laboratory more enjoyable.

Above all, I express my sincere gratitude to my parents whose love and support have been the driving force behind all my accomplishments.

## **TABLE OF CONTENTS**

<b>Chapter 1 INTRODUCTION</b>	<b>1</b>
<b>Chapter 2 LITERATURE REVIEW: Catalytic Oxidation of Methane</b>	<b>4</b>
2.1 Noble Metal Catalysts for Methane Oxidation	6
2.1.1 Effects of type of noble metal	11
2.1.2 Effects of support on catalyst activities	11
2.1.3 Effects of time-on-stream	14
2.1.4 Effects of reaction temperature	18
2.1.5 Effects of the type of noble metal precursors	19
2.1.6 State of Pd on support during methane oxidation	21
2.1.7 Mechanism and kinetics of methane oxidation	28
2.2 Metal Oxide Catalysts For Methane Oxidation	33
2.3 Typical Operating Conditions	38
<b>Chapter 3 EQUIPMENT AND PROCEDURES</b>	<b>39</b>
3.1 Description of Catalysts	39
3.2 Characterization Methods and Instruments	43
3.3 Experimental Equipment	45
3.4 Catalytic Activity Measurements —Operating Conditions	51
3.5 Experimental Procedures	52

Chapter 4 EXPERIMENTAL RESULTS AND DISCUSSION	55
4.1 Effects of Pretreatment on Activities of Pd/Al <sub>2</sub> O <sub>3</sub>	55
4.2 Effects of Supports and Pd Precursors	67
4.3 Effects of Second Metal Addition	76
4.4 Effect of Feed Composition and Reaction Pressure	87
4.5 Catalyst Characterization Results (BET, H <sub>2</sub> Chemisorption, XRD)	93
Chapter 5 CONCLUSIONS AND RECOMMENDATIONS	101
REFERENCES	104
APPENDIX A: EXPERIMENTAL DATA	108
APPENDIX B: SAMPLE CALCULATIONS FOR METHANE CONVERSIONS	159
APPENDIX C: SAMPLE CALCULATION FOR Pd DISPERSION FROM H <sub>2</sub> CHEMISORPTION	164
APPENDIX D: SUMMARY OF XRD RUNS AND XRD DATA ANALYSIS	165

## **List of Tables**

Table 2-1. Summary of studies for methane combustion over supported noble metal catalysts	7
Table 2-2. Based-metal oxide catalysts for complete oxidation of methane	34
Table 2-3. Complex metal oxide catalysts for complete oxidation of methane	37
Table 3-1. Description of catalysts	40
Table 3-2. Sample pretreatment and measurement of hydrogen adsorption	45
Table 3-3. Operating conditions of Gas Chromatograph	51
Table 4-1. Comparison of activities of various catalysts	70
Table 4-2. BET, H <sub>2</sub> chemisorption and XRD results of various catalysts	84
Table 4-3. Pd dispersion and crystal sizes for RF34 before and after activation	95
Table 4-4. Summary of Pd and PdO crystal sizes from x-ray diffraction	99

## List of Figures

Figure 3-1. Schematic diagram of reactor	46
Figure 3-2. Schematic diagram of reactor and oven	47
Figure 3-3. Measured temperatures of the oven and inside the reactor	48
Figure 3-4. Schematic diagram of reactor system	50
Figure 4-1. Methane conversion as a function of temperature during activation (State 1) and after activation (State 2) for Catalyst RF34 at various rates (Feed: 0.965% methane, 3.96% oxygen in helium)	56
Figure 4-2. Stability of catalyst RF34 during methane combustion reaction at various feed rates (Feed: 0.965% Methane, 3.96% Oxygen in helium)	59
Figure 4-3. Methane conversion as a function of time on stream at various temperature for catalyst RF34 (Feed: 0.965% methane, 3.96% oxygen in helium; feed rate=82 $\mu\text{mol/s}$ )	63
Figure 4-4. Methane conversion as a function of temperature after activation at various temperatures for catalyst RF34 (State 2) (Feed: 0.965% methane, 3.96% oxygen in helium; feed rate = 82 $\mu\text{mol/s}$ )	65
Figure 4-5. Methane conversion as a function of temperature during activation (State 1) for various catalysts at a feed rate of 82 $\mu\text{mol/s}$ (Feed: 0.965% methane, 3.96% oxygen in helium)	68
Figure 4-6. Methane conversion as a function of temperature after activation (State 2) for various catalysts at a feed rate of 82 $\mu\text{mol/s}$ (Feed: 0.965% methane, 3.96% oxygen in helium)	69
Figure 4-7. Variation of the Conversion (State 2)/Conversion (State 1) ratio as a function of the reaction temperature for various catalysts at a feed rate of 82 $\mu\text{mol/s}$ (Feed: 0.965% methane, 3.96% oxygen in helium)	72
Figure 4-8. Effect of Fe addition on the methane conversion as a function of temperature during activation (State 1) for Pd based catalysts at a feed rate of 82 $\mu\text{mol/s}$ (Feed: 0.965% methane, 3.96% oxygen in helium)	77
Figure 4-9. Effect of Fe content on the activity of Pd-based alumina supported catalysts in State 2 at a feed rate of 82 $\mu\text{mol/s}$ (Feed: 0.965% methane, 3.96% oxygen in helium).	78

Figure 4-10 Effect of Fe content on the activity of Pd-based silica supported catalysts in State 1 at a feed rate of 82 $\mu\text{mol/s}$ (Feed: 0.965% methane, 3.96% oxygen in helium)	79
Figure 4-11. Effect of Fe content on the activity of silica supported Pd-based catalysts in State 2 at a feed rate of 82 $\mu\text{mol/s}$ (Feed: 0.965% methane, 3.96% oxygen in helium)	80
Figure 4-12. Variations in the ratio of activities of State 2 to State 1 as a function of the reaction temperature for various catalysts at a feed rate of 82 $\mu\text{mol/s}$ (Feed: 0.965% methane, 3.96% oxygen in helium)	82
Figure 4-13. Effect of Cu content on the activity of silica supported Pd catalysts in State 1 at a feed rate of 82 $\mu\text{mol/s}$ (Feed: 0.965% methane, 3.96% oxygen in helium)	83
Figure 4-14. Effect of Cu content on the activity of silica supported Pd catalysts in State 2 at a feed rate of 82 $\mu\text{mol/s}$ (Feed: 0.965% methane, 3.96% oxygen in helium)	85
Figure 4-15. Variations in the ratio of activities of State 2 to State 1 as a function of the reaction temperature for various catalysts at a feed rate of 82 $\mu\text{mol/s}$ (Feed: 0.965% methane, 3.96% oxygen in helium)	86
Figure 4-16. Methane conversion as a function of temperature at various feed composition over RF34 in both State 1 and 2 (Feed rate: 82 $\mu\text{mol/s}$ )	88
Figure 4-17. Methane conversions as a function of temperature after activation for Catalyst RF34 at feed rate of 82 $\mu\text{mol/s}$ at various feed compositions	89
Figure 4-18. Fractional conversion of methane as a function of the reciprocal of feed rate (Run 43)	91
Figure 4-19. Methane conversion as a function of temperature at various pressures and constant methane partial pressure and residence time for Catalyst RF34 after activation (State 2)	92
Figure 4-20. Subtracted XRD patterns for Catalyst YW114	97
Figure 4-21. Subtracted XRD patterns for activated and unreduced RF36	98

# **CHAPTER 1**

## **INTRODUCTION**

Methane is widely used as a fuel for domestic heating and power generation because it is easy to transport and it is clean. During recent years, there has been an increase in the use of methane in automobiles as a substitute for gasoline. Methane is a desirable fuel due to its low C/H ratio and it produces less carbon dioxide per unit of energy than any other hydrocarbon. The increased use of methane requires improved catalysts to clean-up exhaust gases because methane at low concentrations is the most difficult hydrocarbon to oxidize.

Catalytic methane oxidation (also called catalytic combustion) is the usual method for eliminating low concentrations of methane from exhaust streams, and such complete oxidation can occur at relative low temperatures ( $\leq 400^{\circ}\text{C}$ ) and for mixtures containing only a small concentration of methane. Hence, catalytic oxidation is the preferred method for exhaust clean-up. However, catalysts with increased activity at low temperature are required to effectively decrease methane emissions from exhaust, especially during start-up of engines.

Since the time of Davy (1) who firstly reported the combustion of methane over platinum and palladium, numerous investigations into catalytic combustion of methane over supported metal catalysts have been carried out. It has been widely reported that supported palladium is the most



active catalyst for methane oxidation (*e.g.* 2). Current catalysts usually require temperature higher than 400°C for complete oxidation of methane from gas (for gas stream contains <1% CH<sub>4</sub>).

It has been observed by many researchers that the activities of supported palladium catalysts for methane combustion are very time dependent. Significant increases in activity as a result of activation treatments with reactant gases containing methane have been reported for most supported Pd catalysts. Similar treatments with oxygen do not result in the increase in activity. Numerous studies have been conducted with the objective to explain the causes for the increase in activity (see Chapter 2). It was reported that the activity of catalysts is dependent on the size of the metal particles (dispersion) on the surface of supports and on the structure of Pd oxide formed during reaction. However, there is no general agreement on the reason(s) for the marked increase in activity during use.

In this study, catalysts made with various palladium precursors and supports were studied to investigate the correlation between catalyst activity and metal precursor and supports. The activities of supported palladium catalysts with various content of a second metal (Fe and Cu) were also measured in order to investigate the effect of second metal addition on the oxidation activity. The effects of operating conditions, such as pressure and reactant composition, on methane conversions over alumina supported catalysts were also examined.

In addition, the activity with time-on-stream at various pretreatment temperature (350-525°C) was measured over freshly reduced alumina-supported Pd catalysts. The activity of catalysts

after treatments at various temperatures was measured. Catalyst after various treatments and use were characterized by x-ray diffraction, hydrogen chemisorption and low-temperature nitrogen adsorption (BET) in an attempt to discover catalyst structure – activity relationships.

## **CHAPTER 2**

### **LITERATURE REVIEW:**

#### **CATALYTICAL OXIDATION OF METHANE**

The objective of this literature overview is to summarize prior and especially recent literature on catalytic oxidation of methane in order to identify factors which may influence on the activity of supported metal catalysts for methane oxidation. Extensive papers have been published over the past two decades on oxidative coupling of methane and conversion of methane for the production of chemicals, but the emphasis in this overview is on catalysts for the complete oxidation of methane at relatively low temperature in feeds containing excess oxygen. Literature on oxidative coupling of methane is not included in this review.

The first report on catalytic combustion of methane was made by Davy. In 1817, Davy (1) reported the 'flameless' combustion of methane (coal gas) and other organic materials over platinum and palladium wires. Davy observed that in the presence of platinum wires combustion of organic compounds occurred at temperatures much below the normal ignition temperature and for mixtures which were not explosive. In his research, he tried various metal wires for flameless combustion but only platinum and palladium produced this effect. Other metals he examined were copper, silver, iron, gold and zinc.

Since the time of Davy numerous investigations into catalytic combustion of methane have been conducted and reported. One of the influential early studies, whose results have been

extensively referred by many other researchers, was conducted by Anderson *et al.* (2). In 1961, Anderson *et al.* published an extensive study on the catalytic oxidation of methane over 30 different catalysts. They concluded that palladium-containing catalysts are the most active catalysts for methane oxidation, and that methane is the most difficult hydrocarbon to oxidize. These results have now been generally agreed upon by other researchers. The catalysts they studied included noble metals, simple metal oxides (bulk and supported), and complex metal oxides. Since palladium catalysts are widely reported as the most active catalysts for methane oxidation, most of this chapter summarizes literature dealing with the complete catalytic oxidation of methane over supported palladium catalysts. However, selected papers from literature on methane oxidation over other metals such as platinum, copper and iron, simple metal oxides and complex metal oxides or reports on methane oxidation under oxygen-lean reaction conditions is also included in this review.

## 2.1 Noble Metal Catalysts for Methane Oxidation

Numerous studies of methane oxidation over supported noble metal catalyst have been reported since the 1961 study by Andersen *et al.* (2). Various types of reactors, feed compositions, space velocities, temperature and catalyst preparation techniques have been reported. A summary of those reports is presented in Table 2-1. Significant increases in activity as a result of activation treatments with reactant gases containing methane have been reported for most supported Pd catalysts.

Although extensive investigations and studies have been conducted on the complete catalytic oxidation of methane, the catalytic mechanism of this reaction is still not well understood. The requirement(s) of active sites and the explanation(s) of cause(s) for the hysteresis effects of many supported noble catalysts which already have been reported by many investigators are still controversial. The influence of supports, palladium precursors, and pre-treatment history of catalysts on activities for methane oxidation need further investigation. It is often difficult to make absolute comparisons of the activity of various catalysts since various types of reactors, feed compositions, space velocities, temperatures and catalyst preparation techniques were used by different investigators. The unusual hysteresis in activities of the supported Pd catalysts and the lack of a standard definition of catalyst activity further complicate the comparison and interpretation of experimental data. Literature reports of the effects of various treatments on activities for catalytic methane oxidation are discussed in the following studies.

Table 2-1. Summary of studies for methane combustion over supported noble metal catalyst  
(I = inerts).

Catalyst	Catalyst Mass, g	Feed Rate cm <sup>3</sup> (STP)/s and CH <sub>4</sub> :O <sub>2</sub> :I ratio	E <sub>act</sub> , kJ/mol	Comments	Ref
3.5% Pd on Al <sub>2</sub> O <sub>3</sub> 3.5% Pd on Al <sub>2</sub> O <sub>3</sub>	6.5 5.9	0.66 cm <sup>3</sup> pulse of CH <sub>4</sub> into pure O <sub>2</sub>	91.2 87.4	Pulse reactor used. The 0.5% Pd catalyst most active of 30 catalyst tested ( active at 300°C). The Pd in the 3.5% Pd catalyst was present as PdO.	2
0.46 to 2.0% Pd on Al <sub>2</sub> O <sub>3</sub>	0.05 to 0.2	3.3 to 13 5:11:90; I=He	108 to 126	P <sub>total</sub> =1.4 bar. Catalysts reduced <i>in-situ</i> at 300°C before use. Reaction is structure sensitive. TON for Pd up to 50 times larger than for Pt. The presence of two types of PdO were proposed: one, PdO is dispersed on Al <sub>2</sub> O <sub>3</sub> and has low activity for methane oxidation, two, PdO is located on Pd and have high activity of methane oxidation.	3
0.5% Pd on (Y <sub>2</sub> O <sub>3</sub> -ZrO <sub>2</sub> )	0.05 to 0.2	3.3 to 13 5:11:90; I=He	114	P <sub>total</sub> =1.4 bar. Catalysts reduced <i>in situ</i> at 300°C before use. Reaction is structure sensitive. TON for Pd over 40 times larger than for Pt.	3
15%Pd on Al <sub>2</sub> O <sub>3</sub>	Special pellets	0.6 1:20:79; I=N <sub>2</sub>	-	Pd much more active than Ir and Rh. Studied effect of H <sub>2</sub> S poisoning.	4
1 & 5% Pd on δ- and γ- Al <sub>2</sub> O <sub>3</sub> (studied 20 catalysts)	0.12	≈2 1:20:79; I=N <sub>2</sub>	80.4 to 158.9	Pd on δ-Al <sub>2</sub> O <sub>3</sub> more active than Pd on γ-Al <sub>2</sub> O <sub>3</sub> . Treatment at ≈400°C in reaction mixture	5
1.95% Pd/ Al <sub>2</sub> O <sub>3</sub>	0.2 to 0.6	1.75 1:4:95; I=N <sub>2</sub>	-	Treatment with reaction gas at 600°C for 14 hours resulted in a large increase in catalytic activity at low temperature, e.g after the above treatment, reaction starts at 200°C instead of 300°C for the sample without the treatment	6
4% Pd/Al <sub>2</sub> O <sub>3</sub>	0.06	0.42 1:20:79; I=N <sub>2</sub>	-	Studied CH <sub>4</sub> oxidation at high temperature. Observed a hysteresis in activity (Pd PdO )	7
1.44% Pd on Sr <sub>0.8</sub> La <sub>0.2</sub> XAl <sub>11</sub> O <sub>19</sub> X=Al or Mn	0.2	≈10 1:2.2 to 25:74 to 97, I=N <sub>2</sub>	-	Reaction zero order <i>w.r.t.</i> O <sub>2</sub> . Decrease in activity at high temp. attributed to decomposition of PdO ( <i>i.e.</i> PdO is the active species)	8

Catalyst	Catalyst Mass, g	Feed Rate $\text{cm}^3(\text{STP})/\text{s}$ and $\text{CH}_4:\text{O}_2:\text{I}$ ratio	$E_{\text{act}}$ , kJ/mol	Comments	Ref
2.18% Pd/ $\text{Al}_2\text{O}_3$ 2.16% Pd/ $\text{SiO}_2$	0.05 to 0.2	2.0 1:4:94; $\text{I}=\text{N}_2$	137 99	Activation in reaction mixture at 600°C for 16 h increased activity of both catalysts. The <i>light-off</i> temperatures for the activated catalysts were 315°C and 304°C for Pd/ $\text{Al}_2\text{O}_3$ and Pd/ $\text{SiO}_2$ respectively.	9
5% to 25 wt% Pd/ $\text{ZrO}_2$	0.25	5.0 1:4:95; $\text{I}=\text{He}$	76 to 97	Various Pd/ $\text{ZrO}_2$ catalysts were prepared by thermal treatment of amorphous and crystalline $\text{Pd}_1\text{Zr}_3$ . Two catalysts were prepared by impregnation and precipitation. Catalysts were active at 250°C. Reaction orders w.r.t. $\text{CH}_4$ varied from 0.17 to 0.79; order w.r.t. $\text{O}_2$ varied from -0.01 to 0.20.	10
1% Pd oxidized ( $\text{CeO}_2$ - $\text{Al}_2\text{O}_3$ ) 1% Pd/reduced	0.5 g	batch 1.5:5.3:1.5; $\text{I}=\text{He}$	-	The activity of the Pd/(reduced $\text{CeO}_2$ - $\text{Al}_2\text{O}_3$ ) was $\approx 3$ times the activity of a 1% Pd/ $\text{Al}_2\text{O}_3$ catalyst. At the 350°C the activity of the Pd/(reduced $\text{CeO}_2$ - $\text{Al}_2\text{O}_3$ ) was about 1 $\mu\text{mol}/(\text{g cat-s})$ .	11
4% Pd (from $\text{Pd}(\text{NO}_3)_2$ ) supported on $\text{Al}_2\text{O}_3$ , $\text{Ta}_2\text{O}_3$ , $\text{TiO}_2$ , $\text{CeO}_2$ , $\text{ZrO}_2$	-	1:19.8:79.2 $\text{I}=\text{N}_2$	-	The hysteresis for decomposition of PdO to Pd is strongly dependent on the type of support. The order of the hysteresis for decomposition of PdO to Pd and its re-oxidization is: $\text{ZrO}_2 > \text{Al}_2\text{O}_3 > \text{Ta}_2\text{O}_3 > \text{CeO}_2$ The stability of PdO directly affect the oxidation activity of supported Pd catalysts. "The decomposition/reduction of PdO/alumina to Pd <sup>0</sup> /alumina results in a decrease in the activity of palladium for methane oxidation."	12
8.5% Pd on $\text{Al}_2\text{O}_3$ , 1% & 10% Pd on $\text{ZrO}_2$ , 0.77% & 7.7% Pd on Si- $\text{Al}_2\text{O}_3$	0.05 to 0.15 mixed with 1-5 g of support	2:19.6:78.4 $\text{I}=\text{N}_2$	76-92	The reaction is structure insensitive. TOR does not depend on Pd precursor, support, or Pd particle size. Catalyst activation history has influence on the steady-state activity of catalyst.	13
0.5% -10% Pd on $\text{Al}_2\text{O}_3$ 1% Pd/ $\text{SiO}_2$	0.05	1:19.8:79.2 $\text{I}=\text{N}_2$	-	Both water and carbon dioxide have negative influence on activity of methane combustion over Pd catalysts.	14
2% Pd on $\text{Al}_2\text{O}_3$	0.3	5:19:78 $\text{I}=\text{N}_2$	-	Support and treatment conditions have effects on activity of methane combustion over Pd catalysts. Catalytic activity cannot only be correlated to an increase in the size of Pd particles.	15

Catalyst	Catalyst Mass, g	Feed Rate $\text{cm}^3(\text{STP})/\text{s}$ and $\text{CH}_4:\text{O}_2:\text{I}$ ratio	$E_{\text{act}}$ kJ/mol	Comments	Ref
Pd on mordenite, Pd on $\text{Al}_2\text{O}_3$ , Pd on USY zeolite, Pd on $\text{SiO}_2$	-	$\text{CH}_4$ :3000 ppm, $\text{O}_2$ : 10%, $\text{N}_2$ balance gas	-	The activity of $\text{CH}_4$ oxidation is effected by support, water vapor, types of metal, Pd dispersion, Ce addition, and catalyst preparations.	16
Pd/ $\gamma$ - $\text{Al}_2\text{O}_3$ , Pd/0.2-5% MgO / $\gamma$ - $\text{Al}_2\text{O}_3$ , PdO/ $\gamma$ - $\text{Al}_2\text{O}_3$ , PdO/0.2-5% MgO / $\gamma$ - $\text{Al}_2\text{O}_3$	-	1% $\text{CH}_4$ +He or 1:4:95 I= $\text{N}_2$	-	1. The initial valance state of supported Pd and the MgO content in composite supports can effect the catalytic activity of palladium. 2. For supported Pd catalysts, lattice oxygen and adsorptive oxygen on the surface of the support act as oxidizers. For supported PdO catalysts, surface PdO provides oxygen to oxidize $\text{CH}_3$ fragments into $\text{CO}_2$ , while the lattice oxygen in supports acts as reducer by providing electron to $\text{Pd}^{2+}$ and then to $\text{CH}_4$ . 3. MgO can enhance the activity of atomic Pd catalysts (e.g. Pd/ $\text{Al}_2\text{O}_3$ ) while MgO is unfavorable for supported PdO catalyst	17
1.0% Pd/ $\text{ZrO}_2$ , 0.91% Pd/ $\text{ZrO}_2$ , 4.1% Pd/ $\text{ZrO}_2$ , 0.86% Pd/ $\text{ZrO}_2$ , 4.2% Pd/ $\text{ZrO}_2$	0.02-0.05	2:20:78 I= $\text{N}_2$	-	Structure sensitive. Rapid decomposition of Pd leads to localized high temperatures and reducing environments and thus inhibit the formation of stoichiometric PdO which is active in methane oxidation. Slower decomposition of precursors could also lead to epitaxial growth of PdO surface planes that catalyze methane oxidation with higher turnover rates.	18
1.0% wt. Pd/ $\text{ZrO}_2$	-	2 kPa $\text{CH}_4$ , 20 kPa $\text{O}_2$ I= $\text{N}_2$	-	No significant structure difference and change in $\text{PdO}_x$ oxygen content were detected between fresh and activated samples by $\text{H}_2$ - $\text{O}_2$ titration or CO oxidation reactions. Small Pd particles are less active than large Pd particles.	19
Pd/ $\text{Al}_2\text{O}_3$	0.3	150 ml (STP) $\text{CH}_4/\text{Air}=1:95$	-	Activity cannot only be explained by Pd dispersion.	15



Catalyst	Catalyst Mass, g	Feed Rate $\text{cm}^3(\text{STP})/\text{s}$ and $\text{CH}_4:\text{O}_2:\text{I}$ ratio	$E_{\text{act}}$ kJ/mol	Comments	Ref
0.5% Pt/ $\text{Al}_2\text{O}_3$ 0.51% Pt/ $\text{Al}_2\text{O}_3$ 4.7% Ag/ $\text{Al}_2\text{O}_3$	5.8 6.5 6.4	0.66 $\text{cm}^3$ pulse of $\text{CH}_4$ into pure $\text{O}_2$	98.3 102.9 211.7	Pulse reactor used The 0.5%Pt catalyst had activity at 300°C. Order <i>w.r.t.</i> $\text{CH}_4$ was 1.0	2
1.95% Pt/ $\text{Al}_2\text{O}_3$	0.2 to 0.6	1.75 $\text{cm}^3/\text{s}$ 1:4:95 I= $\text{N}_2$	70 to 100	$E_{\text{act}}$ decreased and the activity increased with use at 600°C; use at this condition causes Pt sintering. Reaction is structure sensitive.	20
0.5 to 0.84% Pt on $\text{Al}_2\text{O}_3$	0.05 to 0.2	3.3 to 13 $\text{cm}^3/\text{s}$ 5:11:90; I=He	121 to 164	$P_{\text{total}}=1.4$ bar. Catalysts reduced <i>in situ</i> at 300°C before use. Reaction is structure sensitive.	3
0.3 and 0.5% Pt on $\text{ZrO}_2$	0.05 to 0.2	3.3 to 13 $\text{cm}^3/\text{s}$ 5:11:90; I=He	115 to 136	$P_{\text{total}}=1.4$ bar. Catalysts reduced <i>in situ</i> at 300°C before use. Reaction is structure sensitive.	3
0.3 and 0.5% Pt on ( $\text{Y}_2\text{O}_3\text{-ZrO}_2$ )	0.05 to 0.2	3.3 to 13 $\text{cm}^3/\text{s}$ 5:11:90; I=He	111	$P_{\text{total}}=1.4$ bar. Catalysts reduced <i>in situ</i> at 300°C before use. Reaction is structure sensitive.	3
0.03 to 30% Pt on $\text{Y-Al}_2\text{O}_3$ Pt black	0.004 g of Pt plus $\text{Al}_2\text{O}_3$	recycle batch reactor 1:6:60; I=Ar	102 to 153 94	Maximum activity at 5 to 10% Pt. Reaction is structure sensitive. Reaction orders are 0 and 1 <i>w.r.t.</i> $\text{O}_2$ and $\text{CH}_4$ respectively.	21
0.83 to 1.91% Pt on $\text{SiO}_2$	1.76 to 2.5 g	2.7 $\text{cm}^3/\text{s}$ 3-10:20:70-77;	80 to 90	Reaction order <i>w.r.t.</i> $\text{O}_2$ was 0; order <i>w.r.t.</i> $\text{CH}_4$ varied from 0.49 to 0.96. Order <i>w.r.t.</i> $\text{CH}_4$ decreased with increasing Pt dispersion.	22
15% Rh/ $\text{Al}_2\text{O}_3$ 15% Ir/ $\text{Al}_2\text{O}_3$	special pellets	0.6 $\text{cm}^3/\text{s}$ 1:20:79; I= $\text{N}_2$	-	Rh more active than Ir (both less active than Pd). Studied effect of $\text{H}_2\text{S}$ poisoning.	4

### 2.1.1 Effect of type of noble metal

The oxidation activity of catalyst supported on various noble catalysts has been investigated. Anderson *et al.* (2) investigated the activity of a series of  $\text{Al}_2\text{O}_3$ -supported noble metal catalysts. They concluded that among all the supported metal catalysts they tested (supported Pd, Pt, Ag, Co, Cr, Ce, Ni, Ti catalysts), that the palladium catalysts were the most active for methane oxidation. Deng *et al.* (4) investigated the activity of Pd, Rh and Ir on alumina. They also observed Pd catalysts to be the most active. The  $\text{Pd}/\text{Al}_2\text{O}_3$  catalyst had appreciable activity below  $300^\circ\text{C}$  while temperatures of  $350$  and  $400^\circ\text{C}$  were required for appreciable activity for  $\text{Al}_2\text{O}_3$ -supported Rh and Ir catalysts respectively. In addition, Uchida *et al.* (16) reported that the order of methane oxidation over  $\text{Al}_2\text{O}_3$ -supported noble metal catalysts was  $\text{Pd} > \text{Rh} > \text{Pt}$ , they observed that the activity of methane combustion over mordenite-supported noble metal catalysts also follows the similar order. Farrauto *et al.* (23) also reported that palladium containing catalysts were the most active for methane oxidation. There is general agreement in the literature that Pd is the most active metal for methane oxidation.

### 2.1.2 Effect of support on catalyst activities

The type of support frequently affects the activity and the time-on-stream behavior of catalysts. Baldwin and Burch (24) observed that the catalytic activity changed with treatments in oxidizing atmosphere for  $\text{Al}_2\text{O}_3$  and  $\text{SiO}_2$  supported Pd, but silica supported catalysts need a much shorter activating period;  $\text{Pd}/\text{SiO}_2$  catalysts achieved maximum activity after a activation of minutes to a few hours, while alumina-supported catalysts needed much longer activation

periods of 5 to 6 days. Hopos *et al.* (9) observed that treatment of Pd/Al<sub>2</sub>O<sub>3</sub> in a CH<sub>4</sub> - O<sub>2</sub> - N<sub>2</sub> mixture at 600°C increased the activity of the catalyst several fold, while similar treatment of Pd/SiO<sub>2</sub> did not result in a marked change in activity. The authors (9,24) attribute the different behavior to the difference in the initial state of the Pd on the two different supports. They believe that the changes in the Pd phase which are responsible for the higher activity occur more rapidly on SiO<sub>2</sub> than on Al<sub>2</sub>O<sub>3</sub>, *i.e.* the SiO<sub>2</sub>-supported Pd is converted to the active phase rapidly during CH<sub>4</sub> oxidation and does not required prolonged treatment with the reactant mixture.

Other investigators have reported an effect of support on steady-state activities of catalysts. Cullis and Willatt (26) concluded that the support influenced the ability of Pd to adsorb oxygen and there was a correlation between the adsorption capacity of the supported precious metal and its catalytic activity for methane oxidation. The Pd and Pt catalysts they investigated were supported on powdered refractory metal oxides including  $\gamma$ -aluminum(III) oxide,  $\alpha$ -aluminum(III) oxide, silicon(IV) oxide, titanium(IV) oxide, thorium(IV) oxide, tin(IV) oxide. Recently, Farrauto *et al.* (12) investigated the catalytic properties of Pd dispersed on Al<sub>2</sub>O<sub>3</sub>, Ta<sub>2</sub>O<sub>3</sub>, TiO<sub>2</sub>, CeO<sub>2</sub>, ZrO<sub>2</sub>; they reported that the catalytic activity for methane oxidation is strongly dependent on the nature of support. Uchida *et al.* (16) measured the activity of methane oxidation over supported palladium catalysts using mordenite, USY zeolite,  $\gamma$ -alumina and silica as catalyst support respectively. They concluded that, among all the supports they tested, mordenite was superior to other materials. The order of activity for methane oxidation over supported palladium catalysts was: mordinite > alumina > USY zeolite > silica.

Kikuchi *et al.* (15) studied the effect of various  $\text{Al}_2\text{O}_3$  supports on the catalytic activity of  $\text{Pd}/\text{Al}_2\text{O}_3$  for methane combustion. They found that Pd supported on  $\alpha\text{-Al}_2\text{O}_3$  exhibited higher catalytic activity than Pd supported on  $\gamma\text{-}$  or  $\theta\text{-Al}_2\text{O}_3$ . In their subsequent study, they also investigated the effect of high calcination temperature of  $\text{Al}_2\text{O}_3$  supports on the catalytic activity of Pd for methane combustion. They observed that the catalytic activity of  $\text{Pd}/\text{Al}_2\text{O}_3$  whose support was calcinated at  $1600^\circ\text{C}$  prior to impregnation with  $\text{Pd}(\text{NO}_3)_2$  was about 100 times as large as the activity of  $\text{Pd}/\text{Al}_2\text{O}_3$  whose support was calainated at  $1200^\circ\text{C}$  before using the same preparation methods. They ascribed such a phenomenon to the effects of support properties on the oxidative properties of Pd metal. The effect of support properties on activity of methane combustion over supported Pd catalysts has been also demonstrated by Haneda *et al.* (11). They observed that Pd supported on  $\text{CeO}_2\text{-Al}_2\text{O}_3$ , which had been reduced in flowing  $\text{H}_2$  at  $900^\circ\text{C}$  prior to impregnation with Pd nitrate, was considerably more active than similar  $\text{Pd}/\text{Al}_2\text{O}_3$  catalyst. The  $\text{Pd}/[\text{CeO}_2\text{-Al}_2\text{O}_3 \text{ (reduced)}]$  catalyst had appreciable methane oxidation activity at  $350^\circ\text{C}$ .

Hoyos *et al.* (9) investigated the catalytic activity of methane combustion over alumina-supported and silica-supported palladium. They concluded that the support does not directly affect the combustion of methane over supported Pd catalysts, although they agreed that supports affected the rate of activation of palladium catalysts by reactants. Baldwin and Burch (5,24) made similar conclusions for Pd supported on  $\text{SiO}_2$ ,  $\delta\text{-Al}_2\text{O}_3$  and  $\gamma\text{-Al}_2\text{O}_3$ , even though the Pd on  $\delta\text{-Al}_2\text{O}_3$  was considerably more active than the Pd on  $\gamma\text{-Al}_2\text{O}_3$ . They explained the above difference by a difference in morphology of the palladium catalysts on the different supports. Ribeiro *et al.* (13), stated that the turnover rate for methane combustion over supported Pd

catalysts did not depend on the support. They based their conclusion on their experimental results which only showed small changes in the turnover rate for methane oxidation over Pd supported on various supports.

### 2.1.3 Effects of time-on-stream

For methane oxidation over supported palladium it has been observed that the rate depends on the length of use of the catalysts. Many investigators report that the activity of supported palladium increases with time-on-stream (*e.g.* 3,5,6,9,24). Hoyos *et al.* (9) observed that after aging Al<sub>2</sub>O<sub>3</sub>-supported and SiO<sub>2</sub>-supported Pd at 600°C in a mixture of CH<sub>4</sub>-O<sub>2</sub>-N<sub>2</sub> (ratio O<sub>2</sub>/CH<sub>4</sub> = 4) overnight, the activity of catalysts for methane combustion increased. Baldwin and Burch (5) stated that the rate of methane oxidation over a series of Pd/Al<sub>2</sub>O<sub>3</sub> catalysts increased with the length of exposure to the reaction mixture at high temperature (400 to 600°C). They reported that after reacting with methane containing reaction mixture at 375°C over a period of 120 hours, the activity for complete oxidation of methane over 1% Pd/Al<sub>2</sub>O<sub>3</sub> (pre-calcined in air before testing) became about four times larger than the initial activity. Hicks *et al.* (25,27) also reported the activity increase of supported palladium catalysts with time-on-stream. The turnover rate of various supported palladium catalysts which they tested increased from 2-fold to about 40-fold over a reaction period of 8 hours. Such an enhancement of activity was also observed when supported palladium catalysts were reduced under hydrogen before activation in reactants. Baldwin and Burch (24) stated that the activation of Pd/Al<sub>2</sub>O<sub>3</sub> and Pd/SiO<sub>2</sub> occurs whether the precursor is calcined, or calcined and then reduced prior to aging. Briot and Primet (6) observed that aging of freshly reduced Pd/Al<sub>2</sub>O<sub>3</sub> at 600°C in a CH<sub>4</sub> - O<sub>2</sub> - N<sub>2</sub> mixture (CH<sub>4</sub>:O<sub>2</sub> = 1:4)

significantly increased the activity of the catalyst. In addition to alumina and silica supported palladium catalysts, such activation behavior has also been observed for other supported palladium catalysts. Marti *et al.* (28) reported that the activity of amorphous and crystalline  $\text{Pd}_1\text{Zr}_3$  significantly increased over a period of 1000 minutes with an aging temperature ranging from 573 K to 723 K.

The behavior of time-on-stream over supported palladium catalysts was also observed for supported platinum catalysts. Briot and Primet (6) reported that the activity of pre-reduced  $\text{Pt}/\text{Al}_2\text{O}_3$  at low temperature increased by about 10 fold after the pretreatment in reaction mixtures at 600°C. The activity of a pre-reduced  $\text{Pt}/\text{Al}_2\text{O}_3$  slightly raised for reaction temperature lower than 700 K after the catalyst was maintained at 600°C under a flow of reactants for 14 hours. They also demonstrated that the catalyst activity did not change at high reaction temperature after activated at the same condition (20). Hicks *et al.* (3) also observed the enhancement of activity over supported Pt catalysts.

The activation behavior is more marked for supported palladium catalysts than for supported platinum for the same conditions of pretreatment. It was reported in literature, that the activity of  $\text{Pd}/\text{Al}_2\text{O}_3$  was more than 10 times higher than that of  $\text{Pt}/\text{Al}_2\text{O}_3$  after treatment in a mixture of 4 vol.% oxygen in nitrogen at 600°C for 14 hours (6). Otto (21) stated that the reaction conditions and the pretreatment of supported Pt catalysts affected the type of crystallographic plane exposed and thus modified the specific activity per surface site. He suggested that oxidation tends to disperse Pt, while reduction may cause sintering.

It has been stated by many researchers that the presence of both methane and oxygen seemed to be necessary for the enhancement of the activity of supported palladium catalysts. For examples, Briot and Primet (6) noticed that the catalytic activity of Pd/Al<sub>2</sub>O<sub>3</sub> for methane oxidation did not increase when the catalyst sample was aged in the absence of methane although its activity of methane oxidation increased up to 35 fold at low temperature after reacting with a CH<sub>4</sub> - O<sub>2</sub> - N<sub>2</sub> reaction mixture (CH<sub>4</sub>:O<sub>2</sub> = 1:4) at high temperature (400 to 600°C). They attributed this behavior of supported palladium catalysts to active site modification resulting from the deposition of carbon and the surface reconstruction of the PdO crystallites. In addition, Otto (21) stated that the reaction kinetics of methane oxidation depend on the pretreatment history of the catalyst samples. In his study, he measured the rate of methane oxidation over supported Pt and pretreated the catalyst samples in O<sub>2</sub> or H<sub>2</sub> before testing. Baldwin and Burch (24) also found that supported palladium catalysts could only be activated by reactive mixtures; activation did not happen during pretreatment in air. They suggested that the cause of such behavior was the reconstruction of catalyst surface under different gas treatment. Chojnacki and Schmidt (29) also states that there is a correlation between catalyst morphology and different gas treatments.

Cullis and Willatt (26) made the same statement based on the effects Pd/-Al<sub>2</sub>O<sub>3</sub> activation by various gas mixtures. They found that the catalysts became easier to activate after pretreatment by a mixture of H<sub>2</sub>+He as compared to a He or O<sub>2</sub> treatment, and that the catalyst was easier to activate after an inert gas pretreatment than after an O<sub>2</sub> pretreatment. Fujimoto *et al.* (19) stated that the pretreatment of Al<sub>2</sub>O<sub>3</sub> and ZrO<sub>2</sub> supported palladium catalysts at high temperature (700°C) in O<sub>2</sub> resulted in low activity of the supported palladium catalysts for methane

combustion. This low activity of the catalyst is due to the redispersion of Pd at high temperature and the formation of small PdO particles after the above pretreatment. The small PdO particles were considered to interact strongly with the  $\text{Al}_2\text{O}_3$  or  $\text{ZrO}_2$  support. Cullis and Willatt (26) observed that pretreatment of Pd catalyst in oxygen at 725 K was detrimental toward methane oxidation. They stated that *“treatment of palladium with oxygen at 1000 K provides a tightly bound surface species which is chemically stable and may well represent an intermediate stage in the formation of palladium(II) oxide.”*

In addition to the effect of reactants, other pretreatment factors (*e.g.* aging temperature, temperature ramp of aging temperature, *etc.*) also affect the activity of supported Pd catalysts for methane combustion. Baldwin and Burch (5) concluded that the alumina supported palladium catalyst was more active after aging in a 1% methane/air mixture at 405°C than aging in the same mixture at 373°C. However, Chen and Ruckenstein (30) observed that the extent of reoxidation of Pd will be greater on the palladium initially oxidized at low temperature. Baldwin and Burch (24) measured the rate of methane combustion over supported Pd catalysts with various treatment history (*e.g.* calcination temperature, length of calcination period). They observed that the rate constant of methane combustion over catalysts after various pretreatment were different. In addition, Fujimoto *et al.* (18,19) observed that the activity of supported palladium catalysts which are prepared by controlled decomposition of Pd precursors during catalyst preparation do not increase after activating with reactants. In contrast, the activity of the same catalysts which are prepared by uncontrolled decomposition increase with time-on-stream. They explained this observation by assuming that rapid decomposition of Pd precursors may



cause uncontrolled local exotherms which can result in decomposing of active PdO to less active Pd.

Ribeiro *et al.* (31) investigated the effect of pre-treatment history on Pd/SiO<sub>2</sub>. They stated that “*an in situ aging of Pd/Si-Al<sub>2</sub>O<sub>3</sub> sample in methane, or ethylene had no effect in the sample activation.*” They further stated that “*treatment in situ with air appears to make the catalysts more difficult to activate.*” Based on their observation, they suggested that the large differences in catalytic activity reported in literature is due to the different extent of catalyst activation.

#### 2.1.4 Effects of reaction temperature

The effects of reaction temperature on combustion activity of supported noble metal have been reported by various researchers (*e.g.* 2,6,13,16,32). They found that the rate of methane oxidation over supported palladium catalysts does not always increase with the increase of reaction temperature. Marti *et al.* (10) demonstrate that the steady-state activity of methane oxidation over amorphous and crystalline Pd<sub>1</sub>Zr<sub>3</sub> is relatively constant for temperature from 573 to 723K. Farrauto *et al.* (7) studied the oxidation of methane over a wide temperature range (300 to 900°C) using Pd/Al<sub>2</sub>O<sub>3</sub> catalysts. They observed that the catalytic activity of the catalyst significantly decreased when the reaction temperature was higher than about 800°C; they also observed a restoration of activity when reaction temperature was decreased from 700 to 500°C. Such a temperature effect on catalyst activity has been attributed by investigators to the decomposition of PdO to Pd and the re-oxidation of Pd to PdO during reaction (7,8). Sekizawa *et al.* (8) also studied the effect of reaction temperature on the oxidation activity of supported

palladium. They used 1.44 mass% Pd supported on hexaaluminates ( $\text{Sr}_{0.8}\text{La}_{0.2}\text{XAl}_{11}\text{O}_{19}$ , X = Al and Mn). They observed that the activity of catalyst increased initially with a rise in temperature, but started to decrease after 700°C. In agreement with the above investigators, they attributed this phenomena to the decomposition of PdO with the rise of reaction temperature. Cullis and Willatt (26), however explained that the relatively low activity of supported Pd catalysts at high reaction temperature was because of the migration of oxygen into the bulk of the palladium to form a layer of more stable but less active surface oxides under high reaction temperature. The details in the literature about the requirement of active sites for methane combustion will be summarized in a following section.

#### 2.1.5 Effect of the type of noble metal precursors

The effect of the type of noble metal precursor on catalyst activity for methane combustion has been frequently reported in literature. Stull *et al.* (33) reported that a “*stable platinum oxychloride*” may form when  $\text{Al}_2\text{O}_3$  supported Pt catalysts are prepared by impregnation of  $\text{H}_2\text{PtCl}_6$  and oxidizing in air at 500°C. Cullis and Willatt (34) stated that the activity of methane combustion over Pd/ $\text{Al}_2\text{O}_3$  is inhibited by chlorine. They studied the effect of halogenated hydrocarbons (*e.g.*  $\text{CHCl}_3$ ,  $\text{CH}_2\text{Cl}_2$ ,  $\text{CH}_2\text{ClCH}_2\text{Cl}$ ,  $\text{CH}_2\text{Br}_2$ ) and organosiloxanes on the rate of methane oxidation over supported Pd and Pt catalysts. They concluded that the inhibition of methane oxidation by halogenated hydrocarbons is due to the adsorption of the halogen compound on the sites on catalysts surface where oxygen is normally adsorbed and activated. They stated, “*the catalyst systems with which there is a strong interaction between the precious metal and its support suffer the greatest loss in activity but also exhibit the most marked*

recovery.” They also reported that the catalyst support has an appreciable effect on the resistance of the precious metal to the poisoning by halogenated hydrocarbons. In addition, Hicks *et al.* (25,27) reported that those catalysts, which are prepared by impregnation of aqueous  $\text{PdCl}_2$  solution and oxidation in air at  $500^\circ\text{C}$ , show low turnover rates that steadily increase throughout the run. They attributed such an unusual behavior of the above catalysts to the poisoning by chlorine; they also stated that the slow increase of catalyst activity is due to the slow decomposition of an inactive Pd oxide-chloride species into an active Pd oxide species. Marecot *et al.* (35) investigated the effect of chloride on the propane and propene oxidation over platinum and palladium on alumina. They discovered that catalysts prepared using chloride containing precursor salts (*e.g.*  $\text{H}_2\text{PtCl}_6$ ,  $\text{H}_2\text{PdCl}_4$ ) had lower activities than those prepared using chloride-free precursor salts (*e.g.*  $\text{Pt}(\text{NO}_2)_2(\text{NH}_3)_2$ ;  $\text{Pd}(\text{C}_5\text{H}_7\text{O}_2)_2$ ) regardless of particle size of Pd or Pt. However, Baldwin and Burch (5,24) declare that the removal of chlorinated species from the catalysts was not the sole cause of activation of the catalysts prepared from the chloride precursor. They based their conclusion on their observations that samples prepared from the nitrate precursor also showed activation effects, and the fact that their catalysts did not show activation behavior after aging in air.

Simore *et al.* (36) studied the reversible poisoning of palladium catalysts for methane combustion. They reported that the  $\text{Pd}/\text{Al}_2\text{O}_3$  catalyst prepared from  $\text{Pd}(\text{NO}_3)_2$  was more active than that prepared from  $\text{PdCl}_2$ , and that the removal of the chloride from the first one by washing greatly enhanced the activity for methane oxidation.

### 2.1.6 State of Pd on Support During Methane Oxidation

The effects of supports, noble metal precursors, reaction temperature, and pretreatment history on the rate of methane combustion over supported noble metal catalysts have been summarized in the above literature survey. From the above literature survey, it has noticed that preparation factors such as support, noble metal precursors, reaction temperature, and pretreatment history all affect the catalytic properties of supported noble metal catalysts. Catalytic properties of methane combustion over supported palladium and platinum catalysts have been extensively studied and reported by investigators. However, until now, the requirement(s) of active sites on supported noble metal catalysts for methane combustion are still unclear and there is no general agreement on cause(s) for the marked increase in catalytic activity resulting from pretreatment. A brief review of the effect of the Pd on the activities is presented below.

The increase of the methane oxidation rate has been attributed to the formation of a PdO phase during initial contact between Pd-based catalysts and CH<sub>4</sub>/O<sub>2</sub> reactants. Farrauto *et al.* (7) studied the oxidation of methane over a wide temperature range (300 to 900°C) using Pd/Al<sub>2</sub>O<sub>3</sub> catalysts. They concluded that PdO is the active phase and that the observed low activity of Pd/Al<sub>2</sub>O<sub>3</sub> after heating to 900°C is due to the decomposition of the PdO to palladium metal. Sekizawa *et al.* (8), not only concluded that PdO is more active than Pd for the oxidation of methane, they also found that the dissociation of PdO at high temperature (1200°C) depends on the oxygen partial pressure of reactants. They used 1.44 mass% Pd supported on Sr<sub>0.8</sub>La<sub>0.2</sub>XAl<sub>11</sub>O<sub>19</sub> catalysts, where X=Al or Mn. Briot and Primet (6) observed that in an

oxygen-rich reactants mixture, the catalytic oxidation of methane over supported Pd occurs on a Pd oxide phase, while the catalytic oxidation of methane over supported Pt occurs on a Pt phase. Recently, Farrauto *et al.* (12) conducted an extensive investigation on methane combustion over Pd catalysts with various materials of support in order to give more insight into the correlation between Pd phase and catalyst activity. They concluded that the methane combustion behavior over supported Pd catalysts is correlated with the PdO decomposition-reformation hysteresis. They also concluded that the extent of redox hysteresis for palladium catalysts ( $\text{Pd} \leftrightarrow \text{PdO}$ ) is strongly depended on support materials due to the different interactions between PdO and Pd metal with different supports. They reported that the order of the extent of the hysteresis for supports of Pd/PdO are:  $\text{ZrO}_2 > \text{Al}_2\text{O}_3 > \text{Ta}_2\text{O}_5 > \text{TiO}_2 > \text{CeO}_2$ .

In a recent study with Pd on  $\text{Al}_2\text{O}_3$  and Pd/ $\text{ZrO}_2$ , Ribeiro *et al.* (31) heated a series of  $\text{Al}_2\text{O}_3$  and  $\text{ZrO}_2$  supported palladium catalysts to 1123 K. They observed that at this temperature the PdO phase on the surface of catalysts were decomposed to Pd metal phase which was not active for methane combustion. Then, they calcined the above supported Pd catalysts (which were initially heated to 1123 K in air) at relatively low temperature (973K for Pd/ $\text{Al}_2\text{O}_3$ , 773K for Pd/ $\text{ZrO}_2$ ). However, they observed that the supported Pd catalysts still demonstrated very low catalytic activity for methane combustion although the Pd metal on the surface of catalysts had already been re-oxidized to PdO after the above calcination. They explained this observation by assuming that a dispersed monolayer of a stable PdO phase was formed and spread on the oxide support surface; this stable monolayer of PdO phase was not active for methane combustion. Similar behavior was also observed by Hicks *et al.* (3,27) and Cullis and Willatt (26). Hicks *et al.* (3,27) proposed that there exist at least two types of active sites on PdO surface. One, located

on the surface of palladium oxide dispersed over the alumina support, another, located on the surface of palladium oxides dispersed over the surface of palladium crystallites. The first type which originates from well dispersed Pd is postulated to be much less active than the second type which is formed on large Pd particles. It is postulated that the bond between Pd and oxygen for the first type of sites is much stronger than that of the second type of sites. They concluded that methane oxidation on Pd catalysts is strongly depended on the size of Pd particles. Cullis and Willatt (26) explained this phenomenon by suggesting that a layer of tightly bound and stable surface palladium oxide may form due to the migration of oxygen into the bulk of the palladium at high temperature. They concluded that methane oxidation on Pd is independent of particle size.

For several decades, the correlation between Pd particle size and catalytic activity of methane combustion on supported Pd catalysts has received wide attention. Unfortunately, there is still no general agreement on the effect of Pd crystal size on the activity of supported Pd catalysts. In this research work, we conducted an extensive literature survey of papers in this field. A brief summary of related conclusions and views proposed by investigators in recent literature is given below.

The concept of structure sensitive (demanding) and structure insensitive (facile) reactions was introduced by Boudart (37). *Structure insensitive* reactions are reactions for which the rate is proportional to the metal surface area, *i.e.* rate of reaction increases with increasing metal dispersion, while the specific rate of reaction for *structure sensitive* reactions depends on the size of metal particles (dispersion). Otto (21) proposed that the change of catalyst structure can affect

the turnover rate (TOR) of methane combustion due to following reasons: 1) changes of type of crystallographic plane exposed, 2) disparate surface sites located on corners and edges of metal particles, 3) modification of catalytic sites by support interaction, 4) active sites on the support materials.

For complete oxidation of methane over supported palladium and platinum it has been observed that the rate depends on the length of use of the catalyst. The activity of supported catalysts frequently increases with use (3,5,6,27,38). The increase in rate with use has been ascribed to structure sensitivity, *i.e.* use results in increase in average Pt or Pd size and the activity per unit surface area of metal increasing significantly with increasing Pt or Pd particle size (3,6)

Hicks *et al.* (3,27) conducted an investigation on methane combustion over a series of supported palladium and platinum catalysts. For the platinum supported catalyst they tested, they observed that the turnover frequency changed by 100 fold from the least active to the most active catalyst which they prepared. They attributed this change to the structure of exposed platinum. From their investigation on the palladium catalysts, they reported that the turnover frequency was strongly affected by the size of the palladium particles. They suggested that this occurred because the oxide layer on the palladium crystallites is much more active than the palladium oxide dispersed over the alumina. They concluded that the turnover frequency for methane oxidation over palladium supported catalysts depended on the size of the metal crystallites and possibly on the distribution of sites on the metal surface. They observed a redistribution of sites on the catalyst during reaction by infrared results of adsorbed carbon

monoxide at saturation coverage on palladium catalyst samples. In addition, they also stated that support composition and preparation methods can affect the stabilized size of Pd particles on supports. Briot and Primet (6), Briot *et al.* (38), Fujimoto *et al.* (18,19), Briot and Auroux (20) and Marti *et al.* (28) arrived the same conclusion. They showed that the reaction of methane combustion over supported Pd is structure sensitive. Burch *et al.* (39) in a recent study observed that freshly reduced alumina-supported palladium catalysts absorb oxygen to form PdO during initial reaction with reactants ( $\text{CH}_4\text{-O}_2$  mixture) and the time required for oxygen uptake and catalyst activation was similar. Based on the above observation, they proposed that methane combustion causes bulk oxidation processes that increase the reactivity of active surface  $\text{PdO}_x$  species.

On the other hand, Cullis and Willatt (26), showed that the catalytic activity for methane oxidation is independent of particle size. They demonstrated that the different catalytic behavior of palladium and platinum is because of the different abilities of these metals to adsorb oxygen. Baldwin and Burch (5) investigated the catalytic activity of  $\text{Pd/Al}_2\text{O}_3$ . They concluded that there is no *sensible* correlation between activity of palladium catalysts and palladium particle size. Gillet and Channakhone (40) studied palladium/mica model catalysts by using transmission electron microscopy (TEM) and transmission electron diffraction (TED), they found the decomposition of CO on small Pd particles does not only depend on particle size but also was strongly affected by particle morphology. Chojnacki and Schmidt (41) found a significant change of catalyst morphology after different gas treatment. Baldwin and Burch (24) proposed that the reconstruction of the palladium oxide surface could be a possible explanation for the dramatic increase in the activity of supported palladium oxide catalysts for methane combustion.



Briot and Primet (6) also stated that the change of methane combustion activity cannot only be connected to the increase in the size of Pd particles; the reconstruction of the palladium oxide surface may also be a possible reason. However, Ribeiro *et al.* (31) concluded that the increase in catalytic activity cannot be correlated to PdO redispersion occurring during reaction. They based their conclusion on the observation that the change in size of Pd particles after activation was small. They measured the size of Pd particles for supported palladium catalysts before and after reaction by  $\text{H}_2\text{-O}_2$  titration and X-ray diffraction. On the other hand, Garbowski *et al.* (42) recently reported a correlation of the increase in catalytic activity with a restructuring of the Pd surface. They demonstrated that the development of Pd(200) surface planes during activation may lead to an easier transition from surface Pd metal to surface PdO. They also concluded that the activation does not result from the spreading or roughing of PdO crystallites in gas mixture containing  $\text{CH}_4$  and  $\text{O}_2$ . Kikuchi *et al.* (15) made a similar conclusion and concluded that the catalytic activity of Pd/ $\text{Al}_2\text{O}_3$  for methane combustion was strongly affected by the oxidative properties of Pd metal. Ribeiro *et al.* (31), on the contrary, attributed the large differences in turnover rates of methane combustion reported in the literature to insufficient activation of the catalyst samples.

Recently, Fujimoto *et al.* (19) reported that they observed no significant difference in surface structure or  $\text{PdO}_x$  oxygen content between fresh and activated catalysts although the rate of methane combustion increased by a factor of three as a result of activation. However, they still proposed that the redispersion of Pd leads to small PdO particles which interact strongly with the  $\text{ZrO}_2$  support and  $\text{PdO}_x$  species with sub-stoichiometric oxygen content are less active for methane combustion at low temperature. They suggested that one should consider the possibility

that the structural details of the catalytic surface may be destroyed when  $\text{PdO}_x$  crystallites are reduced before  $\text{H}_2\text{-O}_2$  titrations.

The possibility of other reasons for the activation of catalysts has also been studied by investigators, *e.g.* Hicks *et al.* (25) suggested that the removal of chloride from the catalysts during initial activation period may be one reason for the increase of activity with time-on-stream. Baldwin and Burch (24), however, stated that the activation is not due to the removal of chlorinated species. The effect of chloride Pd precursors on catalyst activity has been further investigated by Simone *et al.* (36). The possibility of carbon deposition was studied by Baldwin and Burch (24). However, no conclusion has been made in their paper. In a recent study, Ribeiro *et al.* (31) observed no correlation between the presence of carbon and the rate increase with time-on-stream.

The following several statements regarding the correlation between the catalytic activity and the state of Pd on support during methane combustion summarize the opinions in the literature:

- 1) PdO is the active phase for methane combustion and the low activities of supported Pd catalysts at high reaction temperature are due to the dissociation of PdO to Pd which is not active for methane combustion (*e.g.* 6,7,8,12,31,39).
- 2) The PdO phase is not always active for methane combustion (*e.g.* 3,6,19,26,27,31). PdO which is dispersed and spread on the support surface is inactive for methane oxidation (6,19,31); at least two types of active sites exist on PdO surface. The active sites located

on the surface of palladium oxide dispersed over the surface of palladium crystallites are more active for methane oxidation than those located on the surface palladium oxide dispersed over the alumina support (3,27); the surface palladium oxide which is formed due to the migration of oxygen into the bulk of palladium at high temperature is inactive for methane oxidation (26).

- 3) Methane oxidation on Pd is structure-sensitive and the activity of methane oxidation on Pd is depended on both the size of palladium particles and the reconstruction of palladium oxide surface during reaction (*e.g.* 3,6,18,19,21,27,38), but other investigators concluded that methane oxidation on Pd was structure-insensitive (*e.g.* 5,26,31,40).
- 4) The reconstruction of PdO during reaction may be an explanation for the dramatic increase in the catalytic activity of supported palladium oxide catalysts for methane combustion (6,24,41).

### 2.1.7 Mechanism and kinetics of methane oxidation

The kinetics of methane oxidation over noble metal catalysts are usually modeled by power-law rate functions, *i.e.*

$$-r_{CH_4} = r_{CO_2} = Ae^{-E/RT} C_{CH_4}^n C_{O_2}^m \quad (2-1)$$

For methane oxidation over noble metal catalysts in excess oxygen, the only detected products are carbon dioxide and water. Carbon monoxide has never been detected in the reaction products.

The order with respect to methane ( $n$ ) is usually 1.0 (5,19,21) and the order with respect to oxygen ( $m$ ) is usually zero (5,8,19,21). However, Marti *et al.* (10) obtain  $n=0.17$  to  $0.79$  and  $m=-0.01$  to  $0.20$ , and Kobayashi *et al.* (22) obtained  $n=0.49$  to  $0.96$ . Haneda *et al.* (11) postulated an Eley-Rideal mechanism, but Otto (21) concluded that an Eley-Rideal mechanism is inconsistent with observations. The effects of either water or carbon dioxide on the rate of methane combustion over supported Pd catalysts have been reported in the literature.

It has been commonly reported that water inhibits methane combustion over supported noble metal catalysts (31,34,43). Most of the earlier work was conducted by Cullis and coworkers (34, 43) who reported the negative effect of water for the reaction of  $\text{CH}_4$  oxidation over supported Pd catalysts. They found that water vapor strongly inhibited methane oxidation over a alumina supported catalyst. Ribeiro *et al.* (31) also observed an inhibitory effect of water in their study of  $\text{CH}_4$  combustion. They reported an order of reaction with respect to water of  $-0.98$  at  $\text{H}_2\text{O}$  concentrations between  $0.03$  and  $0.15\%$ . Recently, Burch *et al.* (14) conducted an extensive investigation on water inhibition over a series of silica or alumina supported palladium catalysts. They observed that water strongly inhibited the complete oxidation of methane even at low partial pressures. They also found that the inhibitory effect of water became much less significant at high reaction temperature (*e.g.* temperatures above  $450^\circ\text{C}$ ).

There is a general agreement among investigator on how water inhibits the catalytic activities for methane oxidation. Cullis and coworkers (34, 43), Ribeiro *et al.* (31) and Burch *et al.* (14) suggested that water reacts with PdO to reversibly form Pd(OH)<sub>2</sub> at the PdO surface, and the formation of Pd(OH)<sub>2</sub> effectively blocks access of CH<sub>4</sub> to the active sites on the PdO surface. However, Card *et al.* (44) observed from the TGA results that Pd(OH)<sub>2</sub> decomposes to PdO at about 247°C when Pd(OH)<sub>2</sub>/C was heated in N<sub>2</sub> at a rate of 10°C/min. Burch *et al.* (14) and Cullis *et al.* (43) explained the proposed stability of Pd(OH)<sub>2</sub> at higher temperature by the stabilization of Pd(OH)<sub>2</sub> due to the ability of the support to retain water.

Although the negative effect of carbon dioxide has been reported in literature, there is no general agreement among investigators about the extent of the inhibition caused by carbon dioxide on methane oxidation over supported Pd catalysts. Cullis *et al.* (43), Cullis and Willatt (34), and Burch *et al.* (14) observed a relatively insignificant effect of CO<sub>2</sub> on catalyst activity. On the contrary, Ribeiro *et al.* (13) found that CO<sub>2</sub> strongly inhibits the rate of methane oxidation over supported Pd catalysts for CO<sub>2</sub> concentration of about 0.5% CO<sub>2</sub> by volume; they also observed a smaller inhibitory effect of CO<sub>2</sub> at lower CO<sub>2</sub> concentrations.

So far, the mechanism by which CO<sub>2</sub> inhibits the rate of methane combustion is still unknown. Recently, Burch *et al.* (14) suggested that CO<sub>2</sub> may react with PdO on the support to form inactive PdO-CO<sub>2</sub> surface species. Also, CO<sub>2</sub> may be replaced by H<sub>2</sub>O to form a PdO-H<sub>2</sub>O surface species which is more stable and less active than PdO-CO<sub>2</sub>. They proposed that CO<sub>2</sub> and H<sub>2</sub>O compete for the same sites on the PdO surface.

Giezen *et al.* (45) reported the orders with respect to H<sub>2</sub>O for methane combustion on supported palladium oxide catalysts over a broad temperature range (230-515°C). They proposed the following rate expression for methane oxidation over palladium oxide combustion catalysts:

$$r = k_0 \cdot (P_{CH_4})^{0.9} \cdot (P_{O_2})^{0.2} \cdot (P_{H_2O})^{-0.8} \cdot \exp[-151000/RT] \quad (2.2)$$

Ribeiro *et al.* (13) also studied the order with respect to H<sub>2</sub>O and CO<sub>2</sub> and obtained an order of -1 with respect to H<sub>2</sub>O and an order of -2 with respect to CO<sub>2</sub> (for CO<sub>2</sub>% > 0.5% by volume). They proposed that the rate expression of methane combustion can be expressed as:

$$r = k[CH_4][O_2]^0[H_2O]^{-1}[CO_2]^{-2} \quad (2.3)$$

Kenichiro *et al.* (19) described the rate expression of methane combustion over supported Pd catalysts at low methane conversions (<10%) by:

$$r = k[CH_4][O_2]^0[H_2O]^{-1} \quad (2.4)$$

They also proposed a pathway for the combustion of methane on PdO crystallites which includes dissociative adsorption of oxygen and step-by-step removal of hydrogen atoms from adsorbed methane.

The activation energy for Pd and Pt catalysts ranges from about 70 to 160 kJ/mol (see Tables 1 and 2). Activation energy for a wet feed was found to be much higher than the activation

energy for a dry feed. Giezen *et al.* (45) reported that the relationship between  $E_{\text{dry}}$  and  $E_{\text{wet}}$  can be expressed in terms of the order with respect to water ( $n$ ) as:  $(E_{\text{dry}}/R) = [1/(1-n)] \cdot (E_{\text{wet}}/R)$  (where  $E_{\text{dry}}=86$  kJ/mol,  $E_{\text{wet}}=151$  kJ/mol, and  $n=-0.8$ ). The activation energy usually decreases with increased time-on-stream (20). Large Pt particles, such as those in Pt black, were reported to have lower activation energy than smaller Pt particles (21). The support also appears to influence the activation energy; SiO<sub>2</sub>-supported Pd has lower activation energies than Al<sub>2</sub>O<sub>3</sub>-supported Pd (9). The results in Tables 1 show that Pd catalysts are the most active, but the catalysts preparation techniques, activation procedures and nature of the support have a large influence on the activity of the catalyst.

## 2.2 Metal Oxide Catalysts for Methane Oxidation

Supported and bulk base-metal oxides have been studied as methane oxidation catalysts. Anderson *et al.* (2) studied various metal oxide catalysts; the most active base-metal oxide catalysts they studied were bulk and clay-supported  $\text{Co}_3\text{O}_4$ ; McCarty and Wise (48) also found that  $\text{Co}_3\text{O}_4$  was the most active of the base metal catalysts. The results of these and other methane oxidation studies over metal oxides are summarized in Table 2-2.

It is difficult to make direct comparisons of catalytic activities of various catalysts because different types of reactors, different feed compositions and space velocities, different reaction temperatures, and different catalyst preparation techniques were used by various investigators. Information on the feed compositions, feed rates and amounts of catalyst used are given in Table 2-2 for various studies with base-metal catalysts. The amounts of catalysts used for the activity determinations varied from 0.04 g (40) to 6 g (2). The types of reactors used for the activity determinations included fixed-bed tubular reactors and batch reactors. In order to obtain some comparison of activities, the activity per gram of catalyst (rate of  $\text{CH}_4$  oxidation) was estimated at  $450^\circ\text{C}$  if sufficient information was provided. These estimated activities are also listed in Table 2-2. The only other base-metal oxide, besides  $\text{Co}_3\text{O}_4$ , which showed appreciable activity at temperatures of  $\leq 450^\circ\text{C}$  was  $\text{CuO}$  (49,50,51). The ZSM-5-supported  $\text{CuO}$  (51) appears to have unusually high activity, but the activity at low temperatures was not studied; all the experiments were done at  $500^\circ\text{C}$ . Fe on supported alumina (54) also was reported to have some of activity for methane oxidation.



Table 2-2. Base-metal oxide catalysts for complete oxidation of methane.

Catalyst	Catalyst Mass, g	Feed (STP)	E <sub>act</sub> kJ/mol	Rate at 450°C $\mu\text{mol}/(\text{g cat-s})$	Comments	Ref
Cr <sub>2</sub> O <sub>3</sub> MnO <sub>2</sub> Fe <sub>2</sub> O <sub>3</sub> Co <sub>3</sub> O <sub>4</sub> NiO	0.04 g for all cases	3.3 cm <sup>3</sup> /s 1.5% CH <sub>4</sub> 4.2% O <sub>2</sub> 94.3% He	101 82 105 64 100	0.02 1.64 0.35 6.35 1.43	All catalysts were bulk metal oxides with BET areas of 5 to 13 m <sup>2</sup> /g. Activation energies based on runs with <15% CH <sub>4</sub> conversion.	48
2.1% CuO/Al <sub>2</sub> O <sub>3</sub> 4.8% CuO/Al <sub>2</sub> O <sub>3</sub> 9.2% CuO/Al <sub>2</sub> O <sub>3</sub> 100% CuO	0.5 g for all cases	1.8 cm <sup>3</sup> /s 1% CH <sub>4</sub> 4% O <sub>2</sub> 95% N <sub>2</sub>	106 93 99 101	0.27 0.38 0.30 0.59	Appreciable activity at 400°C (>0.1 $\mu\text{mol}/\text{g}$ for 4.8% and 100% CuO catalyst). Some deactivation after treatment at 1070°C.	49
2.1% CuO/Al <sub>2</sub> O <sub>3</sub> 4.8% CuO/Al <sub>2</sub> O <sub>3</sub> 9.2% CuO/Al <sub>2</sub> O <sub>3</sub> 4.8% CuO/ZnAl <sub>2</sub> O <sub>4</sub>	0.5 g for all cases	1.8 cm <sup>3</sup> /s 1% CH <sub>4</sub> 4% O <sub>2</sub> 95% N <sub>2</sub>	107 92 98 110	0.61 0.96 0.79 0.26	The ZnAl <sub>2</sub> O <sub>4</sub> supported CuO had a lower activity, but did not deactivate when treated at temperatures above 1070°C	50
0.25 to 2.8 wt% Cu on ZSM-5	0.8 to 2.5 g	265 ppm CH <sub>4</sub> , 22% O <sub>2</sub> , 78% He	-	-	99% conversion achieved 500°C and space velocities of up to 8000 h <sup>-1</sup> . Cu on Mordenite and SiO <sub>2</sub> had lower activity.	51
20% Ce <sub>2</sub> O <sub>3</sub> / Al <sub>2</sub> O <sub>3</sub> 20% CeO <sub>x</sub> / Al <sub>2</sub> O <sub>y</sub>	0.5 g 0.5 g	CH <sub>4</sub> : O <sub>2</sub> = 1:0.5 to 6.2	-	-	Used a circulating batch reactor. Order w.r.t. to O <sub>2</sub> = 0 for unreduced catalyst and 0.5 for reduced catalyst	11 & 52
Cr <sub>2</sub> O <sub>3</sub> $\beta$ -Ga <sub>2</sub> O <sub>3</sub>	1.0 g	1.7 cm <sup>3</sup> /s 2% CH <sub>4</sub> , 16% O <sub>2</sub> , 82% N <sub>2</sub>	-	-	Chromium and gallium oxides required 445°C for 10% conversion. All the gallates were less active	53
1.9% Fe/ $\gamma$ -Al <sub>2</sub> O <sub>3</sub> 2.4% Fe/ $\alpha$ -Al <sub>2</sub> O <sub>3</sub>	-	1% CH <sub>4</sub> in air	44 47	-	Active at T>400°C. The E <sub>act</sub> seem wrong; from figure E <sub>act</sub> ≈65 kJ/mol	54

Catalyst	Catalyst Mass, g	Feed (STP)	E <sub>act</sub> kJ/mol	Rate at 450°C $\mu\text{mol}/(\text{g cat-s})$	Comments	Ref
Co <sub>3</sub> O <sub>4</sub>	4 to 6 g	0.66 cm <sup>3</sup> pulse of CH <sub>4</sub> in pure O <sub>2</sub>	69.0	0.30	Rate calculated for	2
8.9% Co <sub>3</sub> O <sub>4</sub> /clay			92.1	0.34	1% CH <sub>4</sub> in O <sub>2</sub>	
9.8%Co <sub>2</sub> O <sub>4</sub> /Al <sub>2</sub> O <sub>3</sub>			87.4	0.07	CH <sub>4</sub> concentration	
			94.6	0.05	=0.169 $\mu\text{mol}/\text{cm}^3$ .	
			102.1	0.04		
4.5%Cr <sub>2</sub> O <sub>3</sub> /Al <sub>2</sub> O <sub>3</sub>			92.5	0.01	A pulse reactor was	
			120.9	0.002	used for these studies.	
20%Mn <sub>2</sub> O <sub>3</sub> /Al <sub>2</sub> O <sub>3</sub>			129.3	0.001		
			100.0	0.001		
8.8%CuO/Al <sub>2</sub> O <sub>3</sub>			131.0	0.000		
			150.2	0.000		
1.5%CeO <sub>2</sub> /Al <sub>2</sub> O <sub>3</sub>			135.6	0.000		
4.1%Fe <sub>2</sub> O <sub>3</sub> /Al <sub>2</sub> O <sub>3</sub>						
16%V <sub>2</sub> O <sub>5</sub> /Al <sub>2</sub> O <sub>3</sub>						
4.8%NiO/Al <sub>2</sub> O <sub>3</sub>						
4.8%MoO <sub>3</sub> /Al <sub>2</sub> O <sub>3</sub>						
13.2%TiO <sub>2</sub> /Al <sub>2</sub> O <sub>3</sub>						

Complex oxides with the perovskite structure and overall chemical formula  $ABO_3$  have also received attention as methane oxidation catalysts in recent years (48). These catalysts have usually been examined as candidates for high temperature, flameless oxidation. Results for this type of catalysts are summarized in Table 2-3. None of the catalysts is as active as noble metal catalysts, but the activation energies for some of the catalysts are quite low ( $<70$  kJ/mole; see Table 2-3). It is not known whether these low activation energies are due to the intrinsic kinetics or whether mass transfer effects have resulted in low apparent activation energies. The mechanism of oxidation over the mixed oxide catalysts is different from the mechanism over noble metal catalysts; a Mars-van Krevelen mechanism is the likely mechanism over the mixed oxide catalysts (48).

None of the metal oxides was as active as palladium catalysts. However, the relatively high activities of  $Co_3O_4$  and  $CuO$  may provide some clues for preparation of bimetallic catalysts containing both a noble and a base metal. The low activation energies of some of the mixed metal oxide may also provide some guidance for development of low-temperature methane oxidation catalysts.

Table 2-3 Complex metal oxide catalysts for complete oxidation of methane.

Catalyst	Mass of Cat, g	Feed (Rate at STP)	E <sub>act</sub> kJ/mol	Rate at 450°C $\mu\text{mol}/(\text{g cat}\cdot\text{s})$	Comments	Ref
LaFe <sub>2</sub> O <sub>3</sub> LaMnO <sub>3</sub> La <sub>5</sub> Sr <sub>5</sub> MnO <sub>3</sub> La <sub>5</sub> Sr <sub>5</sub> MnO <sub>3</sub> LaNiO <sub>3</sub>	0.04g for all cases	3.3 cm <sup>3</sup> /s 1.5%CH <sub>4</sub> 4.2 % O <sub>2</sub> 94.3%He	75 73 60 70 79	0.67 2.20 0.84 2.58 9.74	Rates at 450°C were calculated assuming a surface area of 25 m <sup>2</sup> /g. The reaction mechanism is of the Mars-Van Krevlen type. The order w.r.t. to CH <sub>4</sub> and CO <sub>2</sub> are 1.0 and 0.5	48
La <sub>1-x</sub> Sr <sub>x</sub> CoO <sub>3</sub>	1.0 g	5.0 cm <sup>3</sup> /s, 1% CH <sub>4</sub> in air	-	0.89	Rate at x=0.2 (max activity). Surface area of catalyst for x=0.2 was 4.0 m <sup>2</sup> /g	55
Na-, K-, Rb- and Cs- $\beta$ - gallates	1.0 g	5.0 cm <sup>3</sup> /s 1% CH <sub>4</sub> in air	-	-	All the gallates requires T>570°C for 10% conversion of CH <sub>4</sub> . The activity of the gallates is less than the activity of Ga <sub>2</sub> O <sub>3</sub> (see Table 2.1.1)	53
ZnCrO <sub>4</sub> CuCrO <sub>4</sub> PdCrO <sub>4</sub> CoAl <sub>2</sub> O <sub>4</sub> /Al <sub>2</sub> O <sub>3</sub> Co-ThO <sub>2</sub> - MgO- kieselguhr	3 to 23 g	0.66 cm <sup>3</sup> pulse of CH <sub>4</sub> in pure O <sub>2</sub>	64.4 96.7 104.6 91.6 80.3	0.03 0.002 0.000 0.001 0.03	Rate calculated for 1% CH <sub>4</sub> in O <sub>2</sub> . CH <sub>4</sub> concentration = 0.169 $\mu\text{mol}/\text{cm}^3$ . A pulse reactor was used for these studies.	2

## 2.3 Typical Operating Conditions

Most of the results reviewed above were obtained in fixed bed reactors operated at constant feed rates and constant temperature. All of the studies, with the exception of one (3), were done at atmospheric pressure. The  $\text{O}_2\text{:CH}_4$  ratio, for the  $\text{O}_2$ -rich oxidation studies reported above, varied from 2.2 to 10; in one study  $\text{CH}_4$  pulses were injected into pure  $\text{O}_2$  (2). The most commonly used  $\text{O}_2\text{:CH}_4$  ratio is 4.0. The most common  $\text{CH}_4$  content was 1 mol% and the inert diluent was usually helium or nitrogen. The amounts of catalysts used varied greatly; for the supported Pd catalyst, the amount varied from 0.05 g (3) to 6.5 g (2) and the metal loadings of the catalysts varied from 0.46 to 15 mass% Pd.

Most investigators did not dilute the catalyst in the fixed bed, but Farrauto *et al.* (7) diluted the catalyst bed with  $\alpha$ -alumina to improve temperature control. The catalyst bed temperature was usually measured by a thermocouple located in the catalyst bed (*e.g.* 5,7,9,10). It is usually claimed that mass and energy transfer effects did not influence the rate of methane oxidation.

Product analysis was usually done by on-line gas chromatography. Various other techniques, such as X-ray diffraction (5,8,10), electron microscopy (6,8,20), temperature programmed oxidation (6,8) and infrared spectroscopy (9), were used to obtain information about the catalyst structure and the reaction mechanism.

## **CHAPTER 3**

### **EQUIPMENT and PROCEDURES**

In this chapter, the methods of preparation and characterization of a series supported metal catalysts are presented. The equipment and operating conditions used to determine the catalytic activity of these catalysts for the complete oxidation of methane are also described.

#### **3.1 Description of Catalysts**

The catalytic activity of 11 supported metal catalysts was investigated in this study. The 11 catalysts are described in Table 3-1. The catalysts were prepared using various metal precursors and supports. All catalysts studied were prepared by using the impregnation method (catalyst supports were impregnated with solutions of the metal precursor). Two palladium salts, one iron salt and one copper precursor salt were used to prepare metal precursor solutions for impregnation. The metal precursors used were:  $\text{PdCl}_2$ ,  $\text{Pd}(\text{C}_5\text{H}_7\text{O}_2)_2\text{O}_2$ ,  $\text{FeCl}_3 \cdot 6\text{H}_2\text{O}$  and  $\text{Cu}(\text{NO}_3)_2 \cdot 3\text{H}_2\text{O}$ . In this study, three oxides were used as catalyst support. They were silica ( $\text{SiO}_2$ ), magnesia ( $\text{MgO}$ ), and alumina ( $\text{Al}_2\text{O}_3$ ). The three oxide supports were prepared by R. Fiedorow. The alumina was prepared from aluminum isopropoxide followed by calcination of the resulting boehmite at  $500^\circ\text{C}$  for 5 hours (Fiedorow and Wanke, 1997). The silica was prepared by hydrolysis of tetraethyl ortho-silicate in ethanol at a pH of about 9, *i.e.* similar to that

described by Lopez *et al.* (1991). The washed and dried silica precipitate was calcined at 500°C for 5 hours. The magnesia was prepared by calcination at 600°C for 5 hours of basic magnesium carbonate,  $(\text{MgCO}_3)_4 \cdot \text{Mg}(\text{OH})_2 \cdot 5\text{H}_2\text{O}$ , obtained from Aldrich Chemicals.

**Table 3-1 Description of Catalysts** (*All metal contents are in mass %*)

Catalyst Name	Catalyst	Palladium Precursor	Solvent
RF34	5% Pd/ $\text{Al}_2\text{O}_3$	$\text{PdCl}_2$	Water
RF30	5% Pd/ $\text{Al}_2\text{O}_3$	$\text{Pd}(\text{C}_5\text{H}_7\text{O}_2)_2$	Chloroform
YW114	5% Pd/ $\text{SiO}_2$	$\text{PdCl}_2$	Water
RF35	5% Pd/ $\text{SiO}_2$	$\text{Pd}(\text{C}_5\text{H}_7\text{O}_2)_2$	Chloroform
RF16	5% Pd/MgO	$\text{PdCl}_2$	Water
YW102	(5% Pd + 5% Fe)/ $\text{Al}_2\text{O}_3$	$\text{PdCl}_2$ , $\text{FeCl}_3 \cdot 6\text{H}_2\text{O}$	Water
YW103	(5% Pd+0.5% Fe)/ $\text{Al}_2\text{O}_3$	$\text{PdCl}_2$ , $\text{FeCl}_3 \cdot 6\text{H}_2\text{O}$	Water
YW104	5% Fe/ $\text{Al}_2\text{O}_3$	$\text{FeCl}_3 \cdot 6\text{H}_2\text{O}$	Water
YW107	(5% Pd+5% Fe)/ $\text{SiO}_2$	$\text{PdCl}_2$ , $\text{FeCl}_3 \cdot 6\text{H}_2\text{O}$	Water
YW112	(5% Pd+0.5% Fe)/ $\text{SiO}_2$	$\text{PdCl}_2$ , $\text{FeCl}_3 \cdot 6\text{H}_2\text{O}$	Water
YW113	(5% Pd+0.1% Cu)/ $\text{SiO}_2$	$\text{PdCl}_2$ , $\text{Cu}(\text{NO}_3)_2 \cdot 3\text{H}_2\text{O}$	Water

Before impregnation, all supports were ground into fine powders in a ceramic mortar, and measured amount of supports were wetted with solvent (water or chloroform) before adding the desired amount of solution containing the metal precursor salt. Usually 5 gram samples of support were impregnated with sufficient metal precursor to obtain catalysts with the desired metal content (usually 5 mass % metal).

For all supported palladium catalysts studied, the palladium loading was 5 mass %. The palladium precursor salts used were  $\text{PdCl}_2$  and the  $\text{Pd}(\text{C}_5\text{H}_7\text{O}_2)\text{O}_2$ . For supported palladium catalysts prepared from the chloride precursor the impregnation solutions were prepared by dissolving  $\text{PdCl}_2$  in deionised water. A small amount of hydrochloric acid (usually several drops) was added to facilitate the dissolution of palladium(II) chloride. For supported palladium catalysts prepared from the organic palladium precursor, the catalysts were prepared by impregnation of carrier with chloroform solution containing palladium acetylacetonate ( $\text{Pd}(\text{C}_5\text{H}_7\text{O}_2)_2$ ). In addition to the supported palladium catalysts, 5 bimetallic catalysts were also prepared in this study in order to investigate the effect of the addition of other metal (*e.g.* Cu, Fe) on the catalytic properties of supported palladium catalysts. Catalysts, containing Pd (5%) + Cu (0.1%) or Pd (5%)+Fe (0.5 to 5%) were prepared by co-impregnation of  $\text{SiO}_2$  or  $\text{Al}_2\text{O}_3$  with aqueous solutions of palladium and copper or iron precursors. The second metal precursor salts (*e.g.*  $\text{FeCl}_3 \cdot 6\text{H}_2\text{O}$  or  $\text{Cu}(\text{NO}_3)_2 \cdot 3\text{H}_2\text{O}$ ) were dissolved in deionised water before co-impregnation with palladium precursors. Monometallic Fe/ $\text{Al}_2\text{O}_3$  catalyst was prepared by impregnating the alumina or silica supports with the aqueous iron precursor solution which was prepared by dissolving  $\text{FeCl}_3 \cdot 6\text{H}_2\text{O}$  salts in deionised water.

After impregnation, the beaker containing the sample of wet catalyst precursor was dried at  $80^\circ\text{C}$  by fixing the beaker on a rotating disc and heating overnight with an infrared lamp. Subsequently, the catalyst samples were then put into a oven and dried at  $110^\circ\text{C}$  overnight. After the above treatments, samples were put into a U-shaped Pyrex tube and were reduced according to the following procedure:



- flushed with nitrogen at room temperature for 30 minutes
- changed flowing gas from nitrogen to hydrogen and treated in flowing hydrogen at the following conditions:
  - heated from room temperature to 150°C in 60 minutes
  - kept at 150°C for 16 hours
  - increased temperature from 150°C to 250°C in 30 minutes
  - kept temperature at 250°C for 2 hours
  - increased temperature from 250°C to 500°C within 30 minutes
  - kept at 500°C for 1 hour
- changed flowing gas from hydrogen to nitrogen and flushed at 500°C for 1 hour
- cooled to room temperature in flowing nitrogen over a period of about 1 to 2 hours and stored catalyst in air until use.

The above treatment procedure results in what is referred to as freshly reduced catalysts.

### 3.2 Characterization Methods and Instruments

In this study, three methods of catalyst characterization were used to obtain the information about the physical and chemical properties of the 11 supported metal catalyst. X-ray diffraction (XRD) measurements were used to determine the phase of metals in the catalyst. Hydrogen chemisorption measurements were used to determine the metal dispersion of catalysts, and low temperature nitrogen adsorption measurements (BET) were used to obtain the total surface area of catalysts.

X-ray diffraction measurements are frequently used to determine the state and crystal size of metals in catalysts (*e.g.* 5, 8, 10, 57). In this study, a Philips x-ray diffractometer system equipped with a graphite monochromator and a Cu tube was used to obtain the XRD patterns. Catalyst samples were ground into fine powers, and the powders were compacted into the cylindrical cavity of a stainless steel XRD sample holder. XRD patterns were obtained in the step scan mode with steps of  $0.1^\circ 2\theta$  and counting for 40 seconds per step for a range of angles scanned from  $10$  to  $90^\circ 2\theta$ , and with steps of  $0.02^\circ 2\theta$  and counting for 100 seconds per step for a range of angles of  $35$  to  $55^\circ 2\theta$ . The  $35$  to  $55^\circ 2\theta$  range was chosen since the intense Pd lines are located within this range. The goniometer angle and the digital output of the proportional x-ray detector (*i.e.* angle-intensity pairs) were sent to an on-line PC for storage and subsequent data analysis. XRD patterns were also measured for supports treated at conditions similar to the catalyst treatments.

The BET method was used to determine total surface areas of the supports and catalysts. Nitrogen was used as the adsorbate and a Coulter<sup>TM</sup> OMNISORP<sup>TM</sup> 360 analyzer was used to

measure the nitrogen adsorption isotherm (58). A value of  $0.0162 \text{ nm}^2$  was used as the cross-sectional area of a nitrogen molecule for the calculation of total surface areas of the catalyst.

An AMI-1 catalysts characterization system (manufactured by *Altamira Instruments*) was used to measure hydrogen adsorption uptakes at room temperature ( $25^\circ\text{C}$ ) on supported Pd catalysts. Before measurement, the catalyst samples were reduced in flowing hydrogen at  $500^\circ\text{C}$ . The following procedure was used to measure the hydrogen adsorption uptake.

- a small amount of sample (usually 0.3 g) was placed into the quartz U-tube

- samples were pretreated as follows:

- flushing argon at initial temperature ( $25^\circ\text{C}$ ) for 15 minutes

- changed flowing gas from argon to hydrogen

- heated from  $25^\circ\text{C}$  to  $250^\circ\text{C}$  at ramp rate of  $10^\circ\text{C}/\text{minute}$

- heated from  $250^\circ\text{C}$  to  $500^\circ\text{C}$  at ramp rate of  $5^\circ\text{C}/\text{minute}$

- kept at  $500^\circ\text{C}$  for 60 minutes

- changed flowing gas from hydrogen to argon

- kept at  $500^\circ\text{C}$  for 120 minutes

- cooled temperature from  $500^\circ\text{C}$  to room temperature ( $25^\circ\text{C}$ )

- injected 15 hydrogen pulses of each containing  $62 \mu\text{mol}$  of  $\text{H}_2$

The flow rate and temperature used during the pretreatment are described in Table 3-2.

Table 3-2. Sample Pretreatment and Measurement of Hydrogen Adsorption

	Flow Rate (ml/minute)	Initial Temp. (°C)	Ramp Rate (°C/per min)	End Temp. (°C)	Hold Time (minute)
Flushed by argon	30	25	0	25	15
Reduced by hydrogen (I)	30	25	10	250	0
Reduced by hydrogen (II)	30	250	5	500	60
Flushed by argon	30	500	0	500	120
Cooled by argon	30	500	-	25	-
pulsed adsorption with hydrogen at 25°C					

### 3.3 Experimental Equipment

In this study, a fixed-bed reactor system was designed and constructed for the measurement of the rate of catalytic methane oxidation. The reactor, shown in Figure 3-1, consists of a 316 stainless steel tube with a length of 280 mm and an inside diameter of 4.6 mm. This tube was fixed tightly inside a 316 stainless steel cylindrical block with a diameter of 32 mm and a length of 152 mm. The stainless cylinder served as a good conducting material of large thermal mass to achieve relatively constant temperature along the wall of the reactor. During reaction, the cylinder and reactor are fixed tightly inside an oven as shown in Figure 3-2. Both ends of the oven were covered by layers of insulation materials in order to prevent heat loss from the two ends of the reactor. A small porous Vycor disc was manufactured in the glassblower shop of the Chemistry Department at University of Alberta and supported by a Vycor tube (about 125 mm in length) at the middle of the reactor. A desired amount of catalyst powder (usually 0.10 g) was placed on the Vycor disc inside the reactor. Layers of quartz wool were placed at the top and

bottom of the catalyst bed to prevent that catalyst powder from leaving the reactor. Two type-K thermocouples were used in the reaction system. Thermocouple A, mounted inside the stainless cylinder, was used to control oven temperature, and Thermocouple B was placed in the middle of catalyst bed inside the reactor. The outputs from Thermocouple A and B were recorded by a strip chart millivolt recorder. Figure 3-3 shows the measured temperatures of the oven and inside the reactor when helium flowed through the reactor. The results in Figure 3-3 show that in the absence of the reactants, the temperatures inside and outside the reactor are equal.

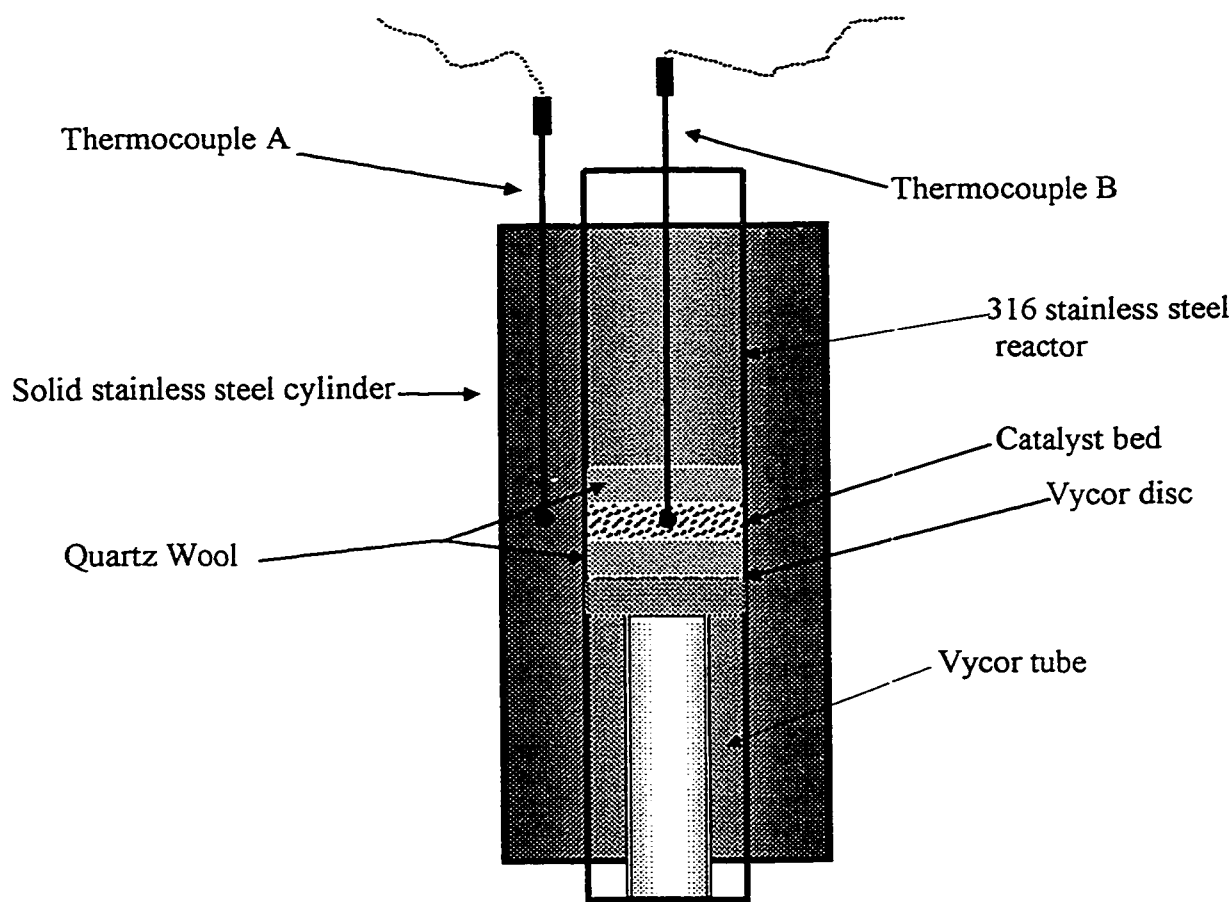


Figure 3-1 Schematic Diagram of Reactor

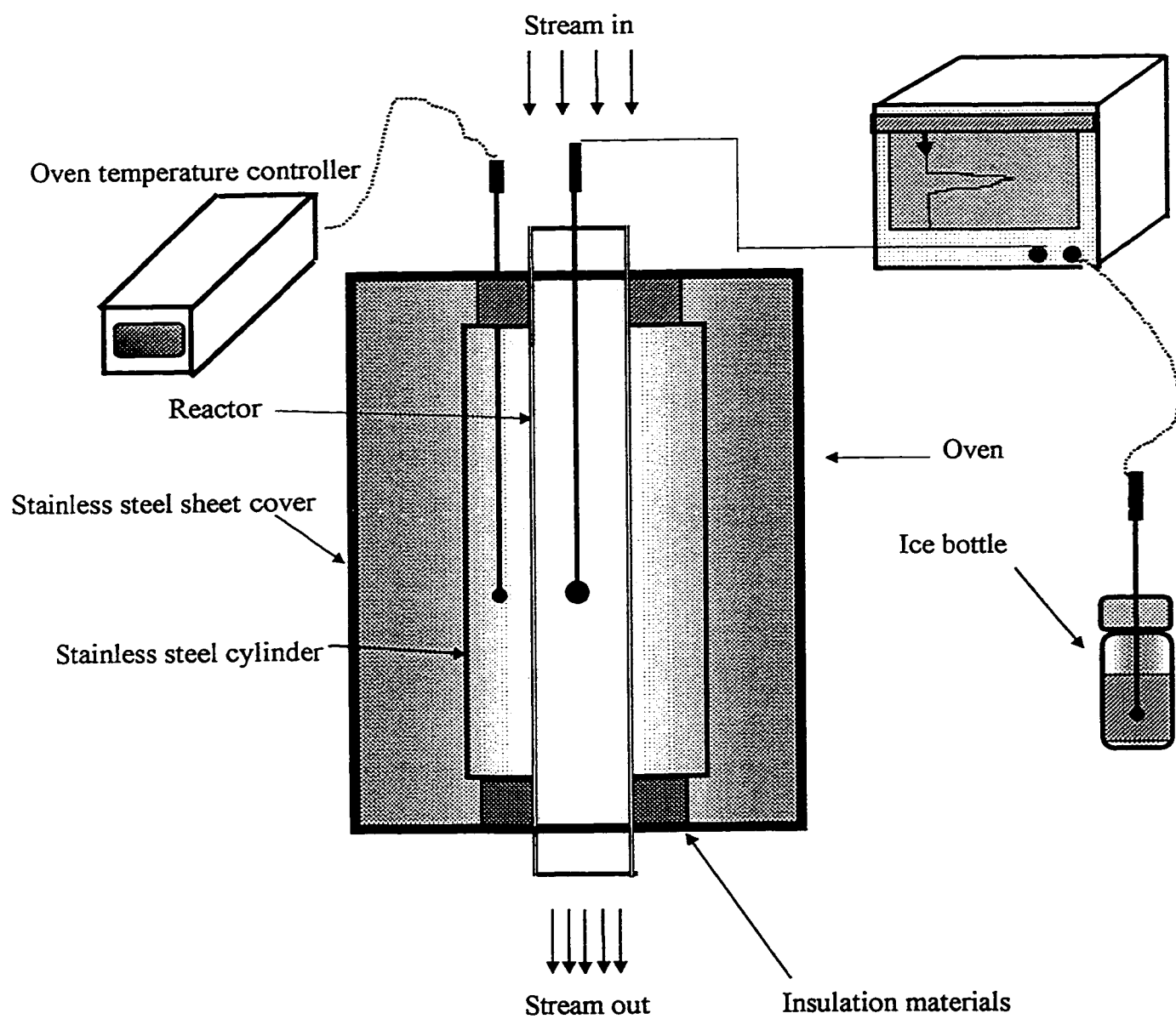


Figure 3-2 Schematic Diagram of Reactor and Oven

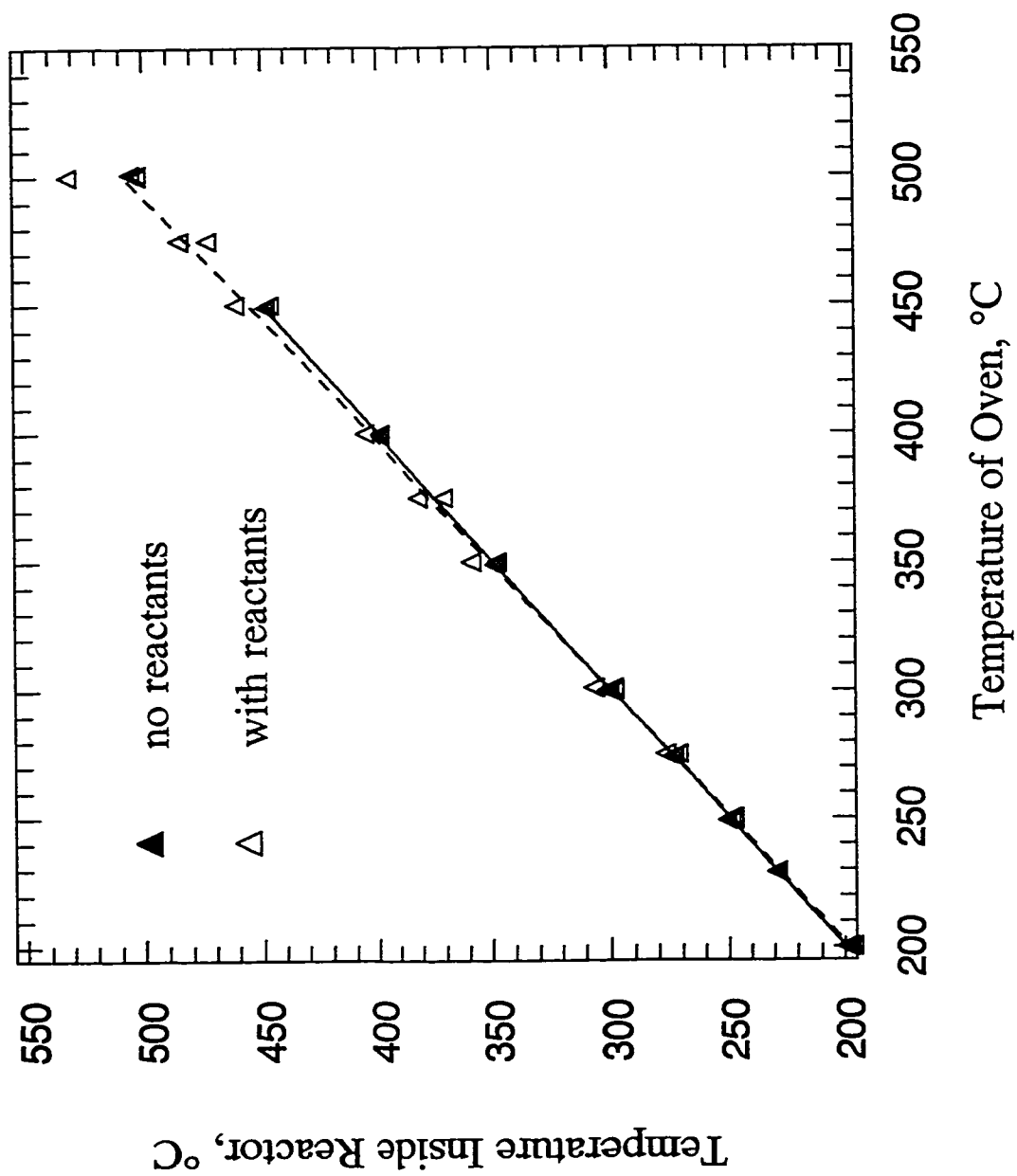


Figure 3-3. Measured temperature of the oven and inside the reactor

There is some difference between the measured temperatures of the oven and inside the reactor in the presence of the reactants especially at relatively high reaction temperature (500°C) when the conversion of methane is relatively high. Therefore, in the following chapters, the temperatures in our experimental results all refer to the temperature inside the reactor. Reactants or helium were fed to the top of reactor and the products leaving the reactor flowed through a gas sample valve of a gas chromatograph (HP5830A).

A schematic diagram of the complete reaction system used in this study is shown in Fig. 3-4. The reactant mixture, which usually contains 0.965 mol% methane, 3.96mol% oxygen in helium, flowed through a three-way flow valve and could be directed to flow downward through the reactor or it could bypass the reactor for analysis by the GC. The flow rate of reacted stream was controlled by a Matheson Mass Flow Controller (Modular Dyna-Blender Model 8250).

The pressure inside the reactor is controlled by a needle valve. Reaction pressure was measured by a pressure gauge. The product streams from the reactor or the by-pass feed was routed to a multiport valve which directed the stream to the vent or the GC. The composition of effluents (reactants or reactant products) were analyzed using the HP 5830A gas chromatography (GC) using a (12 in length, 1/8 in. diameter) carbosieve column maintained at 220°C. The operating conditions of the GC are listed in Table 3-3. The GC was calibrated by standard gas (premixed reactants) before each run. The flow rate of effluents was measured by bubble flow meters. Two types of bubble flow meters were used to measure different ranges of flow rate.



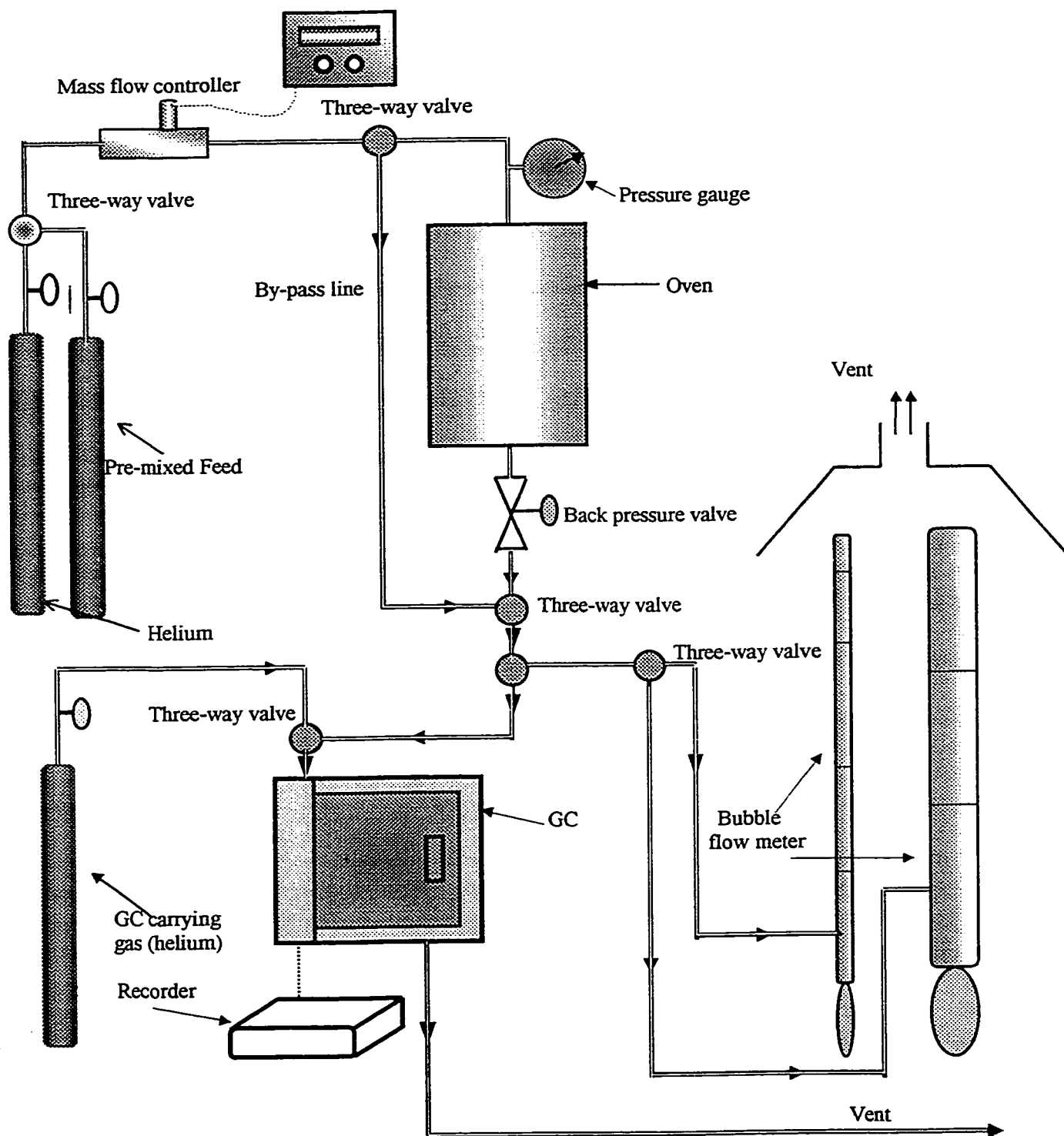


Figure 3-4 Schematic Diagram of Reactor System

Table 3-3. Operating Conditions of Gas Chromatograph

Flow Rate of Helium, (STP)ml/s	0.50
Detector Temperature, °C	260
Detector Type	TCD
Oven Temperature, °C	400
Column Temperature, °C	220

### 3.4 Catalytic Activity Measurements—Operating Conditions

Analyzed gas mixture containing CH<sub>4</sub>, O<sub>2</sub> and He were purchased from Medigas and used as feeds in the present study. Methane contents of 0.2 to 1.0 mol% and oxygen contents of 0.9 to 4.0 mol% were used. Oxygen was always in stoichiometric excess, and helium was the balance gas. A gas mixture containing 0.965 mol% methane and 3.96 mol% oxygen in helium was used for most experiments.

The activities of the catalysts after various treatments were compared using a reactant flow rate of 2.1 mL/s (82  $\mu$ mol/s) at a reactor pressure of ~93 kPa. However, flow rates of 0.5 to 250 mL/s (19.5 to 960  $\mu$ mol/s) and pressure up to 400 kPa were investigated. Reaction temperature of 150 to 600°C were studied. Specific experimental details will be given in the results section.

### 3.5. Experimental Procedures

The following three kinds of experiments were done:

1. Determination of catalytic activities of catalysts as a function of time-on-stream
2. The effects of pretreatment temperature on catalytic activity
3. The effect of reactor pressure on methane oxidation

Runs 1 to 17 were performed to investigate the evolution of catalytic activity of supported palladium catalysts and bimetallic catalysts with time-on-stream. In this type of experiment, a freshly reduced catalyst sample (0.0962 g) was placed on the Vycor disc inside the reactor. The state of catalyst at this time is called State 1. Then, the catalyst sample was purged with helium at  $\sim 0.6$  mL/s ( $23.5 \mu\text{mol/s}$ ). Usually, the oven temperature was initially set to  $150^\circ\text{C}$ . After the temperature inside the catalyst bed was stable, the flowing stream was changed to reactant mixture containing  $\sim 1\%$  methane,  $\sim 4\%$  oxygen in helium. The activity for methane combustion at the initial temperature of  $150^\circ\text{C}$  was measured at feed rates with 0.6, 0.98, 1.6, 2.1 mL/s ( $23.5$ ,  $38.3$ ,  $62.52$ ,  $82 \mu\text{mol/s}$ ). The composition of the stream leaving the reactor was analyzed by using a four-way valve to inject a fixed amount of products into the GC.

The methane conversion was calculated according the procedures and equations described in Appendix B. As indicated in Appendix B, the accuracy of the fractional conversions was very good, i.e. the reported percentage conversions of methane are believed to be accurate to better than  $\pm 1.5\%$ .

Usually, the reaction temperature was increased at an interval of 25 or 50°C until the methane conversion reached 100% at 2.1 mL/s (82  $\mu$ mol/s). Temperature at which complete conversion of methane occurred varied from about 350°C to 600°C for various catalysts. For each temperature, at least three product analyses were done for each feed rate. The system was then kept overnight (about 12 hours) under flowing reactant mixture. The catalyst sample was then purged with helium at  $\sim$ 0.6 mL/s (23.5  $\mu$ mol/s) and cooled gradually to room temperature over about 2 hours. The state of catalysts after the above treatment is called State 2. The conversion of methane for the catalysts in State 2 was then measured at conditions similar to those used for measuring the activity of catalysts in State 1.

Runs 29 to 40 were designed to investigate the effects of pretreatment temperature on the activity of 5% Pd/Al<sub>2</sub>O<sub>3</sub>. Before Runs 29, 31, 33, 35, 37, 39, the Pd dispersions of RF34 catalyst samples, which had been reduced in flowing hydrogen at 500°C, were measured by hydrogen adsorption at room temperature. Details about the Pd dispersion calculation over supported Pd catalysts are given in Appendix B. X-ray diffraction measurements were used to determine the state of Pd in catalyst after the hydrogen adsorption. About 0.1 g of the above freshly reduced catalyst sample was placed on the Vycor disc inside the reactor and the catalyst bed was purged by helium at 2.1 mL/s (82  $\mu$ mol/s). The oven temperature was set at various temperature (350°C in Run 29, 400°C in Run 31 and 37, 375°C in Run 39, 450°C in Run 33, 500°C in Run 35). After the temperatures became stable, the reactant mixture at 2.1 mL/s was fed to the reactor and the composition of effluent was analyzed repeatedly for several hours by GC. When the methane conversion became constant, the catalyst sample was purged by helium at  $\sim$ 0.6 mL/s (23.5  $\mu$ mol/s) and gradually cooled to room temperature over 2 to 4 hours. Runs 30, 32, 34, 36, 38, 40

were performed separately to investigate the activities of catalyst RF34 samples after the above treatments. X-ray diffraction measurements were used to determine the state of Pd in catalyst after Runs 30, 32, 36, 38 and 40. The oxidized samples were reduced by hydrogen at 500°C before the hydrogen adsorption measurements at room temperature (25°C). Then, the X-ray diffraction measurements were conducted on the used and reduced samples to determine the state of Pd in catalyst after Runs 30, 32, 36, 38 and 40.

Runs 18 to 21 and Run 43 were done to determine the effects of reactant composition, temperature and total pressure on methane conversion over alumina supported catalyst RF30 and RF34. Feed containing 0.23% methane and 1.96% oxygen in helium was used in addition to the usual feed (0.965% methane and 3.96% oxygen in helium). Total pressure was varied from 93 to 410 kPa.

## **CHAPTER 4**

### **EXPERIMENTAL RESULTS AND DISCUSSION**

The results of methane oxidation experiments over the various supported catalyst described in Chapter 3 are summarized and discussed in this chapter. Detailed descriptions for each run are presented in Appendix A

#### **4.1 Effects of Pretreatment Activities of Pd/Al<sub>2</sub>O<sub>3</sub>**

The initial experiments (Runs 1, 2, and 3) were done to determine the effect of treatment conditions on activities of Pd/Al<sub>2</sub>O<sub>3</sub>. Additional experiments were done later (Run 29 to 40) to further investigate the effect of pretreatment conditions on activities. In Figure 4-1, the methane conversion is shown as a function of temperature over catalyst RF34. The same catalyst change was used for Runs 1 to 3, starting with a freshly reduced catalyst (State1) at the beginning of Run 1. During Run 1, the temperature was increased gradually from 150 to 475°C and at each temperature the methane conversion was measured at various feed rates (see Appendix A).

The methane conversions for two different feed rates (23.5 and 82 μmol/s) are shown in Fig 4-1. For RF34 in State 1, methane conversion became appreciable only at temperature ≥400°C (Run 1). At temperature ≥ 425°C, the activities increase rapidly; at 475°C the methane conversion was 100%.

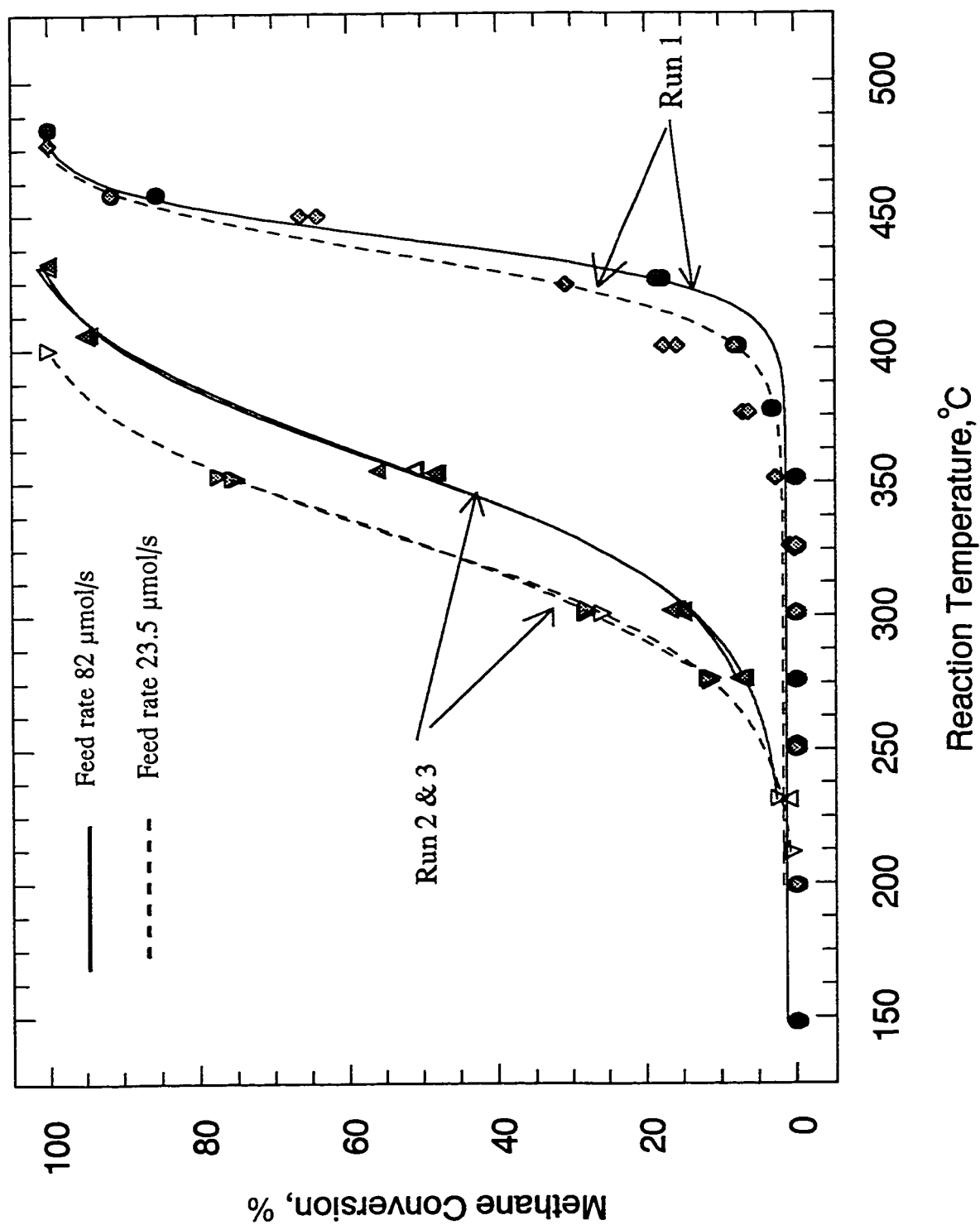


Figure 4-1. Methane conversion as a function of temperature during activation (State 1) and after activation (State 2) for catalyst RF34 at various feed rates (Feed: 0.965% methane, 3.96% oxygen in helium)

After 100% methane conversion was achieved at 475°C, the system was maintained overnight (about 12 hours) under following reactant mixture with a feed rate of about 0.6 mL/s (23.5  $\mu\text{mol/s}$ ). The reactor was then purged with helium and cooled gradually to room temperature over about 2 to 3 hours. The state of catalyst after such treatment as Run 1 is called State 2.

The methane conversion of RF34 in State 2 was measured at conditions similar to those used for Run 1. The activities for methane conversion of RF34 in State 2 is also shown in Fig 4-1. RF34 catalyst had a much higher activity in State 2 than in State 1. Methane conversion of about 5% to 10% were obtained at 275°C, similar conversion in State 1 required temperature 375 to 400°C. Methane conversion of ~100% was obtained at around 375°C in State 2 compared with 475°C in State 1.

After Run 2, the reactor was cooled to 275°C and was maintained at 275°C for about 318 hours at different reactant flow rates. Then, the temperature was increased to 350°C then decreased to 275°C. The reactor was maintained at 275°C for an additional 110 hours at a feed rate of 0.6 mL/s (23.5  $\mu\text{mol/s}$ ). Run 3 was conducted after the above treatment using the same conditions as Run 2. The conversion of methane was measured at different reaction temperatures during Run 3. The methane conversions for Run 3 as a function of temperature are also shown in Fig 4-1. The methane conversion values for Run 2 and Run 3 shown in solid and open triangles for Run 2 and 3 respectively show that no further increase or decrease in activity occurred for RF34 after aging in reactants for another period of around 550 hours after the end of Run 2.



Fig. 4-2 shows the stability of catalyst RF34 in Runs 2 and 3. These results show that the catalytic activity of catalyst RF34 is very stable for a long time at 275°C at various feed rates after aging with reactants overnight at 475°C. This indicates that the active sites on the PdO surface which were formed during activation at high temperature are very stable at low temperature.

The initial observations for methane combustion over RF34 are in agreement with the work of Briot and Primet (6). Both studies observed the dramatic increase in the activity of Pd/Al<sub>2</sub>O<sub>3</sub> especially at low temperature after exposure to reactants at high temperatures. A light-off temperature at around 400°C in State 1 was observed in both investigations. Briot and Primet (6) reported the activity of Pd/Al<sub>2</sub>O<sub>3</sub> remained stable below 390°C and above 460°C in State 1 and below 340°C and above 460°C in State 2. A continuous increase in activity as a function of time in the 340-460°C interval in State 2 was also observed in Briot and Primet's work. However, in our work, the increase in activity as a function of time is just observed in State 1. The difference between our observation and that of Briot and Primet is probably due to the 600°C treatment with reactants in State 1 done by Briot and Primet. This point will be discussed latter.

It is observed that the color of the RF34 sample changed from black in State 1 to brown in State 2 after Run1 and kept its brown color during Runs 2 and 3. This change in color could be due to a change in the Pd dispersion and/or in the Pd oxidation state.

The dramatic increase in activity of methane combustion over RF34 from State 1 to State 2 can be associated with the formation of palladium oxide after aging with reactants which resulted

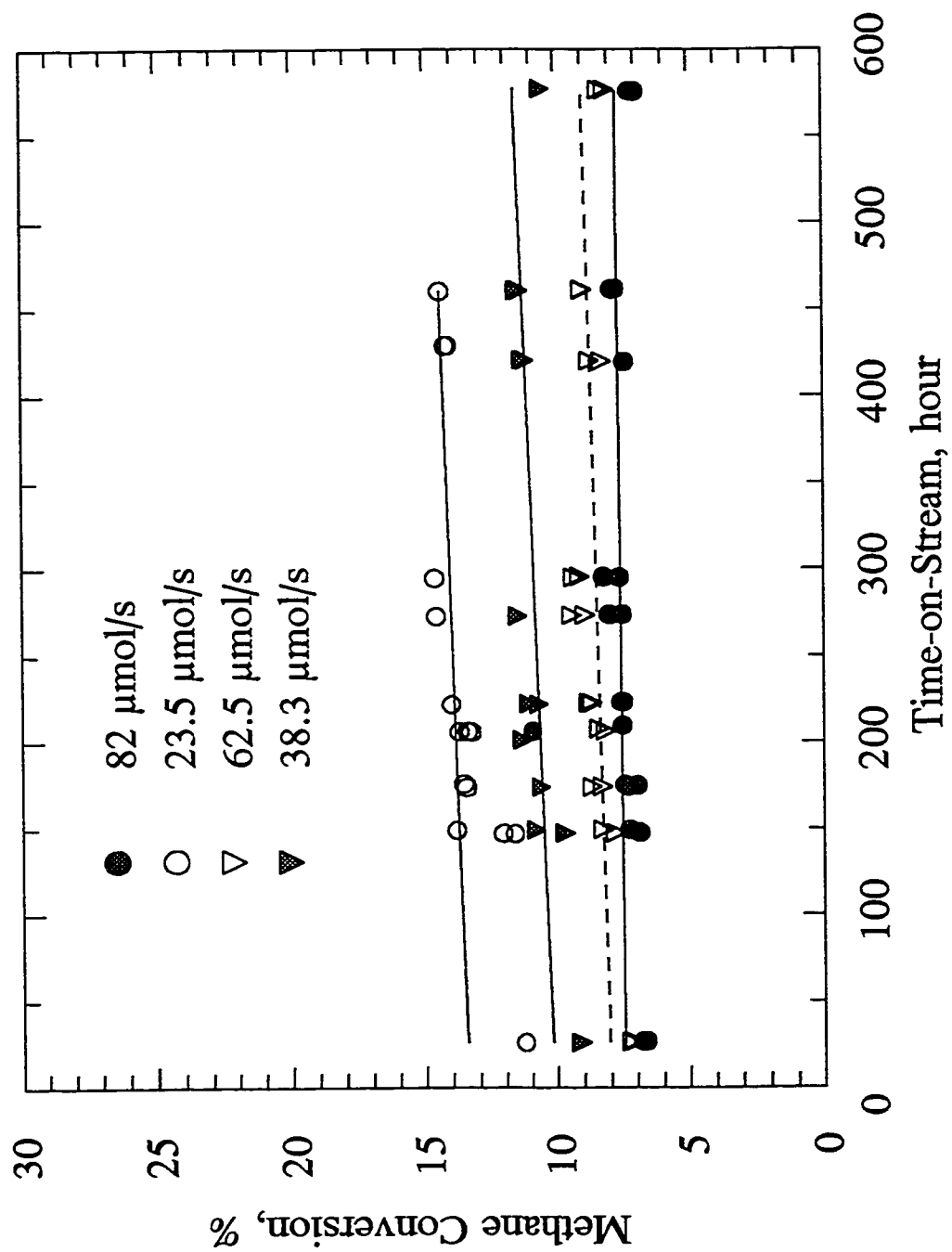


Figure 4-2. Stability of catalyst RF34 during methane combustion reaction at various feed rates  
(Feed: 0.965% Methane, 3.96% oxygen in helium)

in enhancement of the reactivity of adsorbed oxygen. It has been frequently reported in literature that palladium oxide is much more active in methane oxidation than palladium in its reduced state and the increase in catalytic activity of methane combustion over Pd/Al<sub>2</sub>O<sub>3</sub> has been attributed to the oxidation of palladium to form palladium oxides after aging with reactants (*e.g.* 5,6,7,12,13,24,25,27,31). Garbowski *et al.* (42) observed increasing methane combustion activity under both lean and rich conditions as Pd is oxidized to PdO<sub>x</sub> species. Farrauto *et al.* (7) studied the oxidation of methane over a wide temperature range (300 to 900°C) using Pd/Al<sub>2</sub>O<sub>3</sub> catalysts. They concluded that PdO is the catalytically active phase for methane combustion over Pd/Al<sub>2</sub>O<sub>3</sub> and that the observed low activity of Pd/Al<sub>2</sub>O<sub>3</sub> after heating to 900°C is due to the decomposition of the PdO to palladium metal. Sekizawa *et al.* (8), not only concluded that PdO is more active than Pd for the oxidation of methane, they also found that the dissociation of PdO at high temperature (1200°C) depends on the oxygen partial pressure of reactants. They used 1.44 mass% Pd supported on Sr<sub>0.8</sub>La<sub>0.2</sub>XAl<sub>11</sub>O<sub>19</sub> catalysts, where X=Al or Mn. Briot and Primet (6) observed that in an oxygen-rich reactants mixture, the catalytic oxidation of methane over supported Pd occurs on a Pd oxide phase, while the catalytic oxidation of methane over supported Pt occurs on a Pt phase. Recently, Farrauto *et al.* (12) conducted an extensive investigation on methane combustion over Pd catalysts with various materials of support to give more insight into the correlation between Pd phase and catalyst activity. They concluded that the methane combustion behavior over supported Pd catalysts is correlated with the PdO decomposition-reformation hysteresis. In a recent study with Pd on Al<sub>2</sub>O<sub>3</sub> and Pd/ZrO<sub>2</sub>, Ribeiro *et al.* (31) heated a series of Al<sub>2</sub>O<sub>3</sub> and ZrO<sub>2</sub> supported palladium catalysts to 1123 K. They observed that at this temperature the PdO phase on the surface of catalysts were decomposed to Pd metal phase which was not active for methane combustion.

In the current work, a dramatic increase in catalytic activity of Pd/Al<sub>2</sub>O<sub>3</sub> as a function of time was observed at temperature higher than 400°C in State 1. This phenomenon can be explained by the conclusions made by Hick *et al.* (25) in their study. They proposed that during the methane oxidation process over supported palladium catalysts, new surfaces of PdO developed because the PdO lattice obtained from metallic palladium has a porous character. For supported Pd catalyst samples, which were initially reduced, palladium crystallites were oxidized during methane oxidation and led to the formation of new active sites associated with an increase in the rate of methane oxidation. They concluded that all the oxide generated has its surface accessible to the reactants and participates in the methane oxidation.

In agreement with Hick *et al.* (25), Briot and Primet (6) also attributed the increase in the catalytic activity of Pd/Al<sub>2</sub>O<sub>3</sub> with time in the 390 – 460 °C interval in State 1 to the formation of bulk PdO during reaction. The temperature-programmed oxidation (TPO) experiments they performed on Pd/Al<sub>2</sub>O<sub>3</sub> in State 1 and State 2 showed the formation of bulk PdO at temperature above 400°C. Based on the above results, they proposed that the unstable activity of catalyst in the 390-460C is due to formation of bulk PdO at that temperature and the stable activity of Pd/Al<sub>2</sub>O<sub>3</sub> at temperature higher than 460°C in State 1 is due to the complete oxidization of Pd into bulk PdO. They concluded that the stability of the reaction rate with time in both State 1 and State 2 is correlated to the progressive formation of bulk PdO. At any given temperature, the rate of reaction remains constant with time before PdO formation and when the metal particle is fully oxidized into bulk PdO. However, it seems difficult to use their conclusion to explain the instability of the reaction rate in the 340-390°C range for in State 2 that they observed in their

study. Because the Pd should exist in the PdO phase in State 2 after aging with reactants at 600°C according to their TPO results.

However, our experimental results of catalytic measurements over RF34 during Run 2 and Run 3 can be well explained by the conclusions of Briot and Primet. The constant activity of RF34 in State 2 is probably due to the complete oxidation of the palladium which occurred during Run 1 and the overnight exposure to reactants at 475°C.

The only major difference between the experiments of Briot and Primet (6) and the current experiments is the difference in the maximum pretreatment temperature of the supported palladium catalyst. In the Briot and Primet study, the Pd/Al<sub>2</sub>O<sub>3</sub> was aged with reactants at 600°C overnight after 100% methane conversion was obtained at 480°C. In the current study, RF34 was aged with reactants at 475°C overnight when 100% methane conversion was reached at that temperature. Thus, it is tempting to ascribe the difference in the catalytic activity of Pd/Al<sub>2</sub>O<sub>3</sub> with the maximum activation temperature.

Runs 29 to 40 were performed to investigate the effect of pretreatment temperature on the activity of Pd/Al<sub>2</sub>O<sub>3</sub>. Fig 4-3 illustrates the change of methane conversion as function of time on stream at various temperatures for fresh catalysts RF34. After an induction period, the activity of catalyst RF34 increased and then reached a state in which the conversion became constant. It was observed that the evolution of catalytic activity with time over catalyst RF34 was dependent on the activation temperature. The higher the activation temperature, the shorter the period of induction.

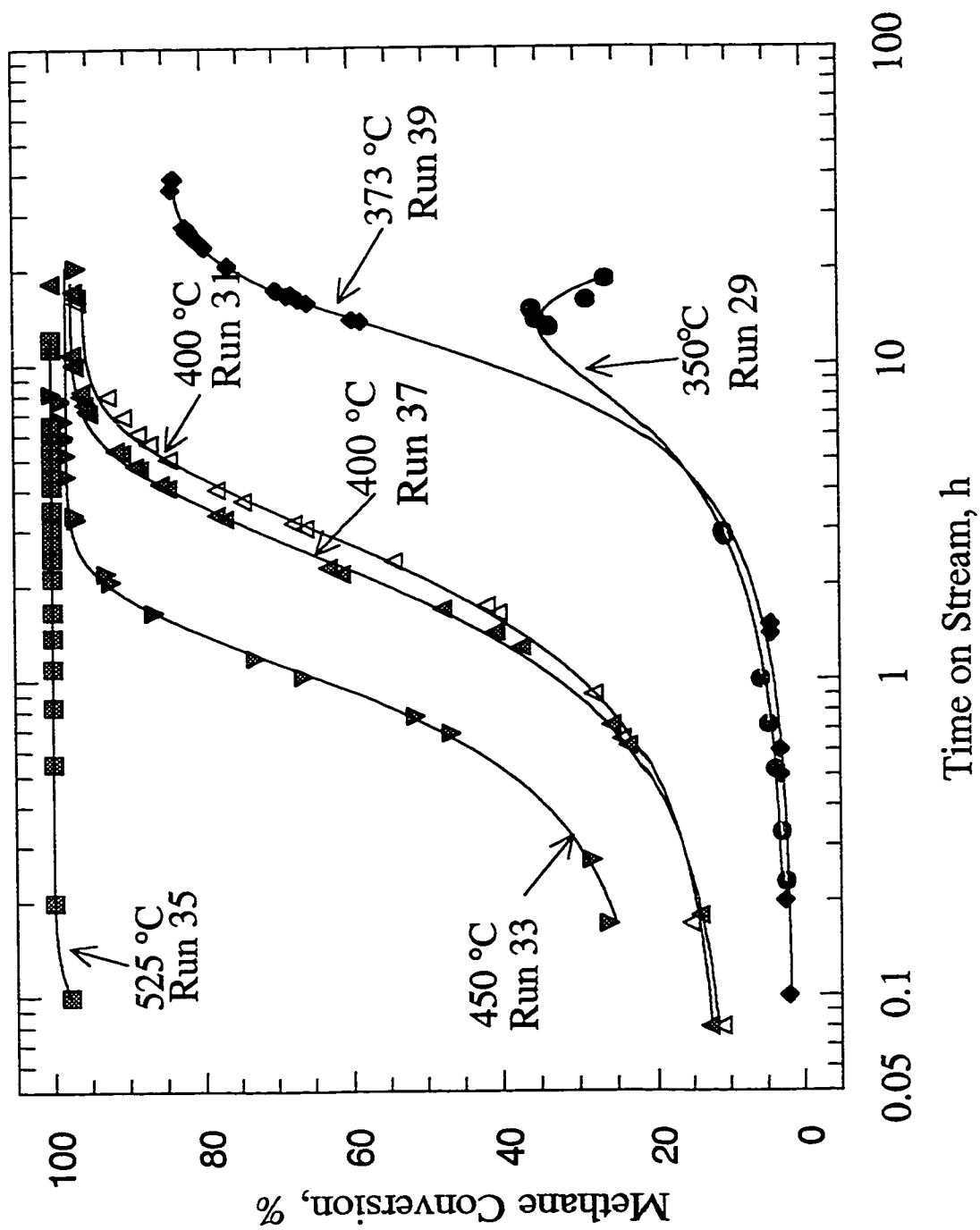


Figure 4-3. Methane conversion as a function of time on stream at various temperatures for Catalyst RF34  
(Feed: 0.965% methane; 3.96% oxygen in helium; feed rate = 2.1  $\mu\text{mol/s}$ ).

The initial activities of RF34 at various activation temperature are all much lower than their steady-state activities. The methane conversion was ~6% after aging with reactants for 1 hour at 350°C and it was ~4.0% after aging with reactants for 1 and half an hour at 375°C, while the methane conversion reach ~98% after being exposed to reactants for 6 minutes at ~500°C. The above difference in the evolution of activity with time at various activation temperature is probably due to the extent of PdO formation at the various temperature.

Briot and Primet (6) reported that bulk PdO would form at temperature ~400°C under heating in oxygen at reduced pressure ( $P_{O_2}=8$  Torr). In their TPO experiments, the formation of bulk PdO was observed at ~390°C for Pd/Al<sub>2</sub>O<sub>3</sub> in State 1 and at ~340°C for Pd/Al<sub>2</sub>O<sub>3</sub> in reduced State 2. Therefore, the initial low activities and slow evolution of activity with time of RF34 at temperature at 350 and 373°C could be due to the slow formation of bulk PdO at temperatures <400°C. During the initial period of induction, most of the Pd on the surface on the RF34 catalyst may exist in the form of Pd which resulted in very low catalytic activities. The much higher initial activity and activation rate at 500°C were probably due to the rapid formation of bulk PdO at higher activation temperature.

Methane conversion as a function of temperature after activation at various temperatures for catalyst RF34 are shown in Fig. 4-4. The steady-state activity of RF34 after activation is correlated with the activation temperature in State 1. The catalyst is more active after activation with feeds at temperatures of 373 to 400°C than after activation with feeds at lower (350°C) or higher (450°C) temperatures.

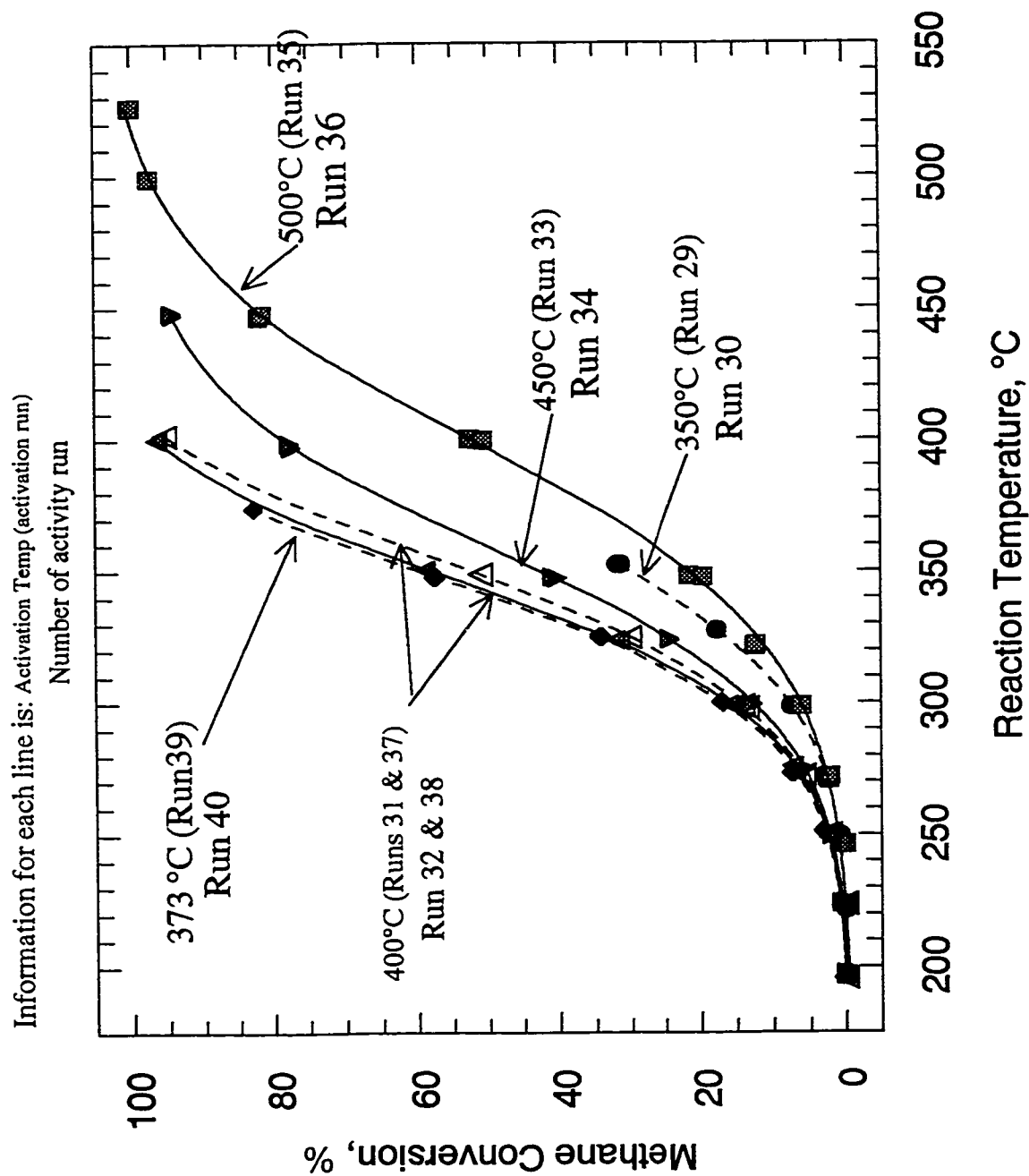


Figure 4-4. Methane conversion as a function of temperature after activation at various temperatures for Cat RF34 (State 2) (Feed: 0.965% methane, 3.96% oxygen in helium; feed rate = 82  $\mu\text{mol/s}$ )



The reasons for this effect of activation temperature on activity is not obvious. Decreases in Pd dispersion or the formation of non-porous PdO are possible causes for the decreases in activities for activation temperature greater than 400°C. The lower activities at an activation temperature of 350°C is probably due to incomplete oxidation of the Pd. Other factors, which may depend on the activation temperature, can also influence the activity of the catalysts. Some of these factors are changes in the support surface, the reconstruction of palladium surface and change in PdO particle size.

As addressed in previous chapter, the effect of pretreatment temperature on the activities of Pd/Al<sub>2</sub>O<sub>3</sub> has been also reported by other investigators. Baldwin and Burch (5) studied the effect of activation temperature over 5% Pd/Al<sub>2</sub>O<sub>3</sub> which was calcined in air for 24 hours before aging with reactants. They observed that the catalyst is more active for the methane combustion reaction after exposure to the reaction mixture at 405°C than after exposure to the reaction mixture at 373°C. Chen and Ruckenstein (30) observed that the extent of reoxidation of Pd will be greater on palladium initially oxidized at low temperature. Baldwin and Burch (24) measured the rate of methane combustion over Pd/Al<sub>2</sub>O<sub>3</sub> catalysts after being calcined in air at 400, 500, 600°C, they observed that the rate constant of methane combustion changed with calcination temperature. Fujimoto *et al.* (18,19) observed that the activity of supported palladium catalysts which are prepared by controlled decomposition of Pd precursors during catalyst preparation do not increase after activating with reactants. While the activity of the same catalysts which are prepared by uncontrolled decomposition increased with time-on-stream. They concluded that incomplete re-oxidation of Pd metal crystallites may lead to the low activity of catalyst as compared with the activity of Pd catalysts which are completed oxidized. Ribeiro *et al.* (31)

suggested that the wide variation in reaction rates reported in the literature could be attributed to the various activations used.

Briot and Primet (6) reported that the bulk PdO which was formed on large diameter palladium particles (16 nm) was much more active than the PdO which was generated on smaller diameter palladium particle (7 nm). However, they also suggested that the effect of the reconstruction of surface under reacting conditions could be a cause of the variation in activities.

## **4.2 Effects of Supports and Pd Precursors**

Experiments were done to investigate the effects of Pd precursors and supports on the activities of supported palladium catalysts (Table 4, Chapter 3 for details of catalysts). The activity of various catalysts in both State 1 (Runs 1, 4, 6, 8, 10, 41, 43) and State 2 (Runs 2, 5, 7, 9, 11, 42, 44) were measured at atmospheric pressure and a feed rate of 82  $\mu\text{mol/s}$  (Feed: 0.965% methane, 3.96% oxygen in helium).

Methane conversion as a function of temperature during activation (State 1) and after activation (State 2) for various catalysts at feed rate of 82  $\mu\text{mol/s}$  are shown in Figures 4-5 and 4-6. Activities of various catalysts at different temperatures are compared in Table 4-1. The values in Table 4-1 were interpolated from Figures 4-5 and 4-6.

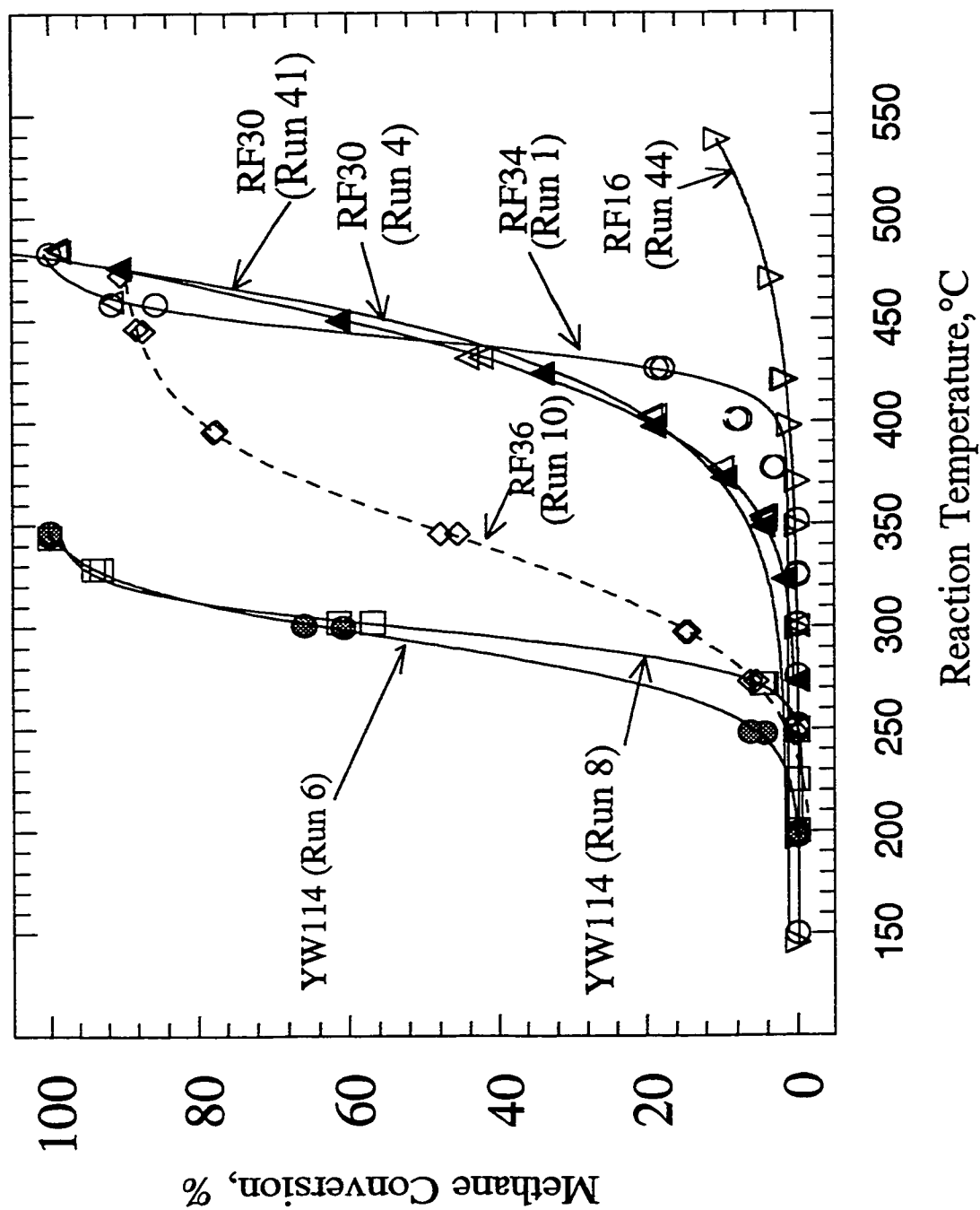


Figure 4-5. Methane conversion as a function of temperature during activation (State 1) for various catalysts at a feed rate of 82  $\mu\text{mol/s}$  (Feed: 0.965% methane, 3.96% oxygen in helium).

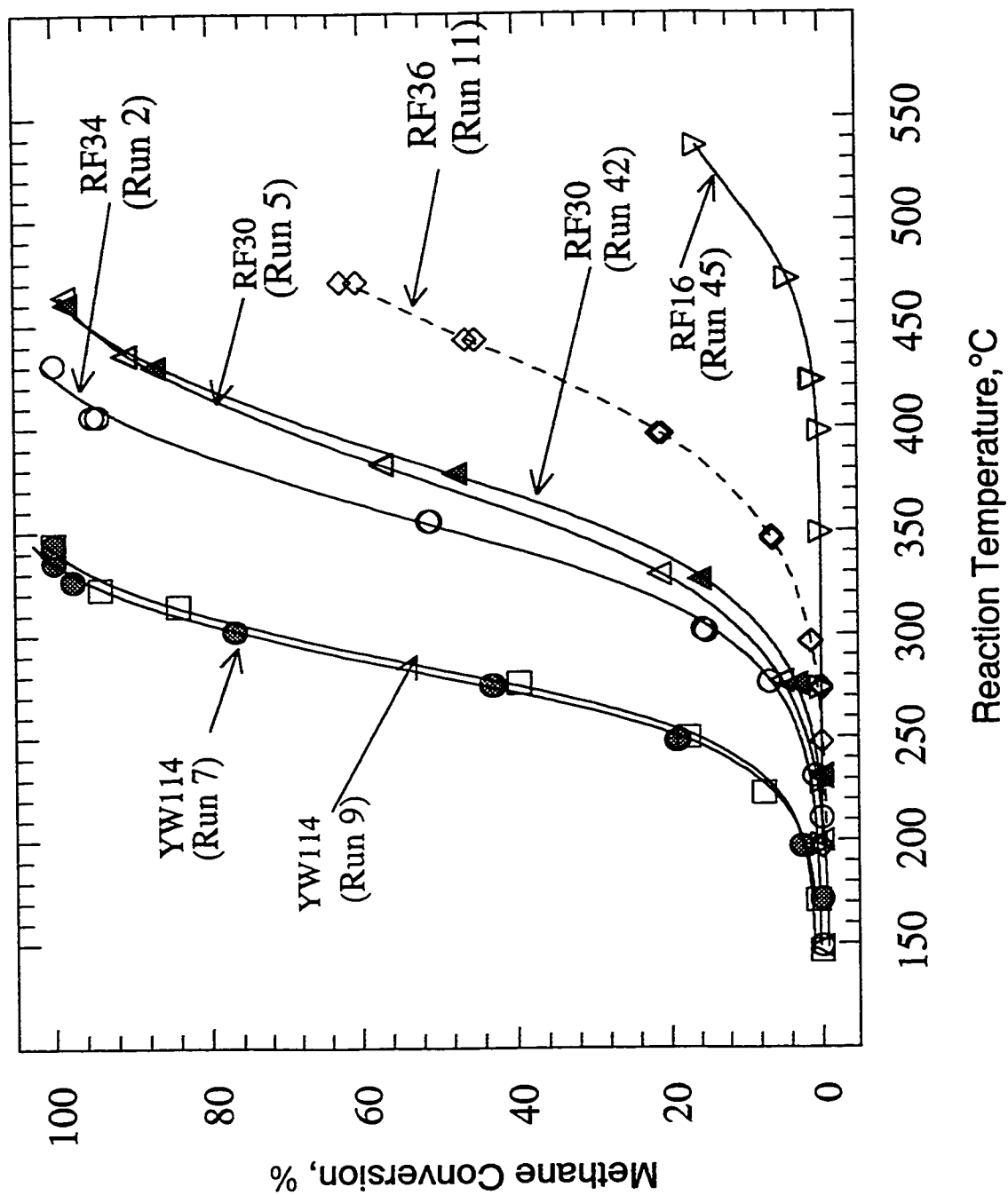


Figure 4-6. Methane conversion as a function of temperature after activation (State 2) for various catalysts at a feed rate of 82  $\mu\text{mol/s}$  (Feed: 0.965% Methane, 3.96% oxygen in helium).

Table 4-1. Comparison of activities of various catalysts.

Catalyst and Runs		Methane Conversion at Various Temperature at a Feed Rate of 82 $\mu\text{mol/s}$ , %													
		Catalyst in State 1							Catalyst in State 2						
		200°C	250°C	300°C	350°C	400°C	450°C		200°C	250°C	300°C	350°C	400°C	450°C	500°C
RF34	Runs 1 & 2	0	0	0	0	8	72		0	3	15	49	88	100	-
RF30	Runs 4 & 5	0	0	0	4	19	54		0	0	10	34	68	95	
RF30	Runs 41 & 42	0	0	0	6	19	60		0	1	7	28	65	95	-
YW114	Runs 6 & 7	0	5	64	100	-	-		3	19	73	100	-	-	-
YW114	Runs 8 & 9	0	0	59	100	-	-		3	18	70	100	-	-	-
RF36	Runs 10 & 11	0	1	15	47	78	88		0	0	1	6	21	45	-

The results in Table 4-1 show that methane conversions of supported palladium catalysts are dependent on reaction temperature, support and palladium precursor. During activation (State 1), silica-supported palladium catalysts (YW114 and RF36) show measurable activity at lower temperature than alumina- and magnesium-supported palladium catalysts. Silica-supported palladium catalyst prepared from  $\text{PdCl}_2$ , YW114, is the most active sample among all the catalysts investigated. For alumina supported Pd catalysts, the sample using organic palladium precursor (RF30) showed measurable activity at lower temperature than the sample using palladium chloride precursor (RF34). MgO supported palladium catalyst (RF16) was the least active sample among all the catalysts investigated.

After activation, catalysts RF34 and YW114, which were prepared with  $\text{PdCl}_2$ , were more active than RF30 and RF36 which were prepared from organic precursor. For catalysts with  $\text{PdCl}_2$  precursor, YW114 was more active than RF34 and RF16. The MgO-supported catalyst, RF16, also had the lowest activity in State 2. For catalysts prepared from the organic palladium precursor, RF30 was more active than RF36 after activation although RF36 was more active than RF30 in State 1.

Variations in the ratio of activity of State 2 to State 1 as a function of the reaction temperature for various catalysts at feed rate of 2.1 mL/s (82  $\mu\text{mol/s}$ ) are shown in Figure 4-7. This plot shows the effect of pretreatment on activities. It is clear that the  $\text{Al}_2\text{O}_3$  supported Pd made with  $\text{PdCl}_2$  (RF34) has largest change in activity; the activities increased by about 80%. Repeat activation studies with catalyst RF30 and YW114 show that activation process is not very reproducible; this is especially notable for catalyst YW114. The unreproducible activation

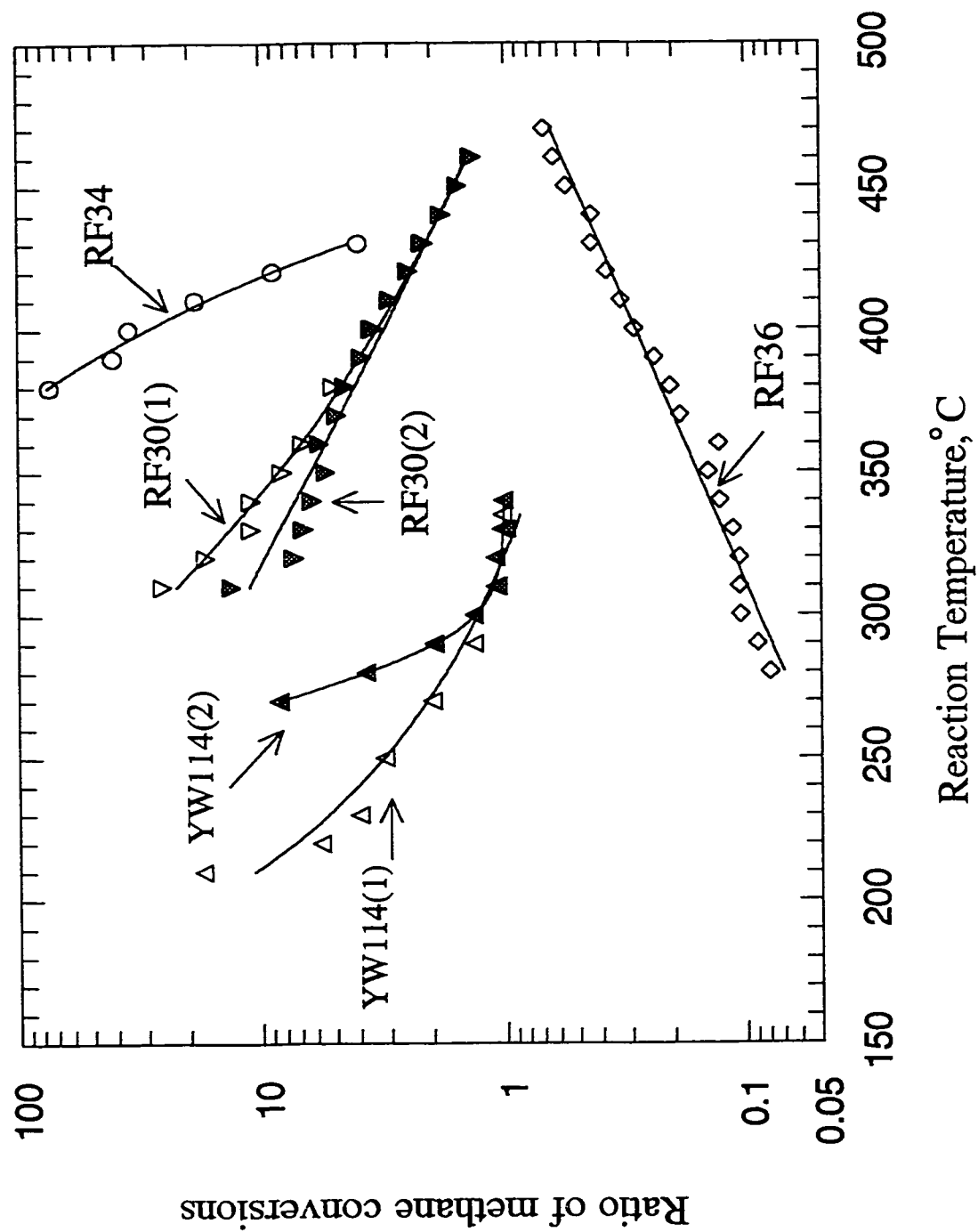


Figure 4-7. Variation of the Conversion (State 2)/Conversion (State 1) ratio as a function of the reaction temperature for various catalysts at a feed rate of 82  $\mu\text{mol/s}$  (Feed: 0.965% methane, 3.96% oxygen in helium).

results of YW114 is probably due to the rapid activation of silica-supported palladium catalyst in State 1.

The difference in  $T_{\text{start}}$  (temperature required to obtain measurable value of methane conversion at 82  $\mu\text{mol/s}$ ) between RF34 and other catalyst samples (RF30, RF36 and YW114) can be attributed to the influence of support property and the initial palladium particle size on the temperature required for bulk PdO formation. It was suggested by Briot and Primet (6) that the temperature for PdO formation appeared to be affected by the Pd particle size. They reported that the temperature for PdO formation decreased slightly from 390°C to 340°C when increasing the metal particle size diameter from 7 to 16 nm over catalyst Pd/Al<sub>2</sub>O<sub>3</sub>. The difference in  $T_{\text{start}}$  between RF34 and RF30 demonstrated in Fig 4-5 is probably due to the large difference in the initial particle sizes of the two catalysts in State 1. The H<sub>2</sub> adsorption results in Section 4.4 will show that the particle size of palladium on RF30 is about 19 times larger than that on RF34.

The difference in  $T_{\text{start}}$  between RF34 and YW114 and RF36 cannot solely be attributed to the difference in the Pd surface area. The particle Pd surface area of YW114 is about 4 times larger than that of RF30 although  $T_{\text{start}}$  for YW114 is about 100 to 130°C lower than  $T_{\text{start}}$  for RF30 (see Section 4.5 for Pd areas and crystal sizes). The support affects the catalyst activities of Pd since the support affects the oxidation of Pd to PdO (Kikuchi *et al.* (15)). Other researchers reported that the reconstruction of Pd on silica-supported catalysts palladium was much more rapid than Pd on alumina. The sintering of palladium oxide particles was more rapid in the case of silica-supported catalysts (24). Therefore, oxidation of Pd to PdO may be different for catalysts RF34 and YW114.



Nature of the Pd precursor also affected the catalytic activities. Catalysts prepared with  $\text{PdCl}_2$  were more active than catalysts prepared with  $\text{Pd}(\text{C}_5\text{H}_7\text{O}_2)_2$  in both State 1 and State 2 (compare activities of YW114 with RF36 and RF34 with RF30 shown in Fig 4-5 and 4-6). This observation differs from those of Cullis and Willatt (34), Hick *et al.* (25, 27), and Marecot *et al.* (35) who reported that chlorine from  $\text{PdCl}_2$  inhibited methane oxidation over supported palladium catalysts. The slightly lower activity of RF34 (using palladium chloride) at low temperature compared to RF30 (using organic palladium precursor) shown in Fig. 4-5 cannot just be explained as the inhibition of methane oxidation by chloride. It is probably due to the difference in the initial particle size of palladium on the surface of catalysts which may cause difference in  $T_{\text{start}}$  and the evolution of catalytic activity with time-on-stream. Baldwin and Burch (24), did not observe an effect of chlorine, their results are similar to those shown in Fig 4-5 and 4-6. Baldwin and Burch investigated the conversion of methane at 350°C as a function of time for supported Pd catalysts made from palladium chloride and palladium nitrate precursors and which were reduced in hydrogen at 400°C prior to testing. The sample made with palladium nitrate precursor had an initial Pd size of 7.6 nm and an initial activity which was higher than the activities of catalyst made with  $\text{PdCl}_2$ . The  $\text{PdCl}_2$  catalyst had an initial Pd size of 1.5 nm. However the activities of the  $\text{PdCl}_2$  catalyst became higher than that of the  $\text{Pd}(\text{NO}_3)_2$  catalyst with time-on-stream.

The catalytic activities of supported palladium catalysts shown in Figures 4-5 and 4-6 can be explained by the effects of two mechanisms during the catalyst activation. One is the formation of a active PdO phase, the other is the losing of active PdO phase by sintering and/or the forming

of inactive PdO. The higher activity of YW114 after activation is probably due to the small interaction between SiO<sub>2</sub> and Pd which favor the formation of PdO. The interaction between Al<sub>2</sub>O<sub>3</sub> and Pd is higher than that for Pd-SiO<sub>2</sub> and this retard the formation of PdO. Bulk PdO appears to form easier on the surface of silica than on alumina. The relative lower activities of RF30 and RF34 than YW114 after activation is probably due to oxidation of Pd to inactive PdO phase on alumina during activation. This is supported by the results of other researchers who reported that there are inactive PdO and active PdO phases on supported palladium catalysts (*e.g.* 3, 26, 27, 31).

The catalysts with large particle palladium size appear to lose active PdO more rapidly during use than catalysts with smaller Pd size (see Section 4.5 for Pd size information). The relatively lower activities of RF30 compared to RF34 were probably due to its dispersion which was about 9 times lower than that of RF34. The large decrease of activity for catalyst RF36 after activation was probably due to its large palladium particle size and the rapid reconstruction of Pd on the surface of the silica support. The above mechanism can also be supported by the relative slower evolution of catalytic activities over RF30 and RF36 shown in Fig 4-5. The deactivation of active PdO may be due to the reconstruction of catalyst morphology during catalyst activation. Baldwin and Burch (24) concluded that the catalytic activity of palladium catalysts were strongly influenced by the morphology of palladium particles. Some evidences for difference in oxidative (PdO structure) properties of RF36 and YW114 compared to the alumina-supported RF34 is in Section 4.5.

### 4.3 Effects of Second Metal Addition

The supported Fe catalysts have been reported in literature to have activity in the combustion of hydrocarbons such as: methane butane, and carbon monoxide (63). Iron contamination also frequently occurs during the use of catalysts in exhaust clean-up. For these reason, the addition of iron to palladium catalyst for methane combustion were investigated in this study.

In Figure 4-8, the methane conversion is shown as a function of temperature over catalyst RF34, YW102 and YW103 to demonstrate the effect of Fe addition on the catalytic activities of supported Pd catalysts in State 1. The activities of supported palladium catalysts in State 1 decreased dramatically by addition adding Fe. The activation temperature ( $T_{\text{start}}$ ) for RF34 is about 25°C lower than that for YW102 and 103. The effect of Fe addition on the activities of catalysts RF34, YW102, and YW103 in State 2 is shown in Figure 4-9. After activation, the activities of RF34 was much higher than that of YW102 and YW103. It is interesting to note that in State 1 YW103, the catalyst with low Fe content, was less active than YW102. However, in State 2, YW 102 (5% Fe + 5%Pd) was less active than YW103(0.5Fe + 5%Pd). This indicates that interaction between Fe and Pd oxides occurred during activation.

The effect of Fe content on the activities of silica supported Pd catalysts (YW114, YW107, and YW112) in State 1 was shown in Figure 4-10. The activities of catalyst YW107 and YW112 which contain Fe were much lower than that of YW114 which is Fe free. The effect of Fe content on the activities of silica supported Pd catalysts (YW114, YW107, and YW 112) in State 2 was shown in Fig. 4-11. Both YW107 and YW112 showed much lower activities than that of

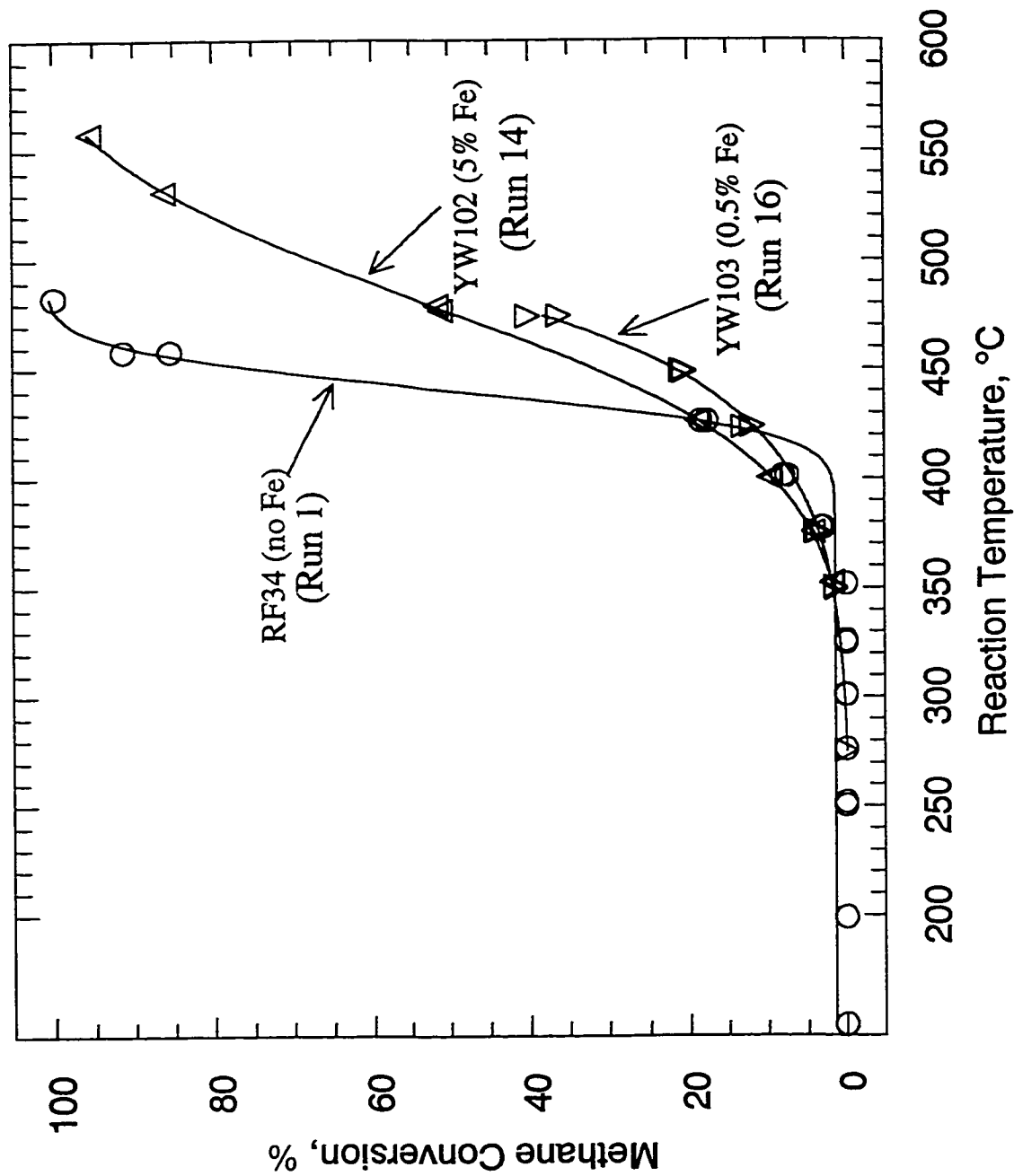


Figure 4-8. Effect of Fe addition on the methane conversion as a function of temperature during activation (State 1) for Pd based catalysts at a feed rate of 82  $\mu\text{mol/s}$  (Feed: 0.965% methane, 3.96% oxygen in helium).

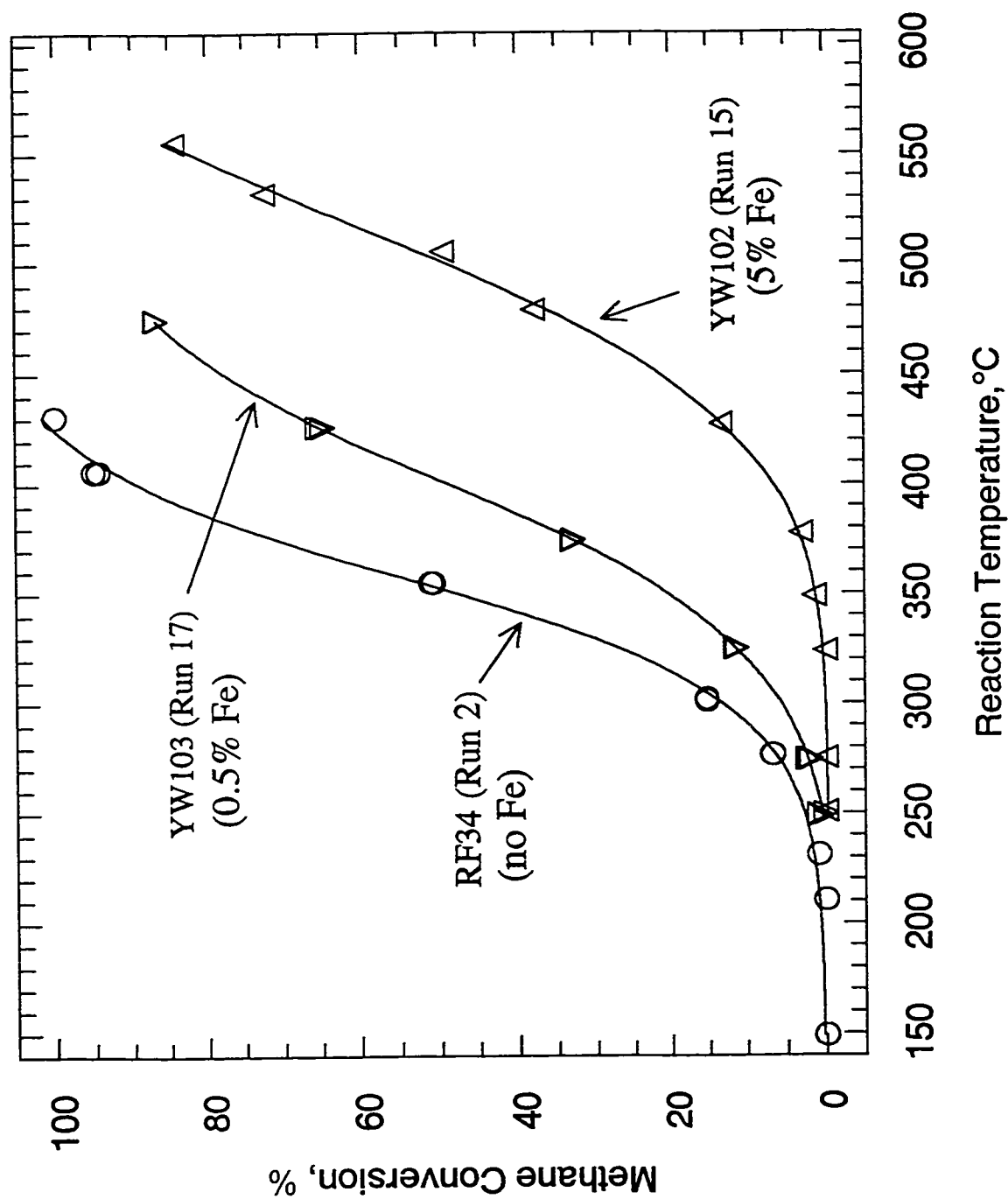


Figure 4-9. Effect of Fe content on the activity of Pd-based alumina supported catalysts in State 2 at a feed rate of 82  $\mu\text{mol/s}$  (Feed: 0.965% methane, 3.96% oxygen in helium).

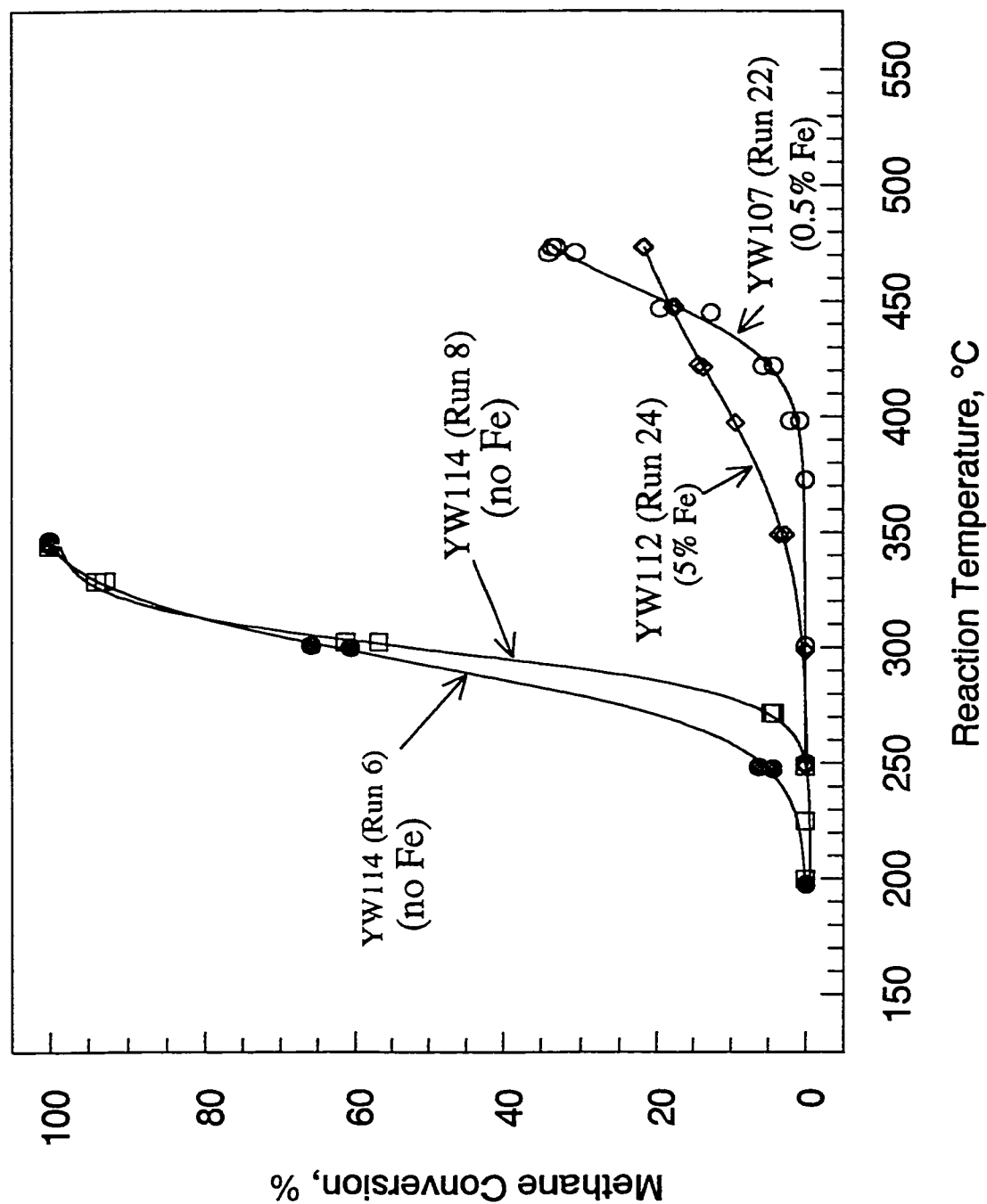


Figure 4-10. Effect of Fe content on the activity of Pd-based silica supported catalysts in State 1 at a feed rate of 82  $\mu\text{mol/s}$  (Feed: 0.965% methane, 3.96% oxygen in helium).

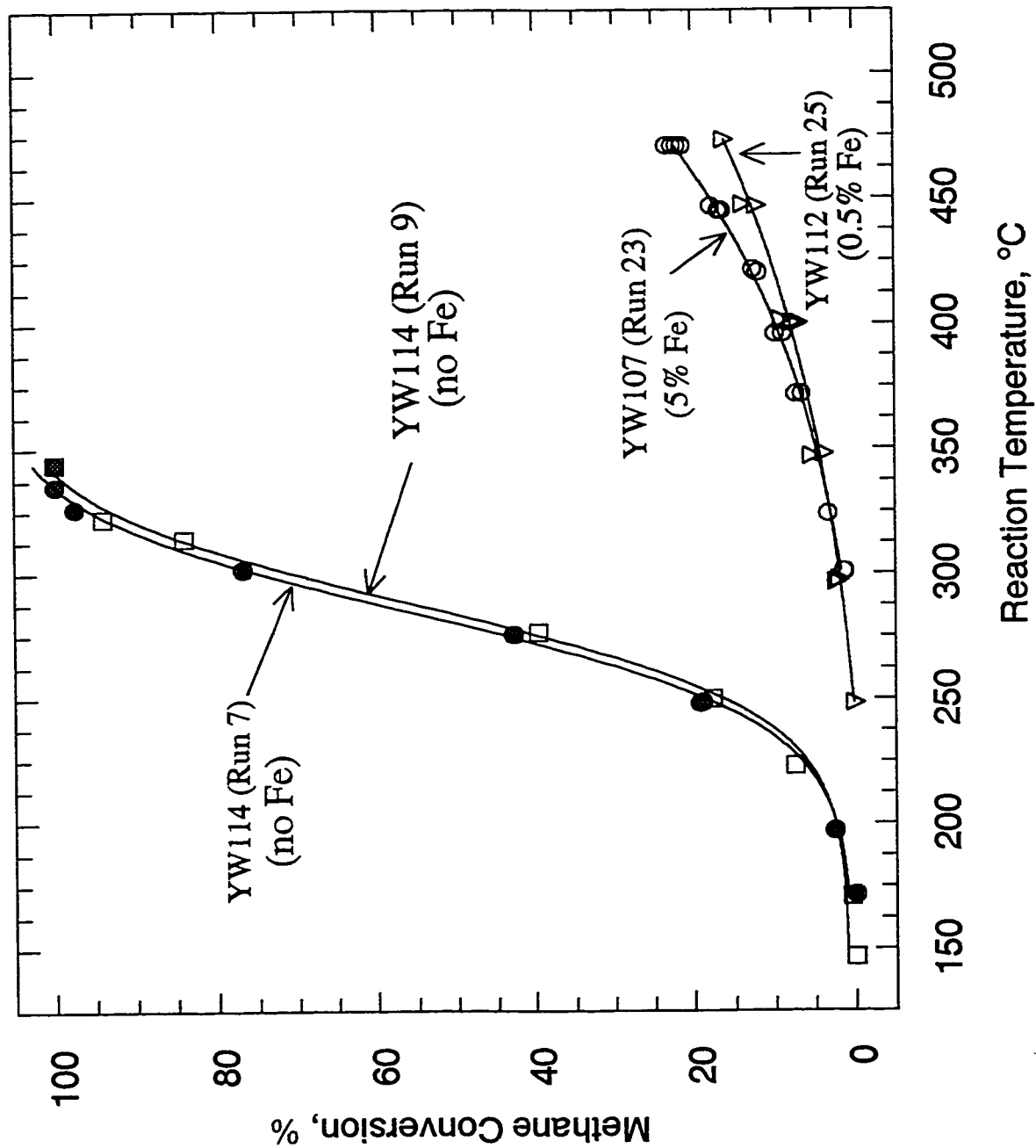


Figure 4-11. Effect of Fe content on the activity of silica supported Pd-based catalysts in State 2 at a feed rate of 82  $\mu\text{mol/s}$  (Feed: 0.965% methane, 3.96% oxygen in helium).

YW114. It is interesting to note that the effect of Fe concentration is less pronounced for SiO<sub>2</sub>-supported Pd than for Al<sub>2</sub>O<sub>3</sub>-supported Pd (compare results in Figures 4-9 and 4-11).

Figure 4-12 shows the variation of the conversion ratio State 2/State 1 as a function of the reaction temperature for various catalysts at feed rate of 82 μmol/s. For alumina supported catalysts, YW103 was activated after aging with reactants and showed a small increase in activity in State 2. YW102 showed lower activity in State 2 than State 1. For silica supported catalysts, no activation were observed for YW107 and YW112.

The results in Figure 4-8 to 4-12 show that the activities of supported palladium decreased after adding Fe. The activities of supported palladium catalysts were influenced by the type of support and by the amount of Fe for the alumina support. Silica supported palladium catalysts seem to be much more sensitive to the deactivation by Fe than alumina supported catalysts. The low activities of the Fe containing catalysts must be due to Pd-Fe interaction such as the covering of Pd or PdO particles with Fe or Fe oxides. Supported iron catalysts are very inactive; conversion of methane over a 5% Fe/Al<sub>2</sub>O<sub>3</sub> catalysts (YW104) were 5% at 473°C (see Run 13, Appendix A).

Cu containing catalysts have been used for NO<sub>x</sub> + CH<sub>4</sub> and CH<sub>4</sub> oxidation reactions (51). The effect of Cu addition on the methane conversion of YW113 in State 1 as the function of reaction temperature was shown in Figure 4-13. YW113 is less active than YW114 and reached 100% methane conversion at 375°C which is about 25°C higher than that of YW114. The effect of Cu addition on the methane conversion of YW113 in State 2 as the function of reaction temperature



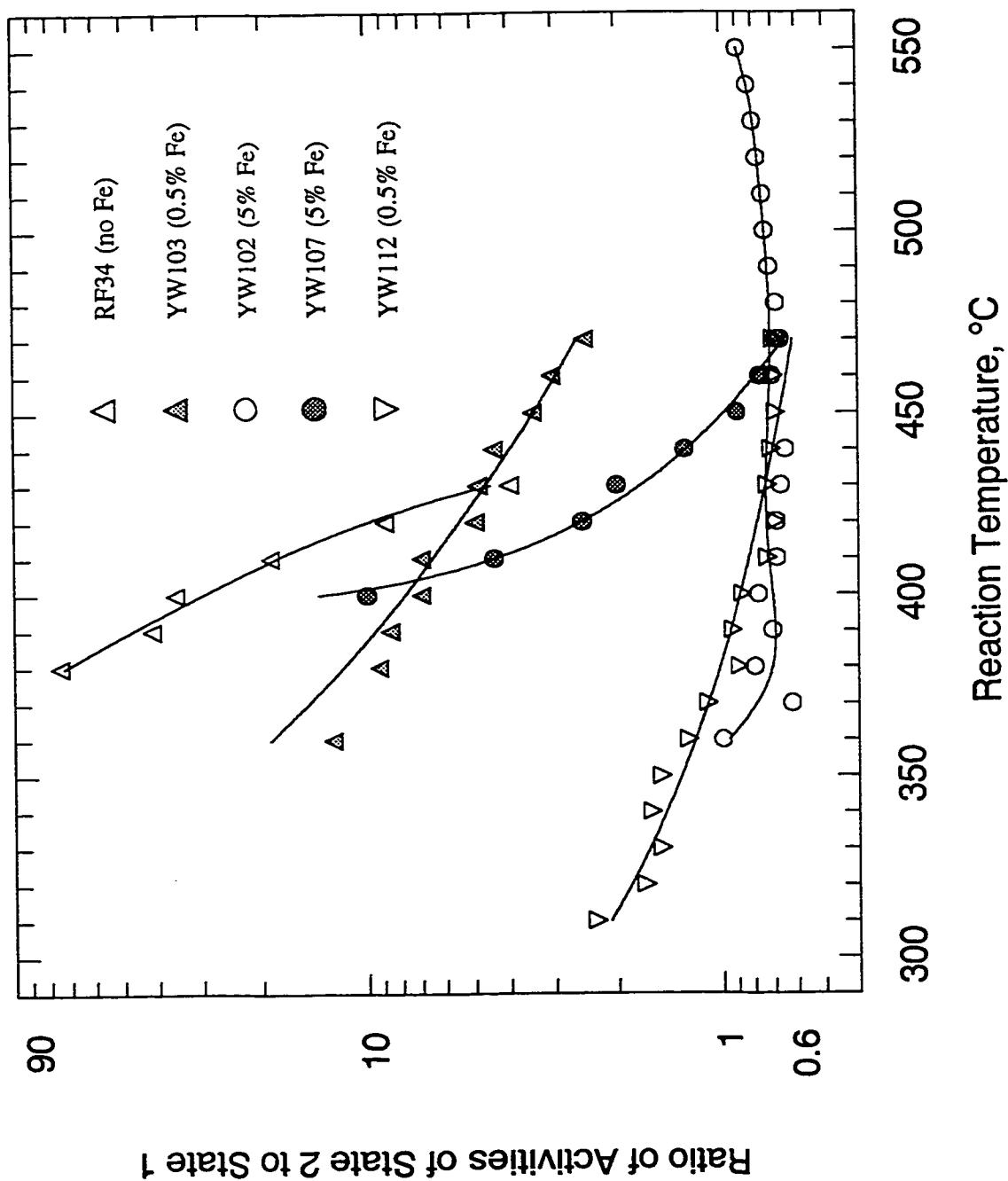


Figure 4-12. Variations in the ratio of activities of State 2 to State 1 as a function of the reaction temperature for various catalysts at a feed rate of 82  $\mu\text{mol/s}$  (Feed: 0.965% methane, 3.96% oxygen in helium).

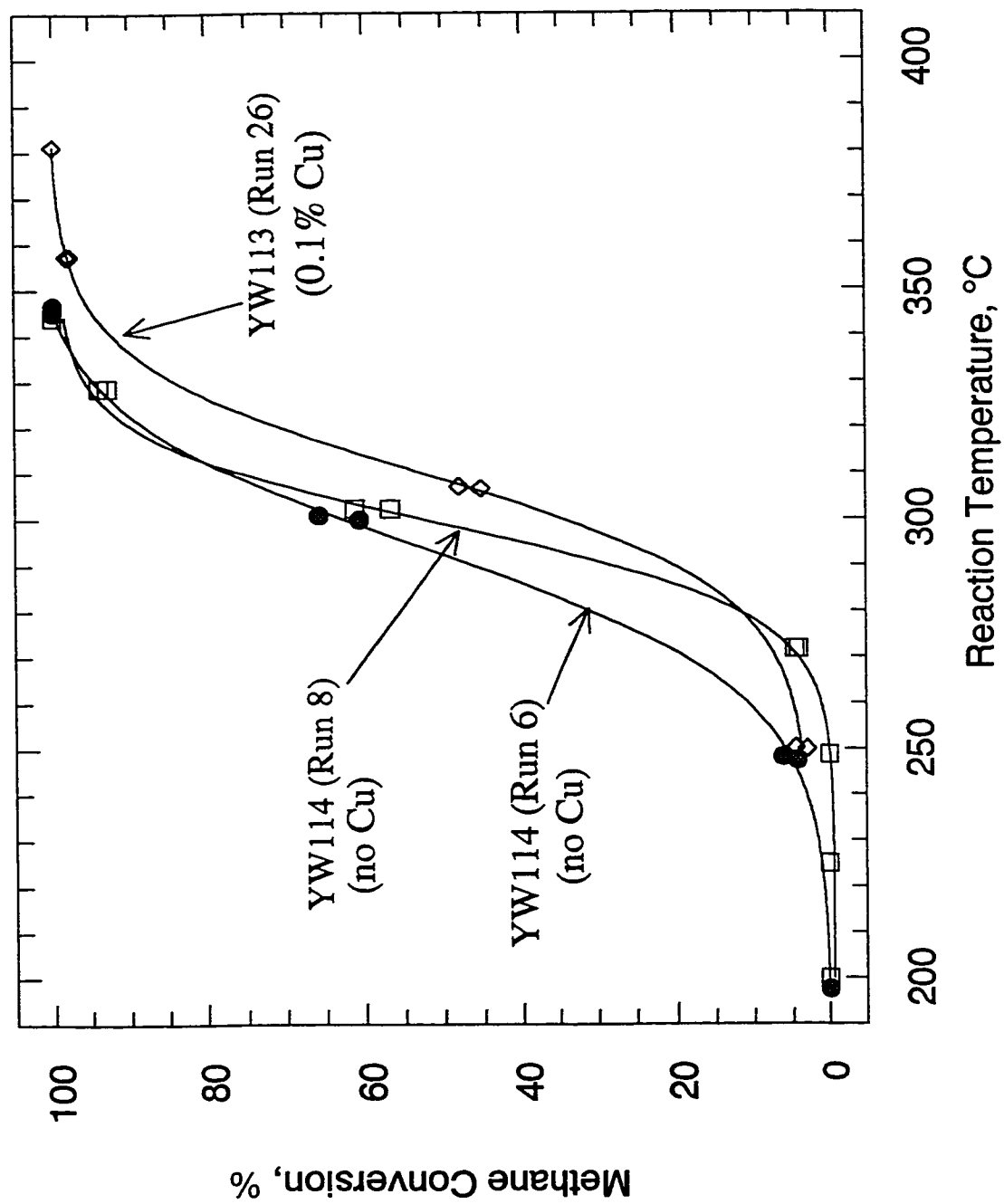


Figure 4-13. Effect of Cu content on the activity of silica supported Pd catalysts in State 1 at feed a rate of 82  $\mu\text{mol/s}$  (Feed: 0.965% methane, 3.96% oxygen in helium).

is shown in Fig 4-14. Catalyst YW113 started to show activity at about 200°C (0.76% methane conversion) which is about 25°C higher than that of YW114 (0.48% methane conversion for 175°C) and YW113 reached 100% conversion at 380°C which is about 40°C higher than that of YW114. The ratios of methane conversions in State 2 to State 1 as the function of temperature are shown in Fig. 4-15. Increase in activities at reaction temperature above 300°C was observed for YW113.

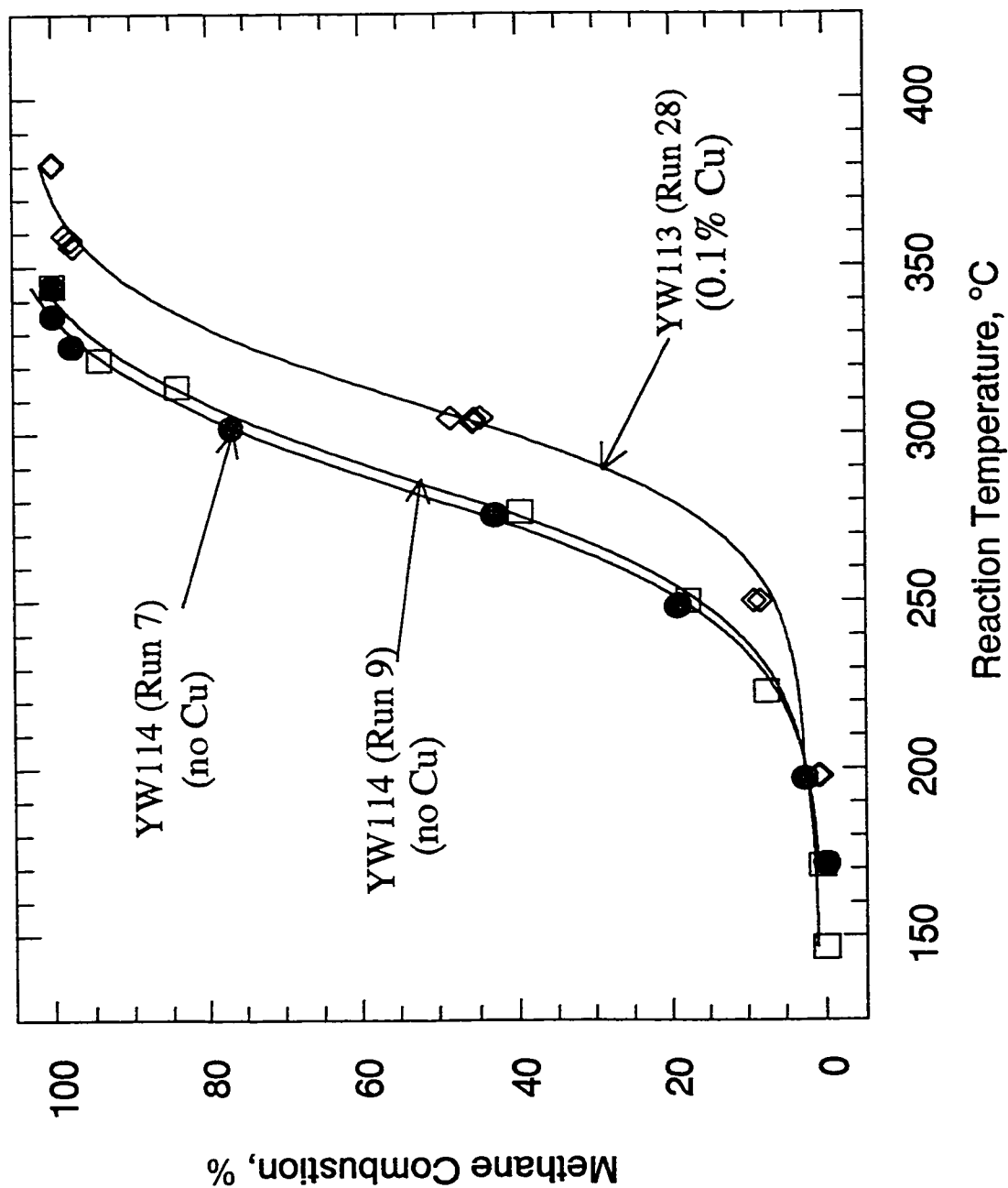


Figure 4-14. Effect of Cu content on the activity of silica supported Pd catalysts in State 2 at a feed rate of 82  $\mu\text{mol/s}$  (Feed: 0.965% methane, 3.96% oxygen in helium).

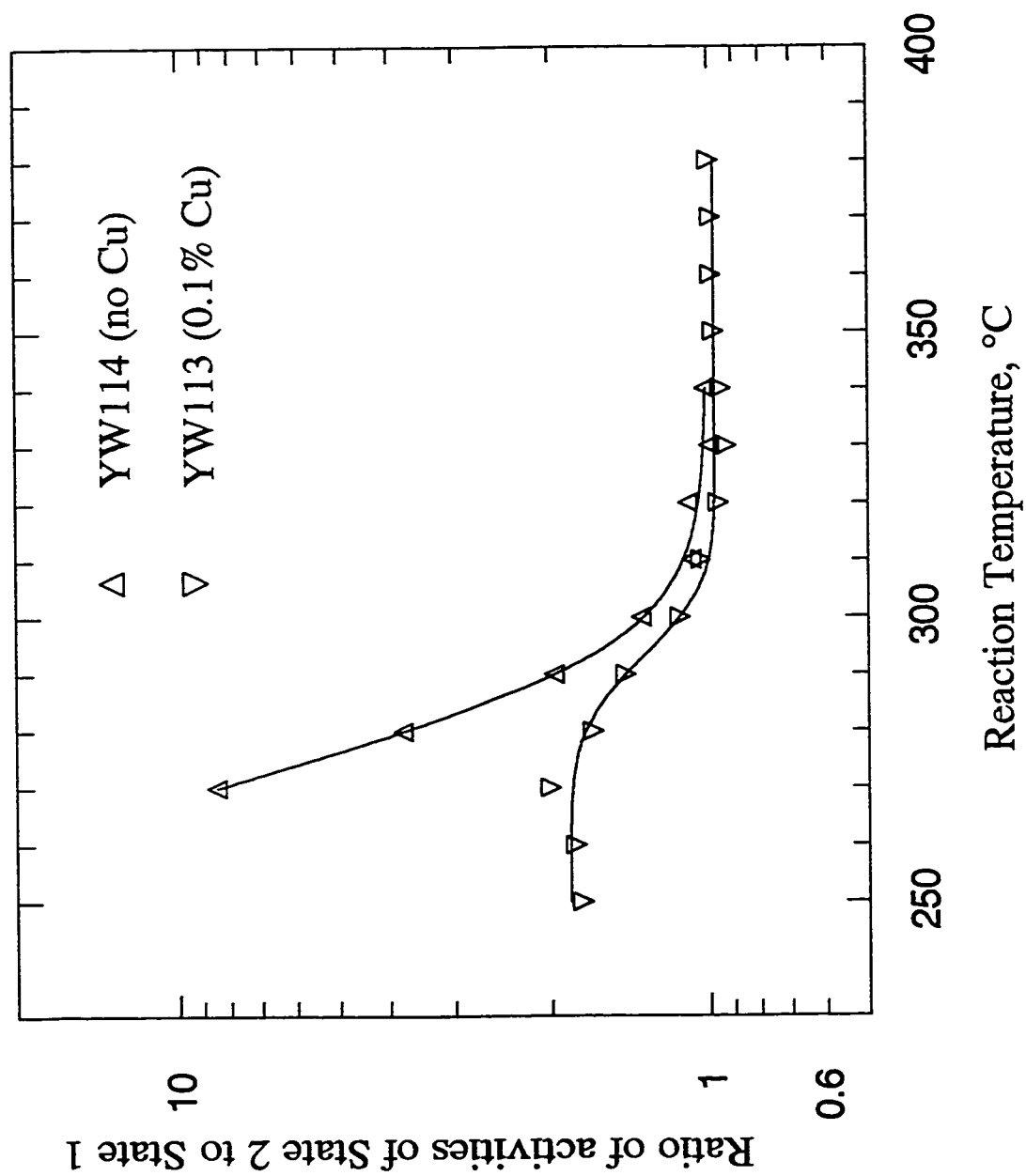


Figure 4-15. Variations in the ratio of activities of State 2 to State 1 as a function of the reaction temperature for various catalysts at a feed rate of 82  $\mu\text{mol/s}$  (Feed: 0.965% methane, 3.96% oxygen in helium).

#### 4.4 Effect of Feed Composition and Reaction Pressure

A limited number of experiments were done with different feed compositions and reaction pressures up to 400 kPa. The effect of reactant composition on activation for RF34 is shown in Figure 4-16. Comparing the compositions for Run 2 with those for Run 20 shows that the composition of the reactant mixture had only a small effect on the final catalytic activities (for Run 2, the catalyst was activated at 475°C with a reactant mixture containing 0.965% CH<sub>4</sub> and 3.96% O<sub>2</sub> and for Run 20 the catalyst was activated at 475°C with a reactant mixture containing 0.232 CH<sub>4</sub> and 1.96% O<sub>2</sub>). The higher methane conversions for Run 19 (Figure 4-16) is probably due to the higher O<sub>2</sub>/CH<sub>4</sub> ratio in the feed for Run 19. The limited data are not sufficient for determination of rate functions.

The effect of total reactor pressure at constant feed composition and approximately constant residence time was measured in Run 43 using catalyst RF30. The residence time was kept approximately constant by keeping the ratio of the feed rate to pressure constant. The methane conversions for this run are shown in Figure 4-17. The results show that conversions were higher at lower reactor pressure. This suggests that the rates of oxidation were inhibited by higher reactant and/or product concentrations such as are obtained with Langmuir-Hinshelwood type rate functions. If the methane oxidation kinetics could be described by a simple first-order power-law rate function over the concentration range investigated, then the conversions at constant residence time and under isothermal conditions would be independent of total pressure. Non-isothermal conditions are more likely at high pressure since the absolute oxidation rate is

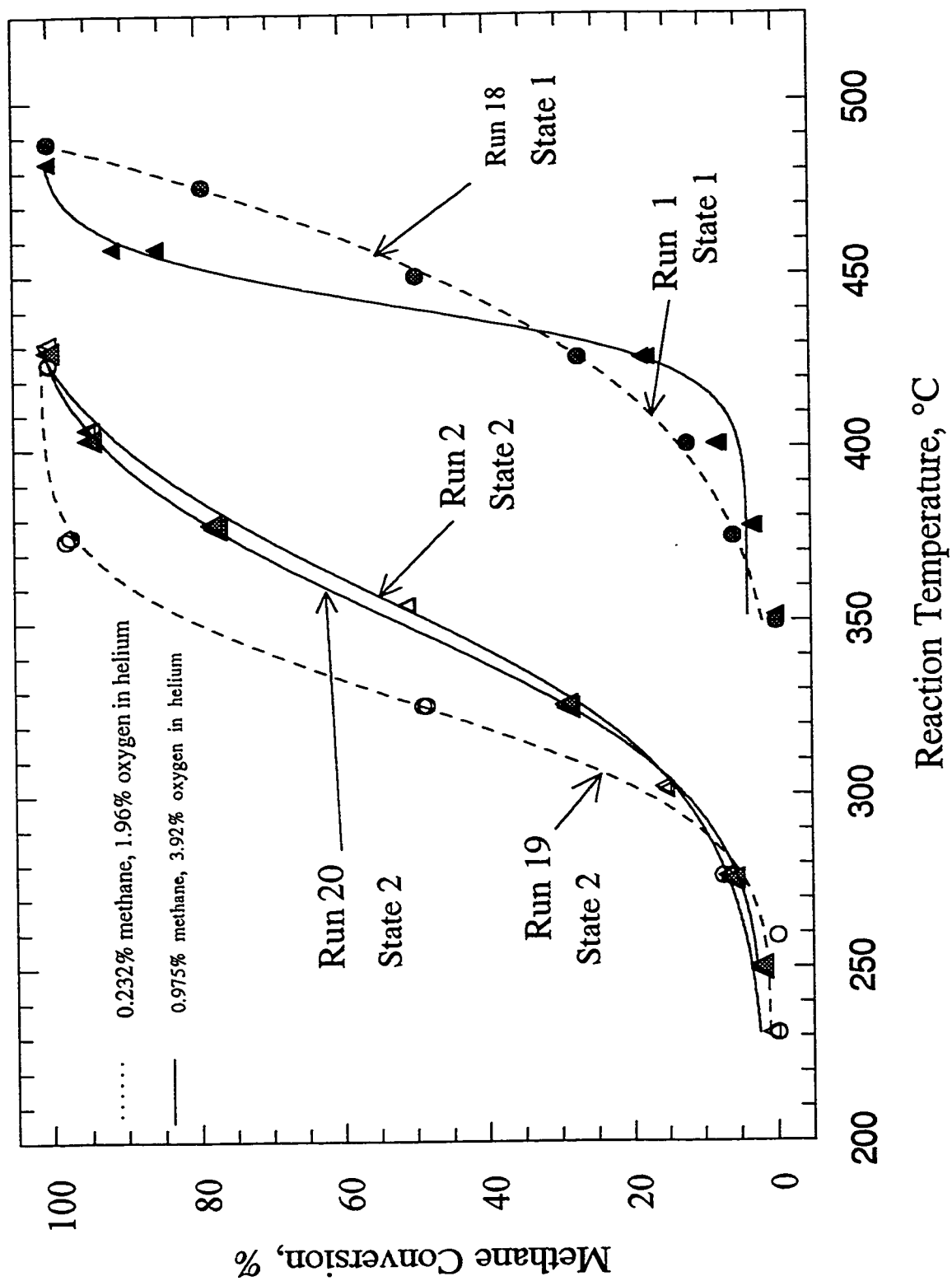


Figure 4-16. Methane conversion as a function of temperature at various feed compositions over RF34 in both States 1 and 2  
(Feed rate: 82  $\mu\text{mol/s}$ )

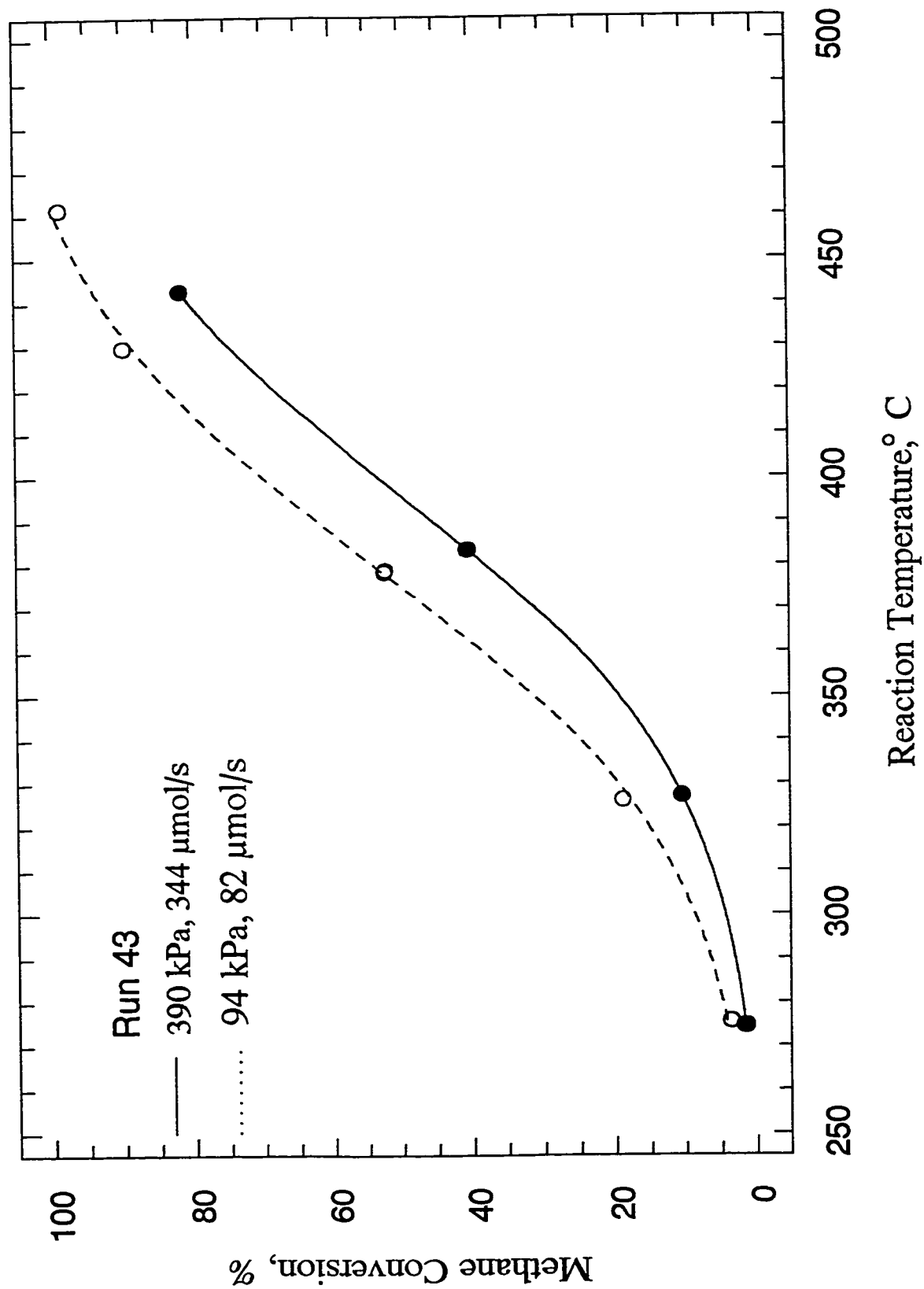


Figure 4-17. Methane conversion as a function of temperature for catalyst RF30 (State 2) at various feed rates and reaction pressures and with constant contact time (Feed: 0.965% methane, 3.96% oxygen in helium).



higher; hence, internal heat transfer effects would tend to increase the conversion at high pressure. This was not observed.

The effect of feed rate on conversion at two different pressures was investigated in Run 43. The results of these determination, plotted as  $\ln(1-X_{CH_4})$  versus the reciprocal of the feed rates, are shown in Figure 4-18. Such a plot should be linear if the reaction is first order in methane in the presence of large oxygen excess. The plots are approximately linear, i.e. the reaction order with respect to methane is close to one for RF30. It also appears that heat and mass transfer effects do not play a major role in the results shown in Figure 4-18 since a four-fold change in pressure (indicated by the change from open to solid symbols in Figure 4-18) did not result in a discontinuity in the oxidation rates.

Runs 19 and 20 were done to determine the effect of total pressure, at constant methane partial pressure, on the rates. Run 20 was done at atmospheric pressure with a feed containing 0.965% methane, i.e. a methane partial pressure of 0.92 kPa. A feed containing 0.23% methane was used for Run 19 and the total pressure for Run 19 was 400 kPa, i.e. a methane partial pressure of 0.92 kPa. The conversions, as shown in Figure 4-19, were relatively independent of total pressure. The slightly higher conversion for Run 19 was probably due to the higher partial pressure of  $O_2$  ( $O_2$  partial pressures were 7.8 and 3.7 kPa for Runs 19 and 20, respectively).

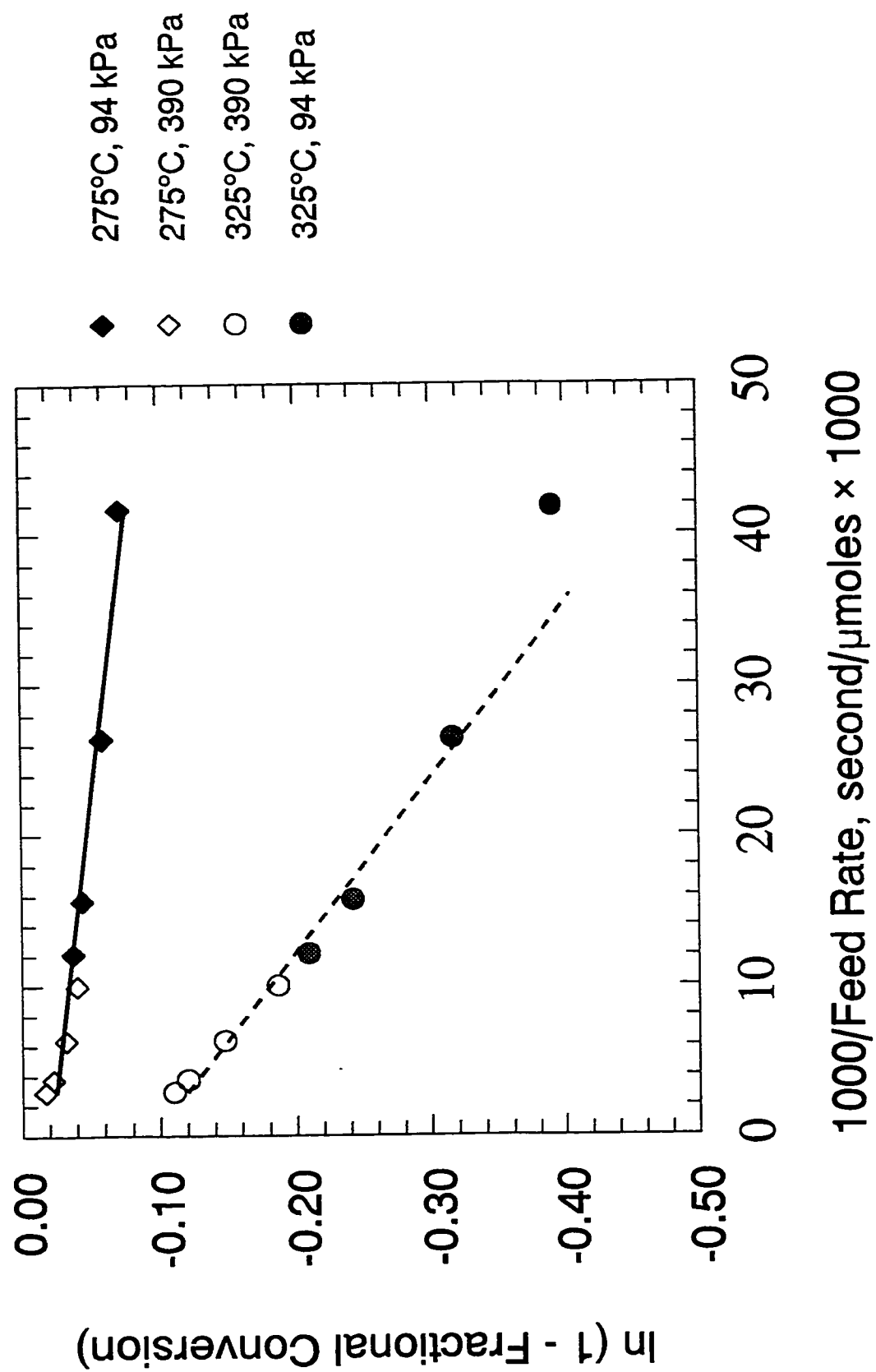


Figure 4-18. Fractional conversion of methane as a function of the reciprocal of feed rate (Run 43).

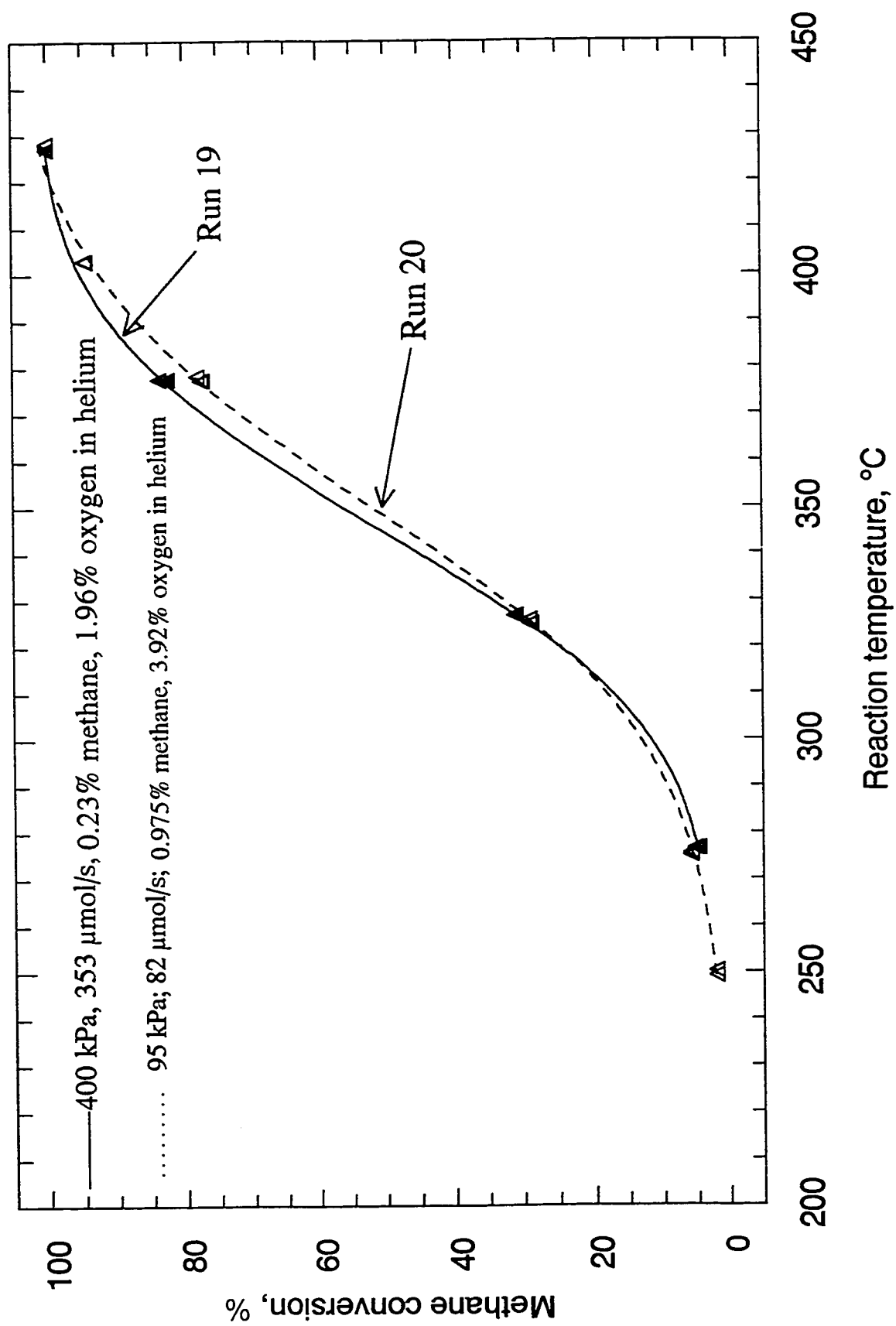


Figure 4-19. Methane conversion as a function of temperature at various pressure and constant methane partial pressures and residence time for catalyst RF34 after activation (state 2).

## 4.5 Catalyst Characterization Results (BET, H<sub>2</sub> Chemisorption, XRD)

The results in the previous chapter showed that the catalytic activities of supported palladium catalysts are a function of the support, palladium precursor, and pretreatment temperature. In addition, it has also been reported in literature that the activities of supported palladium for methane combustion are due to the difference in palladium structure and/or palladium state on the surface of supports of various catalysts. Furthermore, it has been frequently reported that the methane combustion over supported palladium catalysts is structure-sensitive (*e.g.* 3, 6, 18, 19, 20, 21, 27, 28, 38, 39). For this reason, catalysts which were prepared with various palladium supports, palladium precursors and after various treatments were characterized by x-ray diffraction, hydrogen chemisorption and low-temperature nitrogen adsorption (BET) in an attempt to discover catalyst structure – activity relationships.

Total surface areas of catalysts (by the BET method), Pd dispersion (by H<sub>2</sub> chemisorption) and Pd crystal size (by XRD) for various catalysts in State 1 and 2 are summarized in Table 4-2. The total surface area of catalysts RF34 and 30 decreased from 210 and 195 m<sup>2</sup>/g to 185 and 166 m<sup>2</sup>/g after activation with reactants. This shows that the increase in the catalytic activities for methane combustion over these supported palladium catalysts is not due to the change of total surface area of catalysts during activation.

The palladium dispersion, which is defined as the ratio of surface Pd atoms to total Pd atoms, in Table 4-2 show that the palladium dispersion decreased with activation, i.e. the number of surface Pd atoms decreased but the activity increased. The decrease in Pd dispersion was, at

least in part, due to an increase in Pd particle size. The increase in Pd crystal size, which is equal to Pd particle size in well-annealed samples, also increased with activation. The Pd dispersion was calculated using the assumption that one hydrogen atom adsorbs per surface Pd atom (see Appendix C). The Pd crystal size was estimated from XRD line-broadening measurements; the results from the Pd 111 line were used in the size calculations (see Appendix D).

Table 4-2. BET, H<sub>2</sub> chemisorption and XRD results of various catalysts.

Catalyst	Before Activation (State 1)			After Activation (State 2)		
	Surface Area, m <sup>2</sup> /g	Pd Dispersion, %	Pd Crystal Size, nm	Surface Area, m <sup>2</sup> /g	Pd Dispersion, %	Pd Crystal Size, nm
RF34	210	19.7	3.38	185	9.3 to 11.8	4.3 to 6.4
RF30	195	2.1	-	166	1.9	-
YW114	-	10.1	8.12	-	7.8	5.75
RF36	-	1.3	-	-	-	-
RF16	28	1.6	-	20	-	-
YW104	199	-	-	93	-	-
YW103	207	-	-	54	-	-
YW102	197	-	-	122	-	-

The hydrogen chemisorption results suggest that the Pd surface area decreases with activation; the change was most pronounced for RF34 (the Pd dispersion decreased by about 50% as a result of activation). XRD results for RF34 also showed a decrease in Pd area (increase in average Pd crystal size). Hence, it is tempting to ascribe the higher activity resulting from activation to the increase in Pd crystal size, i.e. structure sensitivity. However, for RF30, a catalyst similar to RF34 except that palladium acetylacetonate rather than palladium chloride was used the Pd precursor, the relative change in hydrogen adsorption uptake was much smaller and significant activation still occurred. For YW114, the most active catalyst studied, the hydrogen adsorption

uptake only decreased by about 20% and the average Pd crystal size actually decreased after activation. Hence, the catalytic activity in the activated state is not correlated to the Pd crystal size or hydrogen adsorption uptake of catalysts reduced after activation.

Catalyst RF34 was chosen for further detailed investigations because the activation with reactants resulted in the largest change in activity. Hydrogen chemisorption measurements were done on reduced samples of RF34 after activation at various temperatures. XRD patterns were measured for RF34 in the reduced state, in the oxidized state after activation at various temperatures, and in the reduced state after activation. The results of these measurements are summarized in Table 4-3; more detailed XRD results are presented in Table 4-4.

Table 4-3. Pd dispersions and crystal sizes for RF34 before and after activation.

Runs	Activation Temp,	State 1		State 2		
		Pd Size, nm	Dispersion, %	PdO Size, nm	Pd Size, nm	Dispersion, %
29 & 30	350	3.34	19.3	5.38	4.34	11.8
39 & 40	375	3.29	20.7	5.05	4.39	10.8
37 & 38	400	3.37	18.1	6.21	4.54	10.7
33 & 34	450	3.27	20.5	--	4.48	9.8
35 & 36	525	3.35	20.7	6.50	4.83	9.3
Average for State 1		3.32	19.9			
Standard Deviation		0.04	1.1			

Increasing the activation temperature from 350 to 525°C results in a monotonic decrease in hydrogen adsorption capacity and a similar monotonic increase in PdO and Pd crystal sizes (see Table 4-3). However, the catalytic activity did not vary monotonically with activation

temperature; catalytic activity increased with activation temperature in the 350 to 400°C range followed by a decrease in activity at higher activation temperatures (see Figure 4-6). This indicates clearly that the size of the Pd particles, either as Pd or PdO, are not directly correlated with the methane oxidation activity. The results for catalysts YW114 and RF36 in Table 4-4 further show that large Pd particles do not necessarily result in high activities.

The XRD results for activated and subsequently reduced YW114 were unusual because this reduced catalyst still contains unreduced PdO (see Figure 4-20). This is very unusual since reduction in hydrogen at 500°C usually results in complete reduction of PdO. The XRD results for oxidized RF36 are also unusual since this catalyst still contained Pd metal even after being exposed to reactants (oxidizing atmosphere) at 450°C. A repeat experiment, in which a freshly reduced sample of RF34 was activated with reactants 450°C, yielded similar results, i.e. the oxidation of the Pd during activation was incomplete (see Figure 4-21). Such reduction and oxidation behaviors were not observed with the alumina supported RF34. Additional x-ray patterns are shown in Appendix D.

It is interesting to note that the initial Pd crystal sizes, the PdO crystal sizes in activated samples and the Pd crystal sizes obtained by reduction of the PdO in activated RF34 are well correlated. Pd and PdO sizes are summarized in Table 4-4; Pd sizes used in calculations below were based on the 111 line and PdO sizes were based on the 122 line. The ratio of PdO crystal sizes to Pd crystal sizes in fresh RF 34 varied from about 1.5 to 1.9; this ratio should be 1.24; i.e. the ratio of Pd/PdO densities ( $12.02/9.70=1.24$ ). This indicates that some sintering of Pd occurred during activation. The average ratio of the PdO crystal sizes for RF34 activated at

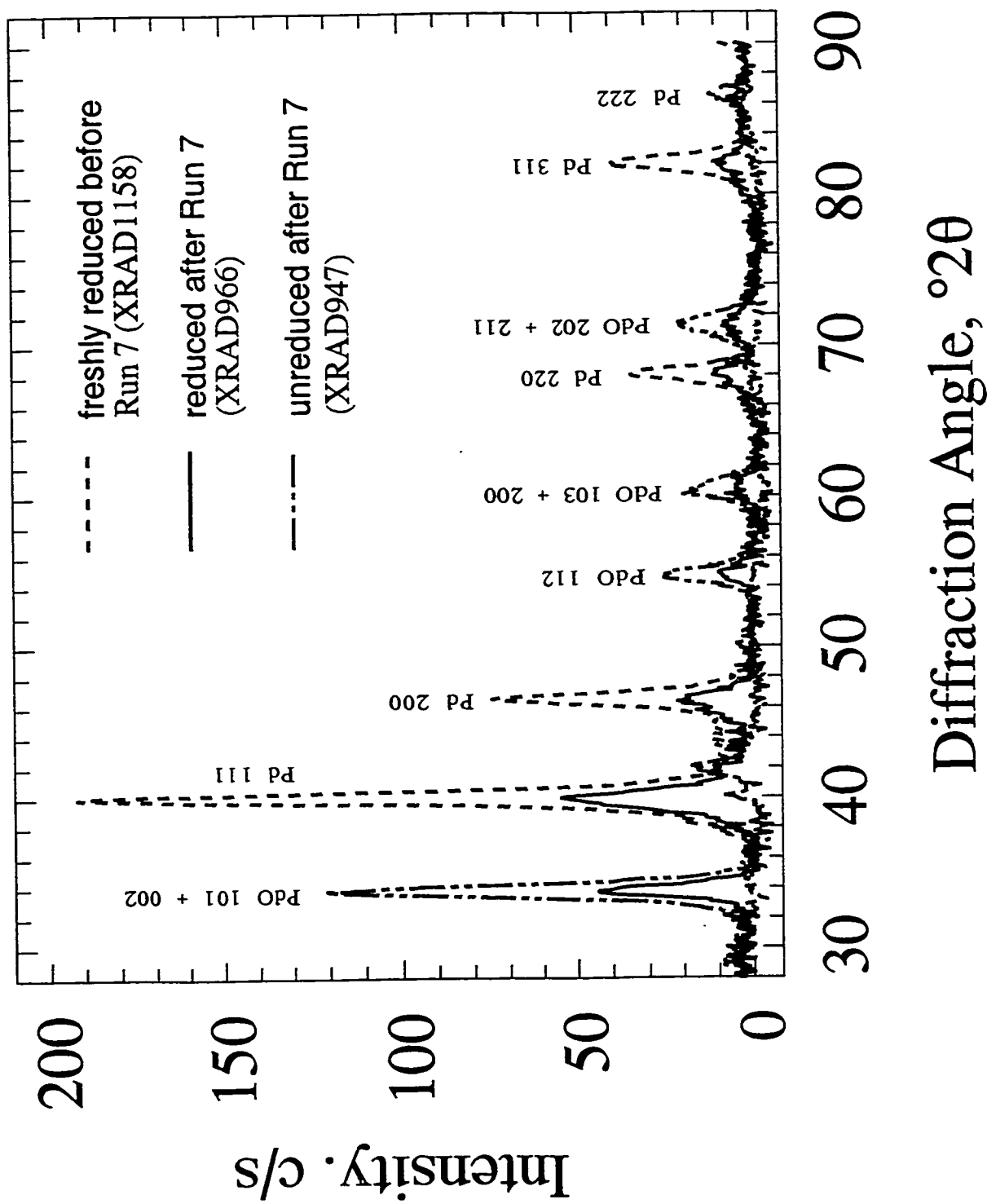


Figure 4-20. Subtracted XRD patterns for Catalyst YW114.



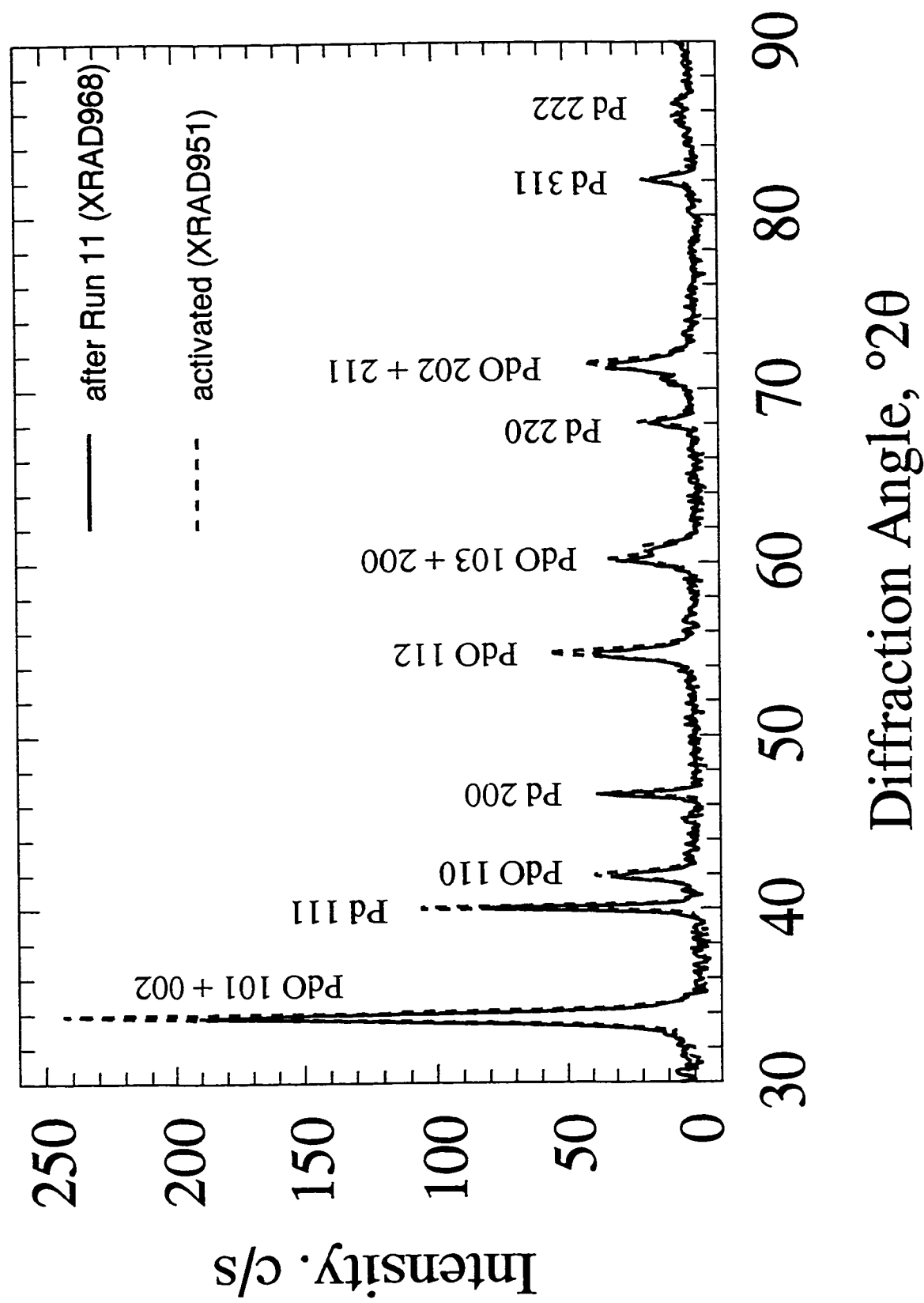


Figure 4-21. Subtracted XRD Patterns for activated and unactivated RF36.

Table 4-4. Summary of Pd and PdO crystal sizes from x-ray diffraction.

Catalyst	Support	Pd Salt	State of Catalyst	Run	Temp	Pd 111	Pd 200	Pd 311	PdO 101†	PdO 122
RF34	Al <sub>2</sub> O <sub>3</sub>	PdCl <sub>2</sub>	reduced State 1	29*	fresh	3.34	3.10	--	--	--
				31*	fresh	3.68	3.94	--	--	--
				33*	fresh	3.27	3.18	--	--	--
				35*	fresh	3.35	3.29	--	--	--
				37*	fresh	3.37	3.72	--	--	--
				39*	fresh	3.29	2.92	3.53	--	--
			reduced State 2	average of fresh		3.38	3.36	--	--	--
				30	350°C	4.34	4.05	3.98	--	--
				40	375°C	4.39	3.83	3.40	--	--
				32	400°C	6.40	5.51	4.72	--	--
				38	400°C	4.54	4.87	3.72	--	--
YW114	SiO <sub>2</sub>	PdCl <sub>2</sub>	oxidized	34	450°C	4.48	4.02	4.01	--	--
				36	525°C	4.83	4.60	3.92	--	--
				30	350°C	--	--	--	4.79	5.38
				40	375°C	--	--	--	5.94	5.05
				32	400°C	--	--	--	8.43	7.15
RF36	SiO <sub>2</sub>	Pd (C <sub>5</sub> H <sub>7</sub> O <sub>2</sub> ) <sub>2</sub>	reduced	38	400°C	--	--	--	6.19	6.21
				36	525°C	--	--	--	6.82	6.50
			oxidized	7*	fresh	8.12	8.31	9.04	--	--
				7	--	5.75	6.66	8.02	7.88¶	10.5¶
RF36	SiO <sub>2</sub>	Pd (C <sub>5</sub> H <sub>7</sub> O <sub>2</sub> ) <sub>2</sub>	oxidized	7	--	---	--	--	8.02	7.89
				11	--	30.1‡	31.5‡	26.2‡	13.7	12.2

† The PdO 101 line overlaps with the less intense 002 line

\* Freshly reduced catalyst used subsequently for indicated run

¶ This sample, reduced after use, still contained PdO

‡ This oxidized catalyst contained elemental (reduced) Pd

different temperatures to Pd sizes in catalysts reduced after activation was 1.24, i.e. equal to the ratio of Pd to PdO densities. Such correspondence between Pd and PdO sizes in fresh and activated states was not observed for silica-supported catalyst YW114; for this catalyst, the PdO crystals after activation reduction were actually smaller than the Pd crystals from which the PdO crystals were formed. These results lead to the conclusion that the PdO in the activated alumina-supported catalyst is present as solid, nonporous PdO and each PdO crystal is reduced to a Pd crystal. For the silica supported catalyst the PdO was probably not present as solid PdO; PdO particles in activated YW114 may be porous or multicrystalline, i.e. each PdO particle may consist of several PdO crystals. The XRD results clearly showed that the structure of the PdO particles on silica is different from those on alumina; it is this difference in structure which is the likely reason for the difference in oxidation behavior of silica and alumina supported palladium.

Catalyst YW114, in which PdO appears to be difficult to reduce, was very active, while catalyst RF36, in which the Pd appears to be difficult to oxidize, had a very low activity. The difference between catalysts YW114 and RF36 was the Pd precursor; both catalysts used the same silica support. Use of Pd acetylacetonate (RF36) resulted in the low activity. Similarly results were obtained with alumina supported, the use of Pd acetylacetonate (RF30) resulted in a catalyst with lower activity than a catalyst made with Pd chloride (RF34). The reasons for these unusual oxidation and reduction behaviors are not known, but it seems to be support and Pd precursor dependent. More detailed examination of the oxidation and reduction behavior of supported catalysts is recommended since it appears that these characteristics are related to the activity for methane oxidation.

## CHAPTER 5

### CONCLUSIONS AND RECOMMENDATIONS

The effects of various factors on the catalytic activity of supported Pd catalysts for the oxidation of methane were investigated. The observations and conclusions of these catalytic studies and the associated catalyst characterization results are summarized below.

1. The support had a marked effect on the initial and steady-state activities. The order of activities, both initial and steady-state activities, for the supports studied was silica > alumina > magnesia.
2. Catalysts made with the palladium chloride were more active than catalysts made with palladium acetylacetonate.
3. Addition of iron and Cu to supported Pd catalysts caused significant catalyst deactivation. The deactivation was more severe for the silica-supported catalysts, but the alumina-supported catalysts were more sensitive to the amount of iron added.
4. The activity as a function of time-on stream for initially reduced catalysts, i.e. activation, was a strong function of the nature of the support and the palladium precursor. The most pronounced activation occurred for RF34, a catalyst made with PdCl<sub>2</sub> on the alumina support. No activation occurred for RF36, a silica supported catalyst made from palladium acetylacetone; the activity of this catalyst did not increase with time-on-stream.
5. Experiments at different total pressures and different feed compositions led to the conclusion that heat and mass transfer effects were not significant at the conditions employed.
6. No systematic experiments were done to determine rate functions, but the limited data indicates that for RF30 the order with respect to methane is close to unity.

7. Total surface area measurements showed that changes in total surface area were not responsible for the observed changes in activity.
8. For the alumina-supported catalyst, RF34, the maximum steady-state activity was obtained after activation at temperature of 375 or 400°C.
9. Hydrogen chemisorption measurements on RF34 showed that Pd dispersion decreased monotonically with increasing activation temperatures. X-ray diffraction measurements confirmed the hydrogen adsorption results, i.e. activation at increasing temperatures resulted in increasingly larger Pd crystals. From this it can be concluded with certainty that methane oxidation is not a simple function of Pd particle size.
10. The PdO crystal sizes in the activated state for RF34 were well correlated with the Pd crystal sizes obtained by reduction of the activated catalysts; this was not the case for YW114, the silica supported catalysts.
11. X-ray diffraction results showed that PdO particles on alumina have a different structure than PdO particles on silica.
12. X-ray diffraction studies with catalysts RF36 and YW114 showed that the Pd precursor has very marked influence on the oxidation - reduction behavior of silica supported palladium.

The current study has added some new information on the unusual behavior of supported palladium catalysts in the oxidation of methane. The importance of the support and the Pd precursor have been identified previously, but the observations of the unusual oxidation - reduction behavior of the silica-supported catalysts and the differences of Pd and PdO crystal sizes as a function of support catalysts are new. It is recommended that future studies investigate the structure of PdO on silica as a function of oxidation temperature. Previous studies have

usually attempted to correlate Pd size or dispersion in reduced catalysts with activity. Careful x-ray diffraction studies allow the determination of PdO structures, and comparison of the PdO crystal sizes with sizes of Pd resulting from the reduction of the PdO could provide more detailed understanding of the factors responsible for the large variation in catalytic activity of supported palladium. Determination of the ease of reduction of PdO formed at different activation temperatures, by techniques such as temperature programmed reduction, may also yield information for gaining understanding of the catalyst structure- catalytic activity relationships.

## REFERENCES

1. Davy, H., in The Collected Works of Sir Humphry Davy, Vol VI, pp. 81-88. [From the Phil. Trans. For 1817, read before the Royal Society, January 23, 1817.].
2. Anderson, R.B., Stein, K.C., Feenan, J.J. and Hofer, L.J.E., Ind. Eng. Chem., **53**, 809-812 (1961).
3. Hicks, R.F., Qi, H., Young, M.L., and Lee, R.G., J. Catal., **122**, 280-294 (1990).
4. Deng, Y., Nevell, T.G., Ewen, R.J., Honeybourne, C.L. and Jones, M.G., Appl. Catal. A **101**, 51-62 (1993).
5. Baldwin, T.R. and Burch, R., Applied Catalysis, **66**, 337-358 (1990).
6. Briot, P. and Primet, M. Appl. Catal. **68**, 301-314 (1991).
7. Farrauto, R.J., Hobson, M.C., Kennelly, T. and Waterman, E.M., Appl. Catal., **81**, 227-237 (1992).
8. Sekizawa, K., Machida, M., Eguchi, K. and Airai, H., **142**, 655-663 (1993).
9. Hoyos, L.J., Praliaud, H. and Primet, M., Appl. Catal., **98**, 125-138 (1993).
10. Marti, P.E., Maciejewski, M. and Baiker, A., J. Catal., **139**, 494-509 (1993).
11. Haneda, M., Mizushima, T., Kakuta, N., Ueno, A., Sato, Y., Matsuura, S., Kasahara, K. and Sato, M., Bull. Chem. Soc. Jpn., **66**, 1279-1288 (1993).
12. Farrauto, R.J., Lampert, J.K., Hobson, M.C., Waterman, E. M., Appl. Catal. B: Envi. **6**, 263-270 (1995).
13. Ribeiro, F.H., Chow, M., and Dalla Betta, R.A., J. Catal., **146**, 537-544 (1994).
14. Burch, R., Urbano, F.J., Loader, P.K., Appl. Catal. A: General **123**, 173-184 (1995).

15. Kikuchi, E., Matsuda, T. and Takahashi, N., Symp. on Catalytic Combustion, Presented Before the Division of Petroleum Chemistry, Inc., 213<sup>th</sup> National Meeting, American Chemistry Society, San Francisco, CA, April 13-17, (1997).
16. Uchida, H., Takashima, F. and Imaseki, Y., Science and Technology in Catalysis, 383-386 (1994).
17. Qi, C., An, L. and Wang, H., Appl. Catal. A: General **140**, 17-18 (1996) .
18. Fujimoto, K., Ribeiro F.H., Bell, A.T. and Iglesia, E., Symp. on Heterogeneous Hydrocarbon Oxidation Presented before the Division of Petroleum Chemistry, Inc., 211<sup>th</sup> National Meeting, American Chemistry Society, New Orleans, LA, 110-113, March 24-29 (1996).
19. Fujimoto, K., Ribeiro, F.H., and Iglesia, E., Symp. on Catalytic Combustion, Presented Before the Division of Petroleum Chemistry, Inc., 213<sup>th</sup> National Meeting, American Chemistry Society, San Francisco, CA, **April** 13-17 (1997) .
20. Briot, P., Auroux, A., Jones, D. and Primet, M., App. Catal., **59**, 141-152 (1990).
21. Otto K., Langmuir, **5**, 1374-1369 (1989).
22. Kobayshi, M., Kanno, T., Konishi, A. and Takeda, H., React. Kinet. Catal. Lett., **37**, 89-93 (1998).
23. Farrauto, R.J., Kennelly, T. and Waterman, E.M., US Patent **4 893 465** (1990).
24. Baldwin T.R. and Burch R., Appl. Catal., **66**, 359-381(1990).
25. Hicks, R.F., Qi, H., Young, M.L. and Lee, R.G., J. Catal., **122**, 295-306 (1990).
26. Cullis, C.F. and B Willatt, M., J. Catal., **83**, 267-285 (1983).
27. Hicks, R.F., Qi, H., Young, M.L., and Lee, R.G., J. Catal., **122**, 295-306, 1990.
28. Marti, P.E., Maciejewski, M., and Baiker, A., J. Catal., **139**, 494-509 (1993).
29. Chojnacki, T.P. and Schmidt, L.D., J. Catal., **115**, 473, (1989).



30. Chen, J.J., and Ruckenstein, E., *J. Phys. Chem.* **85**, 1606 (1981).
31. Ribeiro, F.H., Chow, M., and Dalla Betta, R.A., *J. Catal.*, **146**, 537 (1994).
32. GRI Executive Research Letter, S.D. Ban, December, 1993.
33. Stull, D.R., Westrum, E.F., and Sinke, G.C., "The Chemical Thermodynamics of Organic Compounds", Wiley & Sons, New York, 1967
34. Cullis, C.F. and Willatt, B.M., *J. Catal.* **86**, 187 (1984) .
35. Marecot, P., Fakche, A., Kellali, B., Mabilon, G., Prigent, M., and Barrier, J., *Appl. Catal. B: Environmental* **3**, 283-294 (1994).
36. Simone, D.O., Kennelly, T., Brungard, N.L. and Farrauto R.J., *Appl. Catal.*, **70**, 87-100 (1991).
37. Boudart, M., *Advan. Catal.* **20**, 153-166 (1969).
38. Briot, P., Auroux ,A., Jones, D. and Primet, M., *Appl. Catal.*, **59**, 141 (1990).
39. Burch, R., Urbano, F.J., and Loader, P.K., *Catal. Today*, **27**, 243 (1996).
40. Gillet, M.F. and Channakhone, S., *J. Catal.*, **97**, 427 (1986).
41. Chojnacki, T.P. and Schmidt, L.D., *J. Catal.*, **115**, 473 (1989).
42. Garbowski, E., Feumi-Jantou, C., Mouaddib, N., and Primet, M., *Appl. Catal.*, **109**, 277 (1994).
43. Cullis, C.F., Nevell, T.G. and Trimm, D.L., *J. Chem.Soc., Faraday Trans. 1*, **68**, 1406 (1972).
44. Card, R.J., Schmitt, J.L. and Simpson, J.M., *J. Catal.*, **79**, 13 (1983).
45. Van Giezen, J.C., Van Dillen, A.J., and Geus, J.W., 11<sup>th</sup> International Congress on Catalysis – 40<sup>th</sup> Anniversary, North American Catalysis Society, Baltimore, Maryland, USA, June 30 - July 5, Poster 263 (1996).

46. Mouaddib, N., Feumi-Jantou, C., Garbowski, E. and Primet, M., *App. Catal. A: General*, **87**, 129-144 (1992).
47. Carl, R.F., Lund, S.P. and Saley H., *Symp. on Catalytic Combustion Presented Before the Division of Petroleum Chemistry, Inc., 213<sup>th</sup> National Meeting, American Chemical Society, San Francisco, CA, April 13-17, 1997.*
48. McCarty, J.G. and Wise, H., "Perovskite Catalysts for Methane Combustion", *Catal. Today*, **8**, 231-248 (1990).
49. Marion, M.C., Garbowski, E. and Primet, M., *J. Chem. Soc. Faraday Trans.*, **86**, 3027-3023 (1990).
50. Marion, M.C., Garbowski, E. and Primet, M., *J. Chem. Soc. Faraday Trans.*, **87**, 1795-1800 (1991).
51. Kuchеров, A.V., Slinkin, A.A., Goryashenko, S.S. and Slovetskaja, K.I., *J. Catal.* **118**, 459-465 (1989).
52. Haneda, M., Miki, T., Mizushima, T., Kakuta, N. and Ueno, A., *Stud. Surf. Sci. Catal.* **75**, 2079-2082 (1993).
53. Michiue, Y., Fujili, Y. and Tominaga, H., *Chem. Lett. (Jpn)*, 2039-2042 (1990).
54. Yu T. S., Kirichnko, O.A. and Chermashentseva, G.K., *React. Kinet. Lett.*, **49**, 235-240 (1993).
55. Tabata, K., Matumoto, I. and Kohiki, S., *J. Mat. Sci.*, **22**, 1882-1886 (1987).
56. Chou, P. Vannice, M.A., *J. Catal.*, **105**, 342-351 (1987)
57. Guo, I., Yu, T.-T., and Wanke, S.E., *Stud. Surf. Sci. Catal.*, **38**, 21-32, (1988).
58. Pieters, W.J.M. and Venero, A.F., *Stud. Surf. Sci. Catal.*, **19**, 155-163 (1984).

## Appendix A: Experimental Data

Detailed tabulation of the data for the various methane oxidation experiments are presented in this Appendix. The values of the data set are the day on which each run was started. The 'Time-on-Stream' values shown in the second column of the tables are the total time that catalysts has been exposed to reactant conditions; some catalysts charges were used for more than one run. A set of sample calculation illustrating the procedure used to calculate the methane conversion from G.C. results is given in Appendix B.

The variables listed in this appendix have the following estimated accuracies:

Time-on-stream:  $\pm 0.01$  h

Reactor Temperature:  $\pm 0.2^\circ\text{C}$

Reactant Feed Rate:  $\pm 0.5\%$  of reported value

Methane Conversion:  $\pm 1.5\%$  (see Appendix B)

Table A-1. Results for Run 1 (960814)

Catalyst: RF34 (5 mass % Pd supported on  $\text{Al}_2\text{O}_3$ )

Catalyst charge: 96.2 mg

State of catalyst at beginning of run: freshly reduced (State-1)

Reactor pressure: 94 to 96 kPa

Feed composition: 0.965%  $\text{CH}_4$ , 3.96%  $\text{O}_2$ , in He

Data Set	Catalyst Time-in-Stream, h	Oven Temp, $^\circ\text{C}$	Reactor Temp., $^\circ\text{C}$	Reactant Feed Rate, mL/min	Reactant Feed Rate, $\mu\text{mol/s}$	Methane Fractional Conversion, %
960814-A	0.17	150	148	127.48	83.0	0
960814-B	0.33	150	148	94.53	61.6	0
960814-C	1.58	199	199	97.78	63.7	0
960814-D	2.08	199	199	34.64	22.6	0
960814-E	2.17	249	250.22	34.67	22.6	0
960814-F	2.33	250	251.68	23.97	15.6	0
960814-G	2.42	275	276	25.14	16.4	0
960814-H	2.53	275	276	97.78	63.7	0
960814-I	2.67	300	300.79	35.73	23.3	0
960814-J	2.83	300	301.13	35.74	23.3	0
960814-K	3.00	325	324.83	35.8	23.3	0.12
960814-L	3.17	325	326.26	35.77	23.3	0.74
960814-M	3.33	325	326.26	24.93	16.2	1
960814-N	3.5	325	325.79	98.81	64.3	0
960814-O	3.62	325	325.79	127.48	83.0	0

Data Set	Catalyst Time-in-Stream, h	Oven Temp, °C	Reactor Temp., °C	Reactant Feed Rate, mL/min	Reactant Feed Rate, $\mu\text{mol/s}$	Methane Fractional Conversion, %
960814-P	3.75	325	326.26	35.41	23.1	0
960814-Q	3.92	351	351.62	35.07	22.9	2.62
960814-R	4.08	350	351.62	35.09	22.9	2.65
960814-S	4.25	350	351.62	98.84	64.4	0
960814-T	4.38	351	351.62	98.84	64.4	0.89
960814-U	4.50	350	351.62	128.1	83.4	0
960814-V	4.83	350	351.62	34.64	22.6	2.52
960814-W	5	350	351.62	34.64	22.6	2.53
960814-X	5.17	375	376	35.01	22.8	7.01
960814-Y	5.33	375	376	35.01	22.8	6.22
960814-Z	5.58	375	376.38	58.32	39.0	4.02
960814-A1	5.75	375	376.86	58.32	38.0	4.79
960814-B1	6	375	377.33	98.06	63.9	2.95
960814-C1	6.2	375	377.33	97.97	63.8	3.39
960814-D1	6.33	375	377.33	126.9	82.6	2.91
960814-E1	6.5	375	377.33	126.77	82.5	3.21
960814-F1	6.67	400	401	34.47	22.4	17.58
960814-G1	6.88	400	401	34.38	22.4	15.75
960814-H1	7.05	400	401	57.94	37.7	11.01
960814-I1	7.22	400	401	57.9	37.7	11.59
960814-J1	7.47	400	401	97.31	63.4	8.11
960814-K1	7.58	400	401	97.39	63.4	8.49
960814-L1	7.75	400	401	125.87	82.0	7.57
960814-M1	7.88	400	401	126.03	82.1	8.05
960814-N1	8.05	424	423.76	34.89	22.7	30.77
960814-O1	8.22	425	423.76	35.07	22.8	30.93
960814-P1	8.38	425	426	58.79	38.3	23.15
960814-Q1	8.55	425	427.3	58.64	38.1	23.84
960814-R1	8.63	425	423.76	97.36	63.4	17.17
960814-S1	8.8	425	423.76	97.26	63.3	18.64
960814-T1	8.93	425	426	126.42	82.3	17.7
960814-U1	9.05	425	426	126.53	82.4	18.52
960814-V1	9.22	425	426	97.31	63.4	22.29
960814-W1	9.38	450	449.7	33.04	21.5	64.08
960814-X1	9.63	450	449.7	33.04	21.5	66.39
960814-Y1	9.75	451	452	58.65	38.2	55.2
960814-Z1	10.05	452	452	58.67	38.2	63.18

Data Set	Catalyst Time-in-Stream, h	Oven Temp, °C	Reactor Temp., °C	Reactant Feed Rate, mL/min	Reactant Feed Rate, $\mu\text{mol/s}$	Methane Fractional Conversion, %
960814-A2	10.33	452	453.23	96.67	62.9	65.1
960814-B2	10.63	452	453.23	96.63	62.9	78.35
960814-C2	10.88	452	458	124.55	81.1	85.5
*960814-CC2	11.05	452	458	124.41	81.0	91.37
960814-D2	11.17	452	457.05	158.08	102.9	89.98
960814-E2	11.43	450	461.47	95.76	62.4	97.73
960814-F2	11.6	474	476.74	33.59	21.9	100
960814-G2	11.85	474	476.74	33.69	21.9	100
960814-H2	11.93	474	476.74	56.8	37.0	100
960814-I2	12.27	474	476.74	56.68	36.9	100
960814-J2	12.35	475	479	95.22	62.0	100
960814-K2	12.63	475	482.63	123.36	80.3	100

Table A-2. Results for Run 2 (960820)

Catalyst: RF34 (5 mass % Pd supported on Al<sub>2</sub>O<sub>3</sub>)

Catalyst charge: 96.2 mg

Previous runs in which catalyst charge was used: Run 1 (960814)

State of catalyst at beginning of run: activated (State-2)

Reactor pressure: 94 to 96 kPa

Feed composition: 0.965% CH<sub>4</sub>, 3.96% O<sub>2</sub> in He

Data Set	Catalyst Time-in-Stream, h	Oven Temp, °C	Reactor Temp., °C	Reactant Feed Rate, mL/min	Reactant Feed Rate, μmol/s	Methane Fractional Conversion, %
960820-A	24.68	150	149	23.74	15.5	0
960820-B	24.93	211	212.58	24.01	15.6	1.36
960820-D	25.07	210	211.58	34.53	22.5	0.48
960820-E	25.23	210	210.58	58.73	38.2	0
960820-F	25.33	229	229	98.43	64.1	0.82
960820-G	25.42	230	231	98.63	64.2	1.12
960820-H	25.58	230	231	127.43	83.0	0.9
960820-I	25.83	230	231.48	57.61	37.5	1.62
960820-J	26	230	231.48	57.73	37.6	1.56
960820-K	26.08	230	231.48	35.1	22.9	2.17
960820-L	26.17	275	275.61	34.81	22.7	11.29
960820-M	26.4	275	275.61	57.95	37.7	9.13
960820-N	26.57	275	276.59	97.1	63.2	7.44
960820-O	26.7	275	276.59	97.13	63.2	7.26
960820-OO1	26.82	275	276.59	97.13	6.32	7.14
960820-P	26.9	275	276.59	125.63	81.8	6.81
960820-Q	27.07	275	276.59	125.59	81.8	6.72
960820-R	27.19	300	300.79	34.66	22.6	25.77
960820-S	27.32	300	300.79	58.03	37.8	20.71
960820-T	27.63	300	301.27	96.98	63.1	16.99
960820-U	27.73	300	301.27	96.96	63.1	16.86
960820-V	27.9	300	301.27	126.51	82.4	15.25
960820-W	28.07	300	302.24	126.61	82.4	15.69
960820-X	28.15	350	351.62	34.06	22.2	74.96
960820-Y	28.32	350	353.52	57.97	37.7	63.93
960820-Z	28.53	350	353.52	97.66	63.6	53.93
960820-A1	28.9	350	354	98.2	63.9	54.24
960820-B1	29.32	350	355	126.41	82.3	50.87

Data Set	Catalyst Time-in-Stream, h	Oven Temp, °C	Reactor Temp., °C	Reactant Feed Rate, mL/min	Reactant Feed Rate, $\mu\text{mol/s}$	Methane Fractional Conversion, %
960820-C1	29.4	350	355	126.5	82.4	51.14
960820-D1	29.48	400	400.12	34.11	22.2	100
960820-E1	29.77	400	402.48	58.57	38.1	99.04
960820-F1	30.1	400	404.84	98.03	63.8	96.11
960820-G1	30.62	400	406	97.91	63.8	96.31
960820-H1	30.82	400	406	125.73	81.9	94.36
960820-I1	31.98	400	406	125.46	81.7	95.02
960820-J1	45.4	425	429.67	56.39	36.7	100
960820-K1	45.65	426	429.67	94.35	61.4	100
960820-L1	46.13	425	431	121.33	79.0	100
960820-M1	46.57	425	431	121.33	79.0	100

Table A-3. Results for Run 3 (960824, 960825, 960827, 960829, 960830, 960904, 960905, 960909)

Catalyst: RF34 (5 mass % Pd supported on Al<sub>2</sub>O<sub>3</sub>)

Catalyst charge: 96.2 mg

Previous runs in which catalyst charge was used: Run 2 (960820)

State of catalyst at beginning of run: activated (State-3)

Reactor pressure: 94 to 96 kPa

Feed composition: 0.965% CH<sub>4</sub>, 3.96% O<sub>2</sub>, 95% He

Data Set	Catalyst Time-in-Stream, h	Oven Temp, °C	Reactor Temp., °C	Reactant Feed Rate, mL/min	Reactant Feed Rate, μmol/s	Methane Fractional Conversion, %
960824-A	147.18	275	276.59	34.52	22.5	11.66
960824-AA	147.4	275	276.59	34.52	22.5	12.11
960824-B	147.52	275	276.59	58.98	38.4	9.7
960824-C	147.68	275	276.59	98.2	63.9	7.8
960824-D	147.90	275	276.59	126.58	82.4	6.91
960824-E	149.23	275	276.59	35.35	23.0	13.85
960824-F	149.47	275	276.59	58.59	38.2	10.82
960824-G	149.58	275	276.59	98.65	64.2	8.26
960824-H	149.68	275	276.59	126.41	82.3	7.27
960825-A	173.97	275	276.59	36.12	23.5	13.48
960825-B	174.22	275	276.59	60.59	39.5	10.62
960825-C	174.38	275	276.59	100.02	65.1	8.66
960825-D	174.55	275	276.59	100.1	65.2	8.29
960825-E	174.67	275	276.59	127.71	83.2	7.34
960825-F	174.92	275	276.59	127.88	83.3	7.35
960825-G	175.22	275	276.59	127.65	83.1	7
960825-H	175.67	275	276.59	128.04	83.4	7.45
960825-I	175.83	275	276.59	36.9	24.0	13.58
960827-A	205.85	275	276.59	39.47	25.7	13.3
960827-B	206.02	275	276.59	38.74	25.2	13.74
960827-C	206.13	275	276.59	37.32	24.3	13.43
960827-D	206.45	275	276.59	125.72	81.9	10.95
960827-E	206.63	275	275.61	92.82	60.4	8.16
960827-F	208.02	275	276.59	100.24	65.3	8.41
960827-G	208.27	275	276.59	129.27	84.2	7.84
960827-H	209.85	275	276.59	128.42	83.6	7.53
960827-I	201.13	275	276.59	59.91	39.0	11.37
960827-J	221.68	275	276.59	40.86	26.6	13.4
960827-K	221.93	275	276.59	36.84	24.0	14.03



Data Set	Catalyst Time-in-Stream, h	Oven Temp, °C	Reactor Temp., °C	Reactant Feed Rate, mL/min	Reactant Feed Rate, $\mu\text{mol/s}$	Methane Fractional Conversion, %
960827-L	222.18	275	276.59	64.82	42.2	10.7
960827-LL	-	275	275.61	60.97	39.7	11.1
960827-M	222.82	275	276.59	99.67	64.9	8.66
960827-N	223.02	275	276.59	99.77	65.0	8.79
960827-O	223.38	275	276.59	128.37	83.6	7.5
960827-P	223.55	275	276.59	128.27	83.5	7.58
960829-A	272.75	275	276.59	36.22	23.6	14.59
960829-B	273	275	276.59	58.41	38.0	11.53
960829-C	273.42	275	276.59	97.51	63.5	9.42
960829-D	273.62	275	276.59	97.5	63.5	8.92
960829-E	273.83	275	276.59	127.02	82.7	8.01
960829-F	274	275	276.59	127.15	82.8	7.53
960830-A	294.67	275	276.59	35.87	23.4	14.66
960830-B	295.17	275	276.59	95.53	62.2	9.34
960830-C	295.33	275	276.59	129.66	84.4	7.64
960830-D	295.5	275	276.59	129.51	84.3	8.24
960830-E	295.67	275	276.59	94.65	61.6	9.12
960904-A	419.25	275	276.59	118.03	76.9	7.57
960904-B	419.67	275	276.59	128.27	83.5	7.42
960904-C	419.93	275	276.59	97.8	63.7	8.27
960904-D	420.33	275	276.59	97.71	63.6	8.71
960904-E	420.55	275	276.59	59.26	38.6	11.21
960904-F	420.75	275	276.59	59.26	38.6	11.32
960904-G	429	275	276.59	36.31	23.6	14.23
960904-H	429.17	300	276.59	36.77	2.39	14.14
960904-I	429.77	300	301	36.77	23.9	28.28
960904-J	430.17	300	301	36.92	24.0	28.01
960904-K	430.33	300	302.24	59.52	38.8	23.9
960904-L	430.5	300	301	59.38	38.7	23.28
960904-M	430.67	300	302.24	99.26	64.6	18.45
960904-N	430.78	300	302.24	99.16	64.6	18.5
960904-O	430.97	300	301.76	119.35	77.7	17.44
960904-P	431.08	300	302.24	126.66	82.5	16.21
960904-Q	431.33	300	301.76	126.73	82.5	16.69
960905-A	460.25	275	276.59	36.7	23.9	14.42
960905-B	460.67	275	276.59	57.93	37.7	11.42
960905-C	460.73	275	276.59	57.93	37.7	11.56

Data Set	Catalyst Time-in-Stream, h	Oven Temp, °C	Reactor Temp., °C	Reactant Feed Rate, mL/min	Reactant Feed Rate, $\mu\text{mol/s}$	Methane Fractional Conversion, %
960905-D	460.92	275	276.83	98.74	64.3	8.99
960905-E	461.5	275	276.83	99.11	64.5	8.99
960905-F	461.5	275	276.83	126.77	82.5	7.87
960905-G	461.75	275	276.83	128.49	83.7	7.77
960905-H	465.5	300	301	38.93	25.3	27.87
960905-HH	466	300	302.24	36.63	23.9	28.39
960905-I	466.17	300	302.24	58.58	38.2	23.92
960905-J	466.67	300	302.24	98.67	64.3	18.87
960905-K	466.92	300	302.24	98.67	64.3	18.93
960905-L	467.08	300	302.24	128.94	84.0	17.06
960905-M	467.17	300	302.24	128.94	8.40	17.52
960905-N	467.58	350	351.62	39.47	25.7	75.45
960905-NN	467.9	350	352.57	36.76	23.9	77.31
960905-O	468.12	350	352.57	59.39	38.7	69.22
960905-P	468.5	350	354.48	99.5	64.8	65.47
960905-Q	468.6	350	354.48	99.35	64.7	60.67
960905-R	468.7	350	354.48	127.19	82.8	56.06
960909-A	575.67	275	276.59	129.29	84.2	7
960909-B	575.83	275	276.59	129.29	84.2	7.19
960909-C	576.58	275	276.59	98.66	64.2	8.32
960909-D	576.67	275	276.59	98.68	64.3	8.11
960909-E	577.28	275	276.59	59.85	39.0	10.54
960909-F	578.50.	299	300.79	129.6	84.4	14.94
960909-G	578.62	300	301.76	129.6	84.4	14.95
960909-H	578.83	300	301.76	98.77	64.3	17.13
960909-I	579	300	302.24	98.77	64.3	18
960909-J	579.17	300	302.24	59.15	38.5	21.87
960909-K	587.42	351	353.52	125.1	81.5	47.9
960909-L	587.67	351	353.52	125.1	81.5	48.4
960909-M	587.75	350	353.52	97.32	63.4	52.83
960909-P	588.68.	399	405.31	126.97	82.7	91.7
960909-Q	588.78	399	405.79	126.97	82.7	92.06
960909-R	588.93	399	405.31	98.2	63.9	94.69
960909-S	589.07	400	405.31	98.2	63.9	95.56
960909-T	589.35	401	405.31	59.77	38.9	98.42
960909-U	590.8	425	432.26	126.57	82.4	99.3
960909-V	590.88	425	432.26	126.57	82.4	99.26

Data Set	Catalyst Time-in- Stream, h	Oven Temp, °C	Reactor Temp., °C	Reactant Feed Rate, mL/min	Reactant Feed Rate, $\mu\text{mol/s}$	Methane Fractional Conversion, %
960909-W	591.27	426	431.79	98.08	63.9	100
960909-X	591.37	426	432.26	98.33	64.0	100
960909-Y	591.65	426	429.43	59.96	39.0	100
960909-Z	591.77	426	429.43	59.96	39.0	100

Table A-4. Results for Run 4 (960926)

Catalyst: RF30 (5 mass % Pd supported on Al<sub>2</sub>O<sub>3</sub>)

Catalyst charge: 96.2 mg

State of catalyst at beginning of run: freshly reduced (State-1)

Reactor pressure: 94 to 96 kPa

Feed composition: 0.965% CH<sub>4</sub>, 3.96% O<sub>2</sub>, in He

Data Set	Catalyst Time-in-Stream, h	Oven Temp, °C	Reactor Temp., °C	Reactant Feed Rate, mL/min	Reactant Feed Rate, µmol/s	Methane Fractional Conversion, %
960926A	0.17	350	351.62	36.89	24.0	7.3
960926B	0.25	350	351.62	36.89	24.0	7.62
960926C	0.37	350	351.62	58.32	38.0	6.18
960926D	0.5	350	351.62	98.43	64.1	4.98
960926E	0.58	350	351.62	98.43	64.1	4.61
960926F	0.7	350	351.62	126.48	82.4	4.33
960926G	0.83	350	353.52	126.48	82.4	4.26
960926GG	0.95	350	353.52	126.48	82.4	4.61
960926H	1.03	375	377.33	36.95	24.1	16.39
960926I	1.28	375	377.33	58.03	37.8	13.46
960926J	1.37	375	377.33	98.54	64.2	10.24
960926K	1.73	375	377.33	98.76	64.3	10.88
960926L	1.95	375	377.33	126.72	82.5	10.02
960926M	2.06	375	377.33	126.5	82.4	9.96
960926N	2.17	399	401	37.16	24.2	31.43
960926O	2.37	400	401.29	58.3	38.0	26.36
960926P	2.62	400	402	98.55	64.2	20.68
960926Q	2.77	400	402	98.55	64.2	21.29
960926R	2.87	400	403	126.6	82.4	18.8
960926S	3.02	400	403	126.6	82.4	19.35
960926T	3.1	426	429.43	36.91	24.0	56.84
960926U	3.35	426	429.43	57.72	37.6	49.81
960926V	3.68	426	429.43	98.12	63.9	42.41
960926W	3.75	426	429.9	98.12	6.39	43.32
960926WW	3.85	426	430.37	98.12	63.9	42.22
960926X	4.02	426	431.31	127.32	82.9	42.31
960926Y	4.08	426	431	127.32	82.9	44.23
960926Z	4.27	450	454.4	37.68	24.5	88
960926A1	4.57	450	455.35	58.44	38.1	81.96
960926B1	4.68	450	456	98.52	64.2	73.76

Data Set	Catalyst Time-in-Stream, h	Oven Temp, °C	Reactor Temp., °C	Reactant Feed Rate, mL/min	Reactant Feed Rate, $\mu\text{mol/s}$	Methane Fractional Conversion, %
960926C1	5.93	450	458.64	98.45	64.1	91.33
960926E1	6.23	450	459.58	126.4	82.3	91.27
960926F1	6.88	474	475.57	37.89	24.7	100
960926G1	7.02	474	479	58.41	38.0	100
960926J1	7.12	474	483.79	127.19	82.8	98.6
960926K1	7.18	475	485	129.19	84.1	98.98
960926H1*	7.32	475	485	99.36	64.7	100

Table A-5. Results for Run 5 (961016)

Catalyst: RF30 (5 mass % Pd supported on Al<sub>2</sub>O<sub>3</sub>)

Catalyst charge: 96.2 mg

Previous runs in which catalyst charge was used: Run 4 (960926)

State of catalyst at beginning of run: activated (State-2)

Reactor pressure: 94 to 96 kPa

Feed composition: 0.965% CH<sub>4</sub>, 3.96% O<sub>2</sub>, in He

Data Set	Catalyst Time-in-Stream, h	Oven Temp, °C	Reactor Temp., °C	Reactant Feed Rate, mL/min	Reactant Feed Rate, μmol/s	Methane Fractional Conversion, %
961016A	18.15	150	148.58	37.47	24.4	0
961016B	18.27	149	149	37.47	24.4	0
961016C	18.35	200	199.58	36.39	23.7	0
961016D	18.5	229	230	37.34	2.43	0.7
961016E	18.75	229	230	57.89	37.7	0.88
961016F	18.87	230	230	97.56	63.5	0
961016G	19.03	230	231.48	97.56	63.5	0.46
961016H	19.25	230	231.48	125.47	81.7	0
961016I	19.37	230	230	125.47	8.17	0
961016J	19.45	275	276.59	36.5	23.8	9.61
961016K	19.67	275	276.59	57.91	37.7	8.19
961016L	19.82	275	276.59	97.58	63.5	5.92
961016M	19.93	275	277	97.58	63.5	5.99
961016N	20.07	275	277	126.09	82.1	5.11
961016O	20.17	275	277	126.09	82.1	5.16
961016P	20.27	325	327.71	36.6	23.8	38.64
961016Q	20.52	325	327.71	58.46	38.1	31.7
961016R	20.73	325	328.67	97.28	63.3	24.18
961016S	20.83	325	328.67	97.28	6.33	24.11
961016T	20.98	325	328.67	125.63	81.8	21.38
961016U	21.08	325	328.67	125.63	81.8	21.35
961016V	21.33	375	379.24	36.39	23.7	80.66
961016W	21.97	375	380.19	58.03	37.8	72.74
961016X	21.75	375	382	97.08	63.2	62.62
961016Y	21.88	375	382	97.08	63.2	62.23
961016ZZ	22.17	375	382	126.42	82.3	57.16
961016A1*	22.25	375	382	126.42	82.3	57.18

Data Set	Catalyst Time-in-Stream, h	Oven Temp, °C	Reactor Temp., °C	Reactant Feed Rate, mL/min	Reactant Feed Rate, $\mu\text{mol/s}$	Methane Fractional Conversion, %
961016AA1	22.7	375	382.56	126.42	82.3	57.26
961016B1	22.83	424	427.53	36.37	23.7	100
961016C1	23.2	425	430.84	58.06	37.8	97.39
961016D1	23.53	425	434.14	96.92	63.1	93.46
961016E1	23.67	425	434.62	96.92	63.1	93.79
961016F1	23.95	425	435.56	126.04	82.1	90.67
961016G1	24.03	425	435.56	126.04	82.1	90.85
961016H1	24.48	453	463.81	126.4	82.3	98.53
961016I1	24.53	454	461.47	97.84	63.7	100
961016J1	24.9	454	461.47	93.68	61.0	100
961016K1	24.98	455	461.47	93.68	61.0	100

Table A-6. Results for Run 6 (970404)

Catalyst: YW114 (5 mass % Pd supported on  $\text{SiO}_2$ )

Catalyst charge: 96.2 mg

State of catalyst at beginning of run: freshly reduced (State-1)

Reactor pressure: 94 to 96 kPa

Feed composition: 0.965%  $\text{CH}_4$ , 3.96  $\text{O}_2\%$  in He

Data Set	Catalyst Time-in-Stream, h	Oven Temp, °C	Reactor Temp., °C	Reactant Feed Rate, mL/min	Reactant Feed Rate, $\mu\text{mol/s}$	Methane Fractional Conversion, %
970404A	0.17	199	197.58	127.44	83.0	0
970404B	0.33	200	197.58	127.44	83.0	0
970404C	0.45	249	247.51	127.24	83.0	4.36
970404D	0.53	249	248.24	127.24	83.0	6.25
970404E	0.65	299	299.83	126.41	82.3	60.65
970404F	0.77	299	300.79	126.41	82.3	65.87
970404G	0.88	343	345	125.87	82.0	100
970404H	0.97	343	345	125.87	82.0	100
970404I	1.63	343	345.4	125.87	82.0	100
970404J	1.75	343	345.4	125.87	82.0	100
970405A	22.78	345	346.6	127.24	82.9	100
970405B	22.88	345	346.6	127.24	82.9	100

Table A-7. Results for Run 7 (970406)

Catalyst: YW114 (5 mass % Pd supported on SiO<sub>2</sub>)

Catalyst charge: 96.2 mg

Previous runs in which catalyst charge was used: Run 6

State of catalyst at beginning of run: activated (State-2)

Reactor pressure: 94 to 96 kPa

Feed composition: 0.965% CH<sub>4</sub>, 3.96 O<sub>2</sub>% in He

Data Set	Catalyst Time-in-Stream, h	Oven Temp, °C	Reactor Temp., °C	Reactant Feed Rate, mL/min	Reactant Feed Rate, μmol/s	Methane Fractional Conversion, %
970406A	23.05	174	171.53	126.9	82.6	0
970406B	23.16	174	171.53	126.9	82.6	0
970406C	23.38	198	197.08	127.2	82.8	2.66
970406D	23.5	198	197.08	127.2	82.8	2.59
970406E	23.88	249	248.24	126.45	82.3	19.28
970406F	23.98	249	248.73	126.45	82.3	18.94
970406G	24.3	274	275.61	126.01	82.1	42.82
970406H	24.41	274	275.61	126.01	82.1	43.05
970406I	24.9	300	301.76	125.87	82.0	76.89
970406J	25	300	301.76	125.87	82.0	76.86
970406K	25.38	325	326.26	125.7	81.9	97.58
970406L	25.46	325	326.26	125.7	81.9	97.76
970406M	25.8	335	335.37	125.48	81.7	100
970406O	25.9	342	344	125.48	81.7	100



Table A-8. Results for Run 8 (971214)

Catalyst: YW114 (5 mass % Pd supported on SiO<sub>2</sub>)

Catalyst charge: 96.2 mg

State of catalyst at beginning of run: freshly reduced (State-1)

Reactor pressure: 94 to 96 kPa

Feed composition: 0.965% CH<sub>4</sub>, 3.96% O<sub>2</sub> in He

Data Set	Catalyst Time-in-Stream, h	Oven Temp, °C	Reactor Temp., °C	Reactant Feed Rate, mL/min	Reactant Feed Rate, μmol/s	Methane Fractional Conversion, %
971214A	0.08	249	248.73	128.63	83.8	0
971214B	0.32	273	271.73	128.63	83.8	4.16
971214C	0.42	273	271.73	128.63	83.8	4.58
971214D	0.53	300	302.24	127.03	82.7	56.74
971214E	0.62	300	302.24	127.03	82.7	61.22
971214F	0.73	324	328.67	126.16	82.2	92.8
971214G	0.83	324	328.67	126.16	82.2	93.91
971214H	0.95	339	344	125.91	82.0	100
971214I	1.03	339	344	125.91	82.0	100

Table A-9. Results for Run 9 (971215)

Catalyst: YW114 (5 mass % Pd supported on SiO<sub>2</sub>)

Catalyst charge: 96.2 mg

Previous runs in which catalyst charge was used: Run 8

State of catalyst at beginning of run: activated (State-2)

Reactor pressure: 94 to 96 kPa

Feed composition: 0.965% CH<sub>4</sub>, 3.96% O<sub>2</sub> in He

Data Set	Catalyst Time-in-Stream, h	Oven Temp, °C	Reactor Temp., °C	Reactant Feed Rate, mL/min	Reactant Feed Rate, μmol/s	Methane Fractional Conversion, %
971215A	19.7	149	146.6	127.93	83.3	0
971215B	19.81	174	171	127.93	83.3	0.48
971215D	20.15	225	223	127.93	83.3	7.47
971215E	20.25	251	250	127.93	83.3	17.65
971215F	20.36	276	276.59	127.93	83.3	39.6
971215G	20.56	310	314	127.93	83.3	84.07
971215H	20.68	322	322.24	127.93	83.3	94.05
971215I	20.85	340	344.21	127.93	83.3	100
971215J	20.95	340	344.21	127.93	83.3	100



Table A-10. Results for Run 10 (970705)

Catalyst: RF36 (5 mass % Pd supported on SiO<sub>2</sub>)

Catalyst charge: 96.2 mg

State of catalyst at beginning of run: freshly reduced (State-1)

Reactor pressure: 94 to 96 kPa

Feed composition: 0.965% CH<sub>4</sub>, 3.96% O<sub>2</sub>, in He

Data Set	Catalyst Time-in-Stream, h	Oven Temp, °C	Reactor Temp., °C	Reactant Feed Rate, mL/min	Reactant Feed Rate, μmol/s	Methane Fractional Conversion, %
970705-A	0.08	200	197.58	127.95	83.3	0
970705-B	0.45	249	247.27	127.52	83.0	0
970705-C	0.57	249	247.27	127.52	83.0	0.9
970705-D	0.75	275	273.17	127.32	82.9	5.47
970705-DD	0.88	275	273.17	127.32	82.9	6.23
970705-E	1.08	299	297.4	127.05	82.7	14.35
970705-EE	1.2	299	297.4	127.05	82.7	14.83
970705-F	1.42	348	345.4	126.96	82.7	45.57
970705-G	1.5	348	345.4	126.96	82.7	47.93
970705-H	1.87	399	395.37	126.37	82.3	77.77
970705-I	1.97	399	396.31	126.37	82.3	77.41
970705-J	2.43	449	446	125.96	82.0	88.04
970705-K	2.55	449	445	125.96	82.0	87.17
970705-L	2.98	475	472	125.51	81.7	90.15

Table A-11. Results for Run 11 (970708)

Catalyst: RF36 (5 mass % Pd supported on SiO<sub>2</sub>)

Catalyst charge: 96.2 mg

Previous runs in which catalyst charge was used: Run 10

State of catalyst at beginning of run: activated (State-2)

Reactor pressure: 94 to 96 kPa

Feed composition: 0.965% CH<sub>4</sub>, 3.96% O<sub>2</sub>, in He

Data Set	Catalyst Time-in-Stream, h	Oven Temp, °C	Reactor Temp., °C	Reactant Feed Rate, mL/min	Reactant Feed Rate, μmol/s	Methane Fractional Conversion, %
970708-A	21.15	200	196.58	127.46	83.0	0
970708-B	21.65	250	247.51	126.48	82.4	0
970708-C	21.72	250	247.51	126.48	82.4	0
970708-D	21.98	276	274.15	126.98	82.7	0
970708-E	22.08	276	273.17	126.98	82.7	0
970708-F	22.4	299	296	127.04	82.7	1.35
970708-G	22.6	299	296.44	127.04	82.7	1.34
970708-H	22.85	349	345.4	127.4	83.0	6.29
970708-I	23.1	349	347	127.4	83.0	6.43
970708-J	23.4	400	396.55	127.11	82.8	20.96
970708-K	23.48	400	396.55	127.11	82.8	21.48
970708-L	23.73	448	442.63	127.35	82.9	44.92
970708-M	23.83	448	442.63	127.35	82.9	46.18
970708-N	23.98	474	370.29	126.46	82.3	60.51
970708-O	24.23	474	370.29	126.46	82.3	62.62

Table A-12. Results for Run 12 (970225)

Catalyst: YW104 (5 mass % Fe supported on Al<sub>2</sub>O<sub>3</sub>)  
 Catalyst charge: 96.2 mg  
 State of catalyst at beginning of run: freshly reduced (State-1)  
 Reactor pressure: 94 to 96 kPa  
 Feed composition: 0.965% CH<sub>4</sub>, 3.96% O<sub>2</sub> in He

Data Set	Catalyst Time-in-Stream, h	Oven Temp, °C	Reactor Temp., °C	Reactant Feed Rate, mL/min	Reactant Feed Rate, μmol/s	Methane Fractional Conversion, %
970225A	0.08	350	351.38	126.34	82.3	0
970225B	0.25	350	351.38	126.34	82.3	0
970225C	0.55	350	351.38	31.82	20.7	0
970225E	1	399	398.69	125.44	81.7	0
970225F	1.37	424	424	126.25	82.2	1.2
970225G	1.45	424	424	126.25	82.2	1.29
970225H	1.82	449	449.23	126.27	82.2	2.32
970225I	1.9	449	449.23	126.27	82.2	2.41
970225J	2.32	474	473.7	126.12	82.1	4.63

Table A-13. Results for Run 13 (970301)

Catalyst: YW104 (5 mass % Fe supported on Al<sub>2</sub>O<sub>3</sub>)  
 Catalyst charge: 96.2 mg  
 Previous runs in which catalyst charge was used: Run 12  
 State of catalyst at beginning of run: activated (State-2)  
 Reactor pressure: 94 to 96 kPa  
 Feed composition: 0.965% CH<sub>4</sub>, 3.96% O<sub>2</sub> in He

Data Set	Catalyst Time-in-Stream, h	Oven Temp, °C	Reactor Temp., °C	Reactant Feed Rate, mL/min	Reactant Feed Rate, μmol/s	Methane Fractional Conversion, %
970301A	23.82	350	349.71	127.12	82.8	0
970301B	23.93	350	349.71	127.12	82.8	0
970301C	24.17	399	397.74	127.43	83.0	0
970301D	24.28	399	398.21	127.43	83.0	0
970301E	24.65	449	448.29	127.06	83.0	2.5
970301F	24.82	449	448.29	127.06	83.0	2.61
970301G	24.92	474	473.23	127.15	83.0	4.48
970301H	25.02	474	473.23	127.15	83.0	4.42

Table A-14. Results for Run 14 (970106)

Catalyst: YW102 (5 mass % Fe + 5 mass % Pd supported on Al<sub>2</sub>O<sub>3</sub>)

Catalyst charge: 96.2 mg

State of catalyst at beginning of run: freshly reduced (State-1)

Reactor pressure: 94 to 96 kPa

Feed composition: 0.965% CH<sub>4</sub>, 3.96% O<sub>2</sub> in He

Data Set	Catalyst Time-in-Stream, h	Oven Temp, °C	Reactor Temp., °C	Reactant Feed Rate, mL/min	Reactant Feed Rate, μmol/s	Methane Fractional Conversion, %
970106A	0.08	351	352.57	129.97	84.6	1.72
970106B	0.2	351	351.62	129.97	84.6	1.89
970106C	0.32	351	351.62	95.03	61.9	2.26
970106D	0.47	351	351.14	58.07	37.8	3.46
970106E	0.63	351	351.14	48.69	31.7	5.35
970106F	0.73	375	375.19	129.44	84.3	4.21
970106G	0.83	375	374.48	94.24	61.4	5.62
970106H	1.15	375	375.19	58.62	38.2	8.18
970106I	1.32	375	375.19	37	24.1	11.33
970107A	1.4	399	399.64	128.53	83.7	9.57
970107B	1.53	399	400.12	128.53	83.7	9.82
970107C	1.67	400	400.58	94.22	61.7	12.44
970107D	1.8	400	400.58	58.47	38.1	17.36
970107E	1.95	400	400.58	36.9	24.0	23.8
970107F	2.25	424	426.12	129.53	84.3	18.75
970107G	2.42	424	426.12	129.53	84.3	18.94
970107H	2.53	425	426.12	95.77	62.4	23.56
970107I	2.68	425	426.12	58.78	38.1	31.88
970107J	2.95	425	426.12	36.82	23.0	41.62
970107K	3.05	474	476.74	130	84.7	51.04
970107L	3.22	474	479	130	84.7	51.57
970107M	3.32	475	479	94.84	61.8	59.31
970107N	3.45	475	478	58.04	37.8	71.3
970107O	3.55	475	476.74	37.16	24.2	81.07
970107P	3.65	524	530.72	128.23	83.5	86.13
970107Q	3.75	525	530.72	94.64	61.6	89.73
970107R	3.85	550	557.7	128.67	83.8	95.43
970107S	3.95	550	553	36.82	24.0	100

Table A-15. Results for Run 15 (970108)

Catalyst: YW102 (5 mass % Fe + 5 mass % Pd supported on Al<sub>2</sub>O<sub>3</sub>)

Catalyst charge: 96.2 mg

Previous runs in which catalyst charge was used: Run 14

State of catalyst at beginning of run: activated (State-2)

Reactor pressure: 94 to 96 kPa

Feed composition: 0.965% CH<sub>4</sub>, 3.96% O<sub>2</sub> in He

Data Set	Oven Temp, °C	Reactor Temp., °C	Reactant Feed Rate, mL/min	Reactant Feed Rate, $\mu$ mol/s	Methane Fractional Conversion, %
970108A	249	250.71	127.13	82.8	0
970108B	249	250.71	34.9	22.7	0
970108C	274	275.12	127.46	83.0	0
970108D	275	275.61	37.1	24.2	0
970108E	324	323.88	36.64	23.9	2.11
970108F	324	323.88	125.26	81.6	0
970108H	348	348.76	125.81	81.9	1.38
970108I	349	348.76	95.03	61.9	1.49
970108J	349	348.76	59.05	38.5	2.72
970108K	350	349	37.18	24.2	3.85
970108L	376	377.33	125.98	82.0	2.95
970108M	376	377.33	95.02	61.9	3.49
970108N	376	376.38	58.44	38.1	5.43
970108O	376	376.38	37.1	24.2	7.09
970110N	426	427.29	127.29	82.9	13.21
970110O	426	427.07	96.49	62.8	14.99
970110Q	426	426.12	36.91	24.0	26.96
970110P	426	427.07	58.49	38.1	19.74
970110J	475	479	126.54	82.4	37.88
970110K	475	476.74	95.38	62.1	42.3
970110M	475	476.16	37.27	24.3	63.39
970110L	475	476.74	58.65	38.2	53.77
970110A	501	505.51	125.93	82.0	49.47
970110B	501	505	94.88	61.8	55.53
970110C	501	505	58.08	37.8	67.68
97010D	501	502.58	34.07	22.2	79.4
970110E	525	532	125.87	82.0	72.36
970110F	525	529.56	94.24	61.4	76.67
970110G	549	555.35	126.06	82.1	84.16

Table A-16. Results for Run 16 (970205)

Catalyst: YW103 (0.5 mass % Fe + 5 mass % Pd supported on Al<sub>2</sub>O<sub>3</sub>)

Catalyst charge: 96.2 mg

State of catalyst at beginning of run: freshly reduced (State-1)

Reactor pressure: 94 to 96 kPa

Feed composition: 0.965% CH<sub>4</sub>, 3.96% O<sub>2</sub> in He

Data Set	Catalyst Time-on-Stream, h	Oven Temp., °C	Reactor Temp., °C	Reactant Feed Rate, mL/min	Reactant Feed Rate, µmol/s	Methane Fractional Conversion, %
970205A	0.08	275	275.12	127.51	83.0	0
970205B	0.2	275	275.12	127.51	83.0	0
970205C	0.27	275	272.12	35.02	22.8	0
970205D	0.42	350	349.24	127.23	82.8	1.3
970205E	0.92	350	350.19	127.13	82.8	1.36
970205F	1.03	375	375.19	126.58	82.4	3.59
970205G	1.17	375	375	126.58	82.4	3.86
970205H	1.28	424	423.29	126.38	82.3	13.01
970205I	1.42	424	423.76	126.38	83.0	11.9
970205J	1.52	449	448.52	126.7	82.5	20.5
970205K	1.62	449	448.76	126.7	82.5	20.86
970205L	1.73	475	474.4	125.57	81.8	36.2
970205M	1.88	475	474.16	125.57	81.8	40.16
970205N	1.93	475	473.23	23.61	15.4	82.59
970205O	2.15	475	473.23	23.61	15.4	83.84



Table A-17. Results for Run 17 (970208)

Catalyst: YW103 (0.5 mass % Fe + 5 mass % Pd supported on Al<sub>2</sub>O<sub>3</sub>)

Catalyst charge: 96.2 mg

Previous runs in which catalyst charge was used: Run 16

State of catalyst at beginning of run: activated (State-2)

Reactor pressure: 94 to 96 kPa

Feed composition: 1% CH<sub>4</sub>, 4% O<sub>2</sub>, 95% He

Data Set	Catalyst Time-on-Stream, h	Oven Temp., °C	Reactor Temp., °C	Reactant Feed Rate, mL/min	Reactant Feed Rate, μmol/s	Methane Fractional Conversion, %
970208A	31.5	250	249.73	127.79	83.2	0
970208B	31.63	250	248.73	127.79	83.2	0.84
970208C	32.83	249	248.73	34.08	22.2	1.72
970208CC	33.03	250	249.23	128.48	83.7	0.88
970208D	33.3	274	274.39	128.21	83.5	2.22
970208E	33.5	275	274.39	128.21	83.5	1.89
970208F	34.48	326	325	128	83.3	11.26
970208G	34.68	326	325	128	83.3	11.51
970208H	35.26	374	374	126.64	82.5	33.03
970208I	35.39	374	374.48	126.64	82.5	32.91
970208J	35.68	425	426.12	126.9	82.6	65.38
970208K	35.79	425	426.12	126.9	82.6	64.72
970208L	36.18	475	474.63	125.97	82.0	86.85
970208M	36.31	475	474.63	125.97	82.0	86.71
970208N	36.71	475	473.23	23.61	15.4	100
970208O	36.83	475	473.23	23.61	15.4	100

Table A-18. Results for Run 18 (970121)

Catalyst: RF34 (5 mass % Pd supported on Al<sub>2</sub>O<sub>3</sub>)

Catalyst charge: 96.2 mg

State of catalyst at beginning of run: freshly reduced (State-1)

Reactor pressure: 94 to 96 kPa

Feed composition: 0.23% CH<sub>4</sub>, 1.96% O<sub>2</sub>, 97.81% He

Data Set	Catalyst Time-on-Stream, h	Oven Temp., °C	Reactor Temp., °C	Reactant Feed Rate, mL/min	Reactant Feed Rate, µmol/s	Methane Fractional Conversion, %
970121A	0.08	325	325	126.94	82.7	0
970121B	0.2	325	325	95.48	62.2	0
970121C	0.47	325	325.79	37.46	24.4	4.04
970121D	0.58	349	349.71	126.42	82.3	0
970121E	0.73	350	350.19	95.75	62.3	0
970121F	0.88	350	350.67	58.76	38.3	4.6
970121G	1.22	350	350.67	37.41	24.4	7.33
970121H	1.3	374	374.48	125.6	81.8	5.71
970121I	1.42	374	374.48	96.27	62.7	8.24
970121J	1.6	374	375.43	58.8	38.3	10.48
970121K	1.78	375	375.43	37.08	24.1	15.14
970121L	1.87	400	401	127.27	82.9	12.06
970121M	1.97	400	401	95.12	61.9	17.23
970121N	2.15	400	401	58.74	38.2	21.33
970121P	2.25	425	426.12	127.11	82.8	27.31
970121Q	2.37	425	426.12	95.88	62.4	33.58
970121R	2.48	425	426.12	58.56	38.1	45.05
970121S	2.75	425	426.12	36.85	24.0	52.41
970121T	2.83	449	449.7	126.64	82.5	49.53
970121U	2.93	449	449.7	95.39	62.1	58.69
970121V	3.05	450	449.7	58.04	37.8	72.25
970121W	3.27	450	449.7	36.99	24.1	87.86
970121X	3.4	473	475.57	126.24	82.2	79.2
970121Y	3.52	474	475.57	94.85	61.8	89.24
970121Z	3.67	474	475.57	58.26	37.9	100
970121A1	3.77	475	475.57	36.68	23.9	100
970121B1	3.87	490	488.49	126.18	82.2	100

Data Set	Catalyst Time-on-Stream, h	Oven Temp., °C	Reactor Temp., °C	Reactant Feed Rate, mL/min	Reactant Feed Rate, $\mu\text{mol/s}$	Methane Fractional Conversion, %
970121C1	3.97	490	490.84	95.66	62.3	100
Kept running at 476°C with reactants						
970122A	21.42	476	475.57	126.65	82.5	100
970122B	21.55	476	475.57	126.65	82.5	100

Table A-19. Results for Run 19 (970127)

Catalyst: RF34 (5 mass % Pd supported on Al<sub>2</sub>O<sub>3</sub>)

Catalyst charge: 96.2 mg

Previous runs in which catalyst charge was used: Run 18

State of catalyst at beginning of run: activated (State-2)

Feed composition: 0.23% CH<sub>4</sub>, 1.96% O<sub>2</sub>, 97.81% He

Data Set	Catalyst Time-on-Stream, h	Reactor Pressure, Psia	Oven Temp., °C	Reactor Temp., °C	Reactant Feed Rate, mL/min	Reactant Feed Rate, $\mu$ mol/s	Methane Fractional Conversion, %
970127A	21.63	13.76	250	259	126.36	82.3	0
970127B	22.18	13.76	275	276.59	125.88	82.0	6.03
970127C	22.3	13.76	275	276.59	125.9	82.0	7.34
970127D	22.6	57.76	275	276.59	529.32	344.8	5.33
970127E	22.71	57.76	275	276.59	529.32	344.7	4.84
970127F	24.46	13.76	325	325.79	126.61	82.4	48.84
970127G	24.63	13.76	325	325.79	126.61	82.4	48.38
970127H	25.13	57.76	325	326.74	528.26	344.0	31.03
970127I	25.25	57.76	325	326.74	528.26	344.0	31.12
970127J	25.71	13.76	375	374	125.8	81.9	97.79
970127K	25.93	13.76	375	375	125.8	81.9	97.22
970127L	26.3	57.76	375	377.57	528.26	344.0	82.51
970127M	26.43	57.76	375	377.57	528.26	344.0	83.72
970127N	26.86	13.76	425	424.7	126.34	82.3	100
970127O	27.05	13.76	425	425	126.34	82.3	100
970127Q	28.2	60.76	425	427	528.59	344.2	100
970127R	28.25	60.76	425	427	528.59	344.2	100

Table A-20. Results for Run 20 (970128)

Catalyst: RF34 (5 mass % Pd supported on Al<sub>2</sub>O<sub>3</sub>)

Catalyst charge: 96.2 mg

Previous runs in which catalyst charge was used: Run 18 and 19

State of catalyst at beginning of run: activated (State-2)

Reactor pressure: 94 to 96 kPa

Feed composition: 0.965% CH<sub>4</sub>, 3.96% O<sub>2</sub> in He

Data Set	Catalyst Time-in-Stream, h	Oven Temp, °C	Reactor Temp., °C	Reactant Feed Rate, mL/min	Reactant Feed Rate, μmol/s	Methane Fractional Conversion, %
970128A	28.33	249	249.23	126.01	82.1	2.19
970128B	28.48	249	250.22	126.01	82.1	2.17
970128C	28.83	274	275.12	125.72	81.9	6
970128D	28.97	274	275.61	125.72	81.9	5.96
970128E	29.48	324	325	126.17	82.2	28.86
970128F	29.62	324	325.79	126.17	82.2	29.08
970128G	30.02	373	377.33	125.59	81.8	77.31
970128GG	30.13	374	377.33	125.59	81.8	77.54
970128H	30.27	374	378.29	125.59	81.8	78.05
970128I	30.73	399	403	126.07	82.1	94.61
970128J	30.88	400	403	126.07	82.1	94.49
970128K	31.62	425	428.48	125.74	81.9	100
970128L	32.02	425	428.48	125.74	81.9	100
970128M	32.1	425	428.48	125.74	81.9	100
970128N	32.55	425	428.48	125.74	81.9	100

Table A-21. Results for Run 21 (970201)

Catalyst: RF34 (5 mass % Pd supported on Al<sub>2</sub>O<sub>3</sub>)

Catalyst charge: 96.2 mg

Previous runs in which catalyst charge was used: Run 18 to 20

State of catalyst at beginning of run: activated (State-2)

Feed composition: 0.23% CH<sub>4</sub>, 1.96% O<sub>2</sub>, 97.81% He

Data Set	Catalyst Time-on-Stream, h	Reactor Pressure, Psia	Oven Temp., °C	Reactor Temp., °C	Reactant Feed Rate, mL/min	Reactant Feed Rate, $\mu$ mol/s	Methane Fractional Conversion, %
970201A	32.63	13.47	250	252.17	128	83.3	5.22
970201B	32.8	13.47	250	251.2	128	83.3	4.07
970201C	33.05	56.47	250	251.2	543.37	353.8	0
970201E	33.38	56.47	274	275.61	542.89	353.5	5.03
970201F	33.51	56.47	274	275.61	542.89	353.5	6.08
970201G	34.34	13.47	276	278	128	83.3	13.17
970201H	34.46	13.47	276	277.56	128	83.3	13.82
970201HH	35.3	13.47	275	276.59	127.23	82.8	12.39
970201I	37.71	13.47	325	327.46	127.23	82.8	52.74
970201J	37.81	13.47	325	327.46	127.23	82.8	51.9
970201K	38.2	56.47	325	328.19	539.08	351.0	29.29
970201L	38.31	56.47	325	328.19	539.08	351.0	30.31
970201M	38.63	56.47	374	377.81	538.02	350.3	76.83
970201N	38.8	56.47	374	377.57	538.02	350.3	76.86
970201O	38.95	13.47	374	375.19	126.4	82.3	100
970201P	39.13	13.47	375	376.38	125.72	81.9	100
970201R	39.41	13.47	399	401	126.48	82.4	100
970201S	39.83	57.47	400	404.84	538.7	350.8	94.97
970201T	40.13	56.47	400	404.84	539.83	351.5	94.79
970201U	40.71	56.47	425	428.48	540.3	351.8	100
970201V	40.83	56.47	425	428.48	540.3	351.8	100

Table A-22. Results for Run 22 (970319)

Catalyst: YW107 (5 mass % Pd + 5 mass % Fe supported on SiO<sub>2</sub>)

Catalyst charge: 96.2 mg

State of catalyst at beginning of run: freshly reduced (State-1)

Reactor pressure: 94 to 96 kPa

Feed composition: 0.965% CH<sub>4</sub>, 3.96% O<sub>2</sub> in He

Data Set	Catalyst Time-in-Stream, h	Oven Temp, °C	Reactor Temp., °C	Reactant Feed Rate, mL/min	Reactant Feed Rate, μmol/s	Methane Fractional Conversion, %
970319A	0.08	251	250	126.74	82.5	0
970319B	0.22	250	250.22	126.74	82.5	0
970319C	0.32	302	300.79	126.48	82.4	0
970319D	0.4	302	300.79	126.48	82.4	0
970319E	0.47	375	372.81	126.29	82.2	0
970319F	0.57	375	372.81	126.29	82.2	0
970319G	0.67	401	398.21	126.7	82.5	0.76
970319H	0.85	401	398.21	126.7	82.5	2.06
970319I	1	424	421.86	126.5	82.4	4.21
970319J	1.09	424	421.86	126.5	82.4	5.69
970319K	1.19	449	445	126.5	82.4	12.61
970319L	1.37	450	446.76	126.5	82.4	19.5
970319M	1.47	473	470.88	126.17	82.2	30.63
970319N	1.57	473	470.88	126.17	82.2	34.02
970319O	2.69	475	473.23	125.93	82.0	33.03
970319P	2.77	475	473.23	125.93	82.0	33.51

Table A-23. Results for Run 23 (970324)

Catalyst: YW107 (5 mass % Pd + 5 mass % Fe supported on SiO<sub>2</sub>)

Catalyst charge: 96.2 mg

Previous runs in which catalyst charge was used: Run 22

State of catalyst at beginning of run: activated (State-2)

Reactor pressure: 94 to 96 ka

Feed composition: 0.965% CH<sub>4</sub>, 3.96% O<sub>2</sub> in He

Data Set	Catalyst Time-in-Stream, h	Oven Temp, °C	Reactor Temp., °C	Reactant Feed Rate, mL/min	Reactant Feed Rate, μmol/s	Methane Fractional Conversion, %
970324A	19.44	326	323.88	126.66	82.5	3.32
970324B	19.52	325	323.88	126.66	82.5	3.32
970324C	20.49	302	300.79	127.23	82.8	1.32
970324D	20.6	301	300.79	127.23	82.8	1.39
970324E	20.85	373	371.62	127.21	82.8	7.31
970324F	20.94	374	371.62	127.21	82.8	6.53
970324G	21.04	398	395.84	127.19	82.8	9.84
970324H	21.14	398	395.84	126.77	82.5	8.9
970324I	21.35	423	421.4	128.95	84.0	12.56
970324J	21.47	423	420.21	128.95	84.0	11.98
970324K	21.77	448	446.76	128.19	83.5	17.73
970324L	21.85	448	445	128.19	83.5	16.79
970324M	21.99	449	445	128.19	83.5	16.45
970324N	22.2	474	470.88	128.51	83.7	23.34
970324O	22.29	474	470.88	128.51	83.7	22.56
970324P	22.39	474	470.88	128.51	83.7	21.98
970324Q	22.6	475	470.88	128.51	83.7	21.34



Table A-24. Results for Run 24 (970325)

Catalyst: YW112 (5 mass % Pd + 0.5 mass % Fe supported on SiO<sub>2</sub>)

Catalyst charge: 96.2 mg

State of catalyst at beginning of run: freshly reduced (State-1)

Reactor pressure: 94 to 96 kPa

Feed composition: 0.965% CH<sub>4</sub>, 3.96% O<sub>2</sub> in He

Data Set	Catalyst Time-in-Stream, h	Oven Temp, °C	Reactor Temp., °C	Reactant Feed Rate, mL/min	Reactant Feed Rate, µmol/s	Methane Fractional Conversion, %
970325A	0.08	250	248.73	128.11	83.4	0
970325B	0.18	250	249.23	128.11	83.4	0
970325C	0.28	300	298.61	128.76	83.8	0
970325D	0.43	300	298.61	128.76	83.8	0
970325E	0.53	351	349	129.66	84.4	2.77
970325F	0.7	351	349	129.66	84.4	3.52
970325G	0.8	398	397.26	126.8	82.6	9.37
970325I	0.89	423	422.33	126.35	82.3	14.28
970325J	1.03	423	421.4	126.35	82.3	13.63
970325K	1.13	448	447.35	125.93	82.0	17.81
970325L	1.21	448	447.35	125.93	82.0	17.38
970325M	1.3	473	473.23	125.83	81.9	21.75
970325N	1.4	473	473.23	125.83	81.9	21.56
970325O	1.53	474	473.23	126.03	82.1	21.74

Table A-25. Results for Run 25 (970329)

Catalyst: YW112 (5 mass % Pd + 0.5 mass % Fe supported on SiO<sub>2</sub>)

Catalyst charge: 96.2 mg

Previous runs in which catalyst charge was used: Run 24

State of catalyst at beginning of run: activated (State-2)

Reactor pressure: 94 to 96 kPa

Feed composition: 0.965% CH<sub>4</sub>, 3.96% O<sub>2</sub> in He

Data Set	Catalyst Time-in-Stream, h	Oven Temp, °C	Reactor Temp., °C	Reactant Feed Rate, mL/min	Reactant Feed Rate, μmol/s	Methane Fractional Conversion, %
970329A	20.06	249	248.24	127.15	82.8	0
970329B	20.23	249	248.24	127.15	82.8	0
970329C	20.55	298	296.44	127.05	82.7	2.27
970329D	20.68	298	297.4	127.05	82.7	1.88
970329E	21.01	348	346.83	126.96	82.7	5.26
970329F	21.26	349	347.8	126.96	82.7	3.71
970329G	21.71	402	401.29	126.7	82.5	8.93
970329H	21.81	402	400.12	126.7	82.5	7.55
970329I	21.9	401	400.12	126.56	82.4	6.84
970329J	22.2	449	447.35	127.02	82.7	13.7
970329K	22.31	449	446.76	127.02	82.7	11.98
970329L	22.66	475	473.23	126.44	82.3	16
970329M	22.71	475	473.23	126.44	82.3	15.56
970329N	22.81	475	473.23	126.44	82.3	15.48
970329O	22.91	475	473.23	126.52	82.4	15.23
970329P	23.06	475	473.23	126.52	82.4	14.71

Table A-26. Results for Run 26 (970331)

Catalyst: YW113 (5 mass % Pd + 0.1 mass % Cu supported on SiO<sub>2</sub>)

Catalyst charge: 96.2 mg

State of catalyst at beginning of run: freshly reduced (State-1)

Reactor pressure: 94 to 96 kPa

Feed composition: 0.965% CH<sub>4</sub>, 3.96% O<sub>2</sub> in He

Data Set	Catalyst Time-in-Stream, h	Oven Temp, °C	Reactor Temp., °C	Reactant Feed Rate, mL/min	Reactant Feed Rate, µmol/s	Methane Fractional Conversion, %
970331A	0.08	249	250	127.78	83.2	3.09
970331B	0.18	250	250.22	127.75	83.2	4.57
970331C	0.28	301	306.57	126.61	82.4	45.33
970331D	0.4	301	307	126.25	82.2	48.05
970331E	0.5	348	357.33	125.6	81.8	97.82
970331F	0.62	348	357.33	125.6	81.8	98.18
970331G	0.73	374	381.14	125.69	81.8	100
970331H	0.85	374	381.14	125.69	81.8	100

Table A-27. Results for Run 27 (970401)

Catalyst: YW113 (5 mass % Pd + 0.1 mass % Cu supported on SiO<sub>2</sub>)

Catalyst charge: 96.2 mg

Previous runs in which catalyst charge was used: Run 26

State of catalyst at beginning of run: activated (State-2)

Reactor pressure: 94 to 96 kPa

Feed composition: 0.965% CH<sub>4</sub>, 3.96% O<sub>2</sub> in He

Data Set	Catalyst Time-in-Stream, h	Oven Temp, °C	Reactor Temp., °C	Reactant Feed Rate, mL/min	Reactant Feed Rate, µmol/s	Methane Fractional Conversion, %
970401A	10.95	375	381.62	126.61	82.4	100
970401B	11.07	375	381.14	126.61	82.4	100
970401C	12.9	375	381.14	127.05	82.7	100
970401D	13.08	375	381.14	127.05	82.7	100
970401E	13.9	375	381.14	127.12	82.8	100
970401F	14.65	375	380.19	126.88	82.6	100
970401G	14.73	375	380	126.88	82.6	100

Table A-28. Results for Run 28 (970402)

Catalyst: YW113 (5 mass % Pd + 0.1 mass % Cu supported on SiO<sub>2</sub>)

Catalyst charge: 96.2 mg

Previous runs in which catalyst charge was used: Run 26 and 27

State of catalyst at beginning of run: activated (State-2)

Reactor pressure: 94 to 96 kPa

Feed composition: 0.965% CH<sub>4</sub>, 3.96% O<sub>2</sub>, in He

Data Set	Catalyst Time-in-Stream, h	Oven Temp, °C	Reactor Temp., °C	Reactant Feed Rate, mL/min	Reactant Feed Rate, μmol/s	Methane Fractional Conversion, %
970402AA	14.83	199	197.83	125.51	81.7	0.76
970402AA1	14.93	199	197.83	125.51	81.7	1
970402A	15.35	249	250	126.17	82.2	9.1
970402B	15.45	249	250	126.17	82.2	8.29
970402C	15.68	298	304.64	126.51	82.4	48.39
970402D	15.9	299	303.44	126.51	82.4	45.65
970402DD	16.46	299	304.17	125.6	81.8	45.51
970402D1	16.55	299	304.64	125.6	81.8	44.67
970402E	16.6	348	355.9	125.51	81.7	97.44
970402F	16.67	350	359.24	125.51	81.7	98.42
970402FF	16.73	350	357.81	125.51	81.7	97.67
970402G	16.83	374	380.19	126.44	82.3	100
970402H	16.93	374	380.67	126.44	82.3	100

Table A-29. Results for Run 29 (970712)

Catalyst: RF34 (5 mass % Pd supported on Al<sub>2</sub>O<sub>3</sub>)

Catalyst charge: 96.2 mg

State of catalyst at beginning of run: freshly reduced (State-1)

Reactor pressure: 94 to 96 k Pa

Feed composition: 0.965% CH<sub>4</sub>, 3.96% O<sub>2</sub>, in He

Data Set	Catalyst Time-in-Stream, h	Oven Temp, °C	Reactor Temp., °C	Reactant Feed Rate, mL/min	Reactant Feed Rate, µmol/s	Methane Fractional Conversion, %
970712A	0.23	349	347.32	126.03	82.1	2.47
970712B	0.33	349	347.32	126.03	82.1	3.02
970712C	0.52	350	347.32	126.05	82.1	3.81
970712D	0.72	350	347.8	126.39	82.3	4.68
970712E	1	350	347.8	126.39	82.3	5.73
970712F	2.83	350	348.29	125.25	81.6	10.51
970712G	2.92	350	348.29	125.25	81.6	10.76
970712H	13.08	350	350.63	127.21	82.8	33.49
970712I	13.2	350	351.14	127.21	82.8	33.64
970712J	13.83	350	351.38	127.21	82.8	35.16
970712K	14.85	350	351.38	127.21	82.8	35.64
970712L	14.95	350	351.38	128.64	83.8	35.73
970712M	15.87	350	350.67	128.53	83.7	28.31
970712N	15.97	350	350.67	128.53	83.7	28.96
970712O	18.53	350	350.19	128.36	83.6	25.4
970712P	18.63	350	350.19	128.36	83.6	26.71

Table A-30. Results for Run 30 (970713)

Catalyst: RF34 (5 mass % Pd supported on Al<sub>2</sub>O<sub>3</sub>)

Catalyst charge: 96.2 mg

Previous runs in which catalyst charge was used: Run 29

State of catalyst at beginning of run: activated (State-2)

Reactor pressure: 94 to 96 kPa

Feed composition: 0.965% CH<sub>4</sub>, 3.96% O<sub>2</sub>, in He

Data Set	Catalyst Time-in-Stream, h	Oven Temp, °C	Reactor Temp., °C	Reactant Feed Rate, mL/min	Reactant Feed Rate, μmol/s	Methane Fractional Conversion, %
970713A	18.71	200	197.5	128.21	83.5	0
970713B	18.8	200	197.5	128.21	83.5	0
970713C	18.98	223	221.5	128	83.3	0
970713D	19.08	223	221.5	128	83.3	0
970713E	19.36	251	249.7	128.42	83.6	0.83
970713F	19.46	250	249.7	128.42	83.6	0
970713G	19.66	273	272	128.25	83.5	2.75
970713H	19.8	273	272	128.25	83.5	2.94
970713I	20.05	299	298.6	127.99	83.3	7.45
970713J	20.15	299	298.6	127.99	83.3	7.54
970713K	20.36	328	328	127.95	83.3	17.79
970713L	20.58	328	328	127.95	83.3	17.68
970713M	20.85	351	353	127.51	83.0	31.53
970713N	20.98	351	353	127.51	83.0	32.1

Table A-31. Results for Run 31 (970716)

Catalyst: RF34 (5 mass % Pd supported on Al<sub>2</sub>O<sub>3</sub>)

Catalyst charge: 96.2 mg

State of catalyst at beginning of run: freshly reduced (State-1)

Reactor pressure: 94 to 96 kPa

Feed composition: 0.965% CH<sub>4</sub>, 3.96% O<sub>2</sub>, in He

Data Set	Catalyst Time-in-Stream, h	Oven Temp, °C	Reactor Temp., °C	Reactant Feed Rate, mL/min	Reactant Feed Rate, μmol/s	Methane Fractional Conversion, %
970716A	0.08	399	396.31	128.42	83.6	11.15
970716B	0.17	400	396.31	128.42	83.6	15.36
970716D	0.65	400	397.74	127.69	83.1	24.21
970716E	0.9	400	397.74	127.69	83.1	27.94
970716F	1.63	400	399	126.32	82.3	40.41
970716G	1.72	400	399	126.32	82.3	41.89
970716H	2.38	400	400	126.12	82.1	54.2
970716I	3.03	400	400	125.75	81.9	65.97
970716J	3.15	400	401	125.75	81.9	67.52
970716K	3.7	400	401	126.84	82.6	74.43
970716L	4.03	400	401.29	126.84	82.6	78.04
970716M	5.03	400	401.52	126.79	82.6	84.51
970716N	5.65	400	400.3	126.79	82.6	87.02
970716O	6.08	400	402.48	126.79	82.6	88.56
970716P	6.87	400	401.52	126.79	82.6	90.48
970716Q	7.98	400	401.52	126.79	82.6	92.48
970716R	15.92	400	401.52	126.97	82.7	96.44
970716S	16.47	400	401.52	126.97	82.7	96.5
970716T	16.55	400	401.52	126.97	82.7	96.41

Table A-32. Results for Run 32 (970718)

Catalyst: RF34 (5 mass % Pd supported on Al<sub>2</sub>O<sub>3</sub>)

Catalyst charge: 96.2 mg

Previous runs in which catalyst charge was used: Run 31

State of catalyst at beginning of run: activated (State-2)

Reactor pressure: 94 to 96 kPa

Feed composition: 0.965% CH<sub>4</sub>, 3.96% O<sub>2</sub>, in He

Data Set	Catalyst Time-in-Stream, h	Oven Temp, °C	Reactor Temp., °C	Reactant Feed Rate, mL/min	Reactant Feed Rate, μmol/s	Methane Fractional Conversion, %
970718A	16.63	200	195.58	128.64	83.8	0
970718B	16.72	200	195.58	128.64	83.8	0
970718C	17	226	223.54	128.46	83.7	0
970718D	17.08	225	223.54	128.46	83.7	0
970718E	17.38	251	249.73	128.52	83.7	2.22
970718F	17.5	251	248.73	128.52	83.7	2.11
970718G	17.68	274	272.21	127.67	83.1	5.87
970718H	17.77	274	272	127.67	83.1	5.91
970718I	17.98	299	297.88	127.7	83.2	13.57
970718J	18.42	299	298.61	127.7	83.2	14.18
970718K	18.95	326	324.83	127.46	83.0	30.11
970718L	19.05	326	324.83	127.46	83.0	30.25
970718M	19.27	348	348.76	127.15	82.8	51.08
970718N	19.37	349	348.76	127.15	82.8	51.15
970718O	19.78	398	401.52	126.24	82.2	95.42



Table A-33. Results for Run 33 (970725)

Catalyst: RF34 (5 mass % Pd supported on Al<sub>2</sub>O<sub>3</sub>)

Catalyst charge: 96.2 mg

State of catalyst at beginning of run: freshly reduced (State-1)

Reactor pressure: 94 to 96 kPa

Feed composition: 0.965% CH<sub>4</sub>, 3.96% O<sub>2</sub>, in He

Data Set	Catalyst Time-in-Stream, h	Oven Temp, °C	Reactor Temp., °C	Reactant Feed Rate, mL/min	Reactant Feed Rate, µmol/s	Methane Fractional Conversion, %
970725A	0.17	452	449.7	127.06	82.7	26.03
970725B	0.27	451	449.7	127.06	82.7	28.24
970725C	0.68	451	449.7	127.19	82.8	46.69
970725D	0.77	450	449.7	127.19	82.8	51.4
970725E	1.03	450	449.7	126.34	82.3	66.32
970725F	1.18	451	451	126.34	82.3	72.86
970725G	1.65	450	449.7	125.72	81.9	86.5
970725H	2.07	450	451	125.63	81.8	92.15
970725I	2.2	450	451	125.63	81.8	92.84
970725J	3.27	450	451	125.63	81.8	96.76
970725K	3.37	451	451	125.63	81.8	96.98
970725L	4.47	450	451	125.61	81.8	98.03
970725M	5.23	451	451	125.61	81.8	98.08
970725N	5.85	451	449.7	125.61	81.8	98.55
970725O	5.97	450	449.7	125.61	81.8	98.39
970725P	6.7	451	449.7	125.12	81.5	98.5
970725Q	6.78	451	449.7	125.12	81.5	98.83
970725R	7.7	450	449.7	125.12	81.5	98.86
970725S	7.8	450	449.7	125.12	81.5	98.8
970725T	8.15	450	449.7	125.12	81.5	100
970725U	8.58	450	449.7	251.76	163.9	94.16
970725V	8.67	450	449.7	349.96	227.9	91.62
970725W	19.87	450	451	347.52	226.3	86.64
970725X	19.95	450	451	347.52	226.3	87.09
970725Y	20.42	450	449.7	125.52	81.7	96.69
970725Z	20.5	450	449.7	125.52	81.7	96.5

Table A-34. Results for Run 34 (970728)

Catalyst: RF34 (5 mass % Pd supported on Al<sub>2</sub>O<sub>3</sub>)

Catalyst charge: 96.2 mg

Previous runs in which catalyst charge was used: Run 33

State of catalyst at beginning of run: activated (State-2)

Reactor pressure: 94 to 96 kPa

Feed composition: 0.965% CH<sub>4</sub>, 3.96% O<sub>2</sub> in He

Data Set	Catalyst Time-in-Stream, h	Oven Temp, °C	Reactor Temp., °C	Reactant Feed Rate, mL/min	Reactant Feed Rate, µmol/s	Methane Fractional Conversion, %
970728A	20.58	200	197.58	127.38	82.9	0
970728B	20.67	200	197.58	127.58	83.1	0
970728C	21.33	225	224	128.83	83.9	0
970728D	21.42	225	224	128.83	83.9	0.63
970728E	21.77	250	249.23	128.78	83.9	2
970728F	21.93	250	249.23	128.78	83.9	1.89
970728G	22.37	275	274.63	128.85	83.9	6.04
970728H	22.47	275	274.63	128.85	83.9	5.72
970728I	22.68	300	299.34	129.16	84.1	12.95
970728J	22.78	300	299.34	129.16	84.1	12.81
970728K	22.92	325	323.88	129.35	84.2	24.3
970728L	23.13	325	324.36	129.35	84.2	24.43
970728M	23.32	348	347.32	129.21	84.1	40.3
970728N	23.6	349	347.8	129.21	84.2	40.91
970728O	23.87	398	397.26	128.87	83.9	77.46
970728P	24.17	399	398.69	128.87	83.9	77.68
970728Q	24.47	448	447.35	128.52	83.7	94.32
970728R	24.58	449	448.29	128.52	83.7	94.48
970728S	24.87	449	448.29	57.87	37.7	100
970728T	24.95	449	448.29	-	-	100
970728U	25.03	449	448.29	-	-	100

Table A-35. Results for Run 35 (970730)

Catalyst: RF34 (5 mass % Pd supported on  $\text{Al}_2\text{O}_3$ )

Catalyst charge: 96.2 mg

State of catalyst at beginning of run: freshly reduced (State-1)

Reactor pressure: 94 to 96 kPa

Feed composition: 0.965%  $\text{CH}_4$ , 3.96%  $\text{O}_2$ , in He

Data Set	Catalyst Time-in-Stream, h	Oven Temp, °C	Reactor Temp., °C	Reactant Feed Rate, mL/min	Reactant Feed Rate, $\mu\text{mol/s}$	Methane Fractional Conversion, %
970730A	0.1	500	502.58	128.83	83.9	97.91
970730B	0.2	500	502.58	129.48	84.3	100
970730C	0.55	500	522.51	489.56	318.8	100
970730D	0.83	500	527.76	980	638.1	100
970730E	1.1	505	543.63	1301.24	847.3	100
970730F	1.38	501	541.28	1467.71	955.7	98.23
970730G	1.67	501	537.76	1467.71	955.7	96.73
970730H	2.13	500	534.83	1469.51	956.9	94.65
970730I	2.45	500	534.24	1469.51	956.9	93.79
970730J	2.73	500	531.9	1469.51	956.9	92.8
970730K	3.07	500	531.9	1469.51	956.9	92.14
970730L	3.5	500	531.9	1469.51	956.9	91.32
970730M	4.15	500	529.56	1469.51	956.9	90.25
970730N	4.6	500	529.56	1469.51	956.9	89.73
970730O	4.98	500	529	1469.51	956.9	89.07
970730P	5.47	500	526	1469.51	956.9	88.45
970730Q	5.83	500	526	1469.51	956.9	87.84
970730R	6.17	500	526	1469.51	956.9	87.77
970730S	6.48	500	526	1469.51	956.9	87.58
970730T	11.32	500	524.86	1469.51	956.9	84.43
970730U	11.42	500	524.86	1466.28	954.8	84.65
970730V	11.83	500	524.86	1466.28	954.8	84.35
970730W	12.17	500	523.1	1466.28	954.8	84.19

Table A-36. Results for Run 36 (970731)

Catalyst: RF34 (5 mass % Pd supported on Al<sub>2</sub>O<sub>3</sub>)

Catalyst charge: 96.2 mg

Previous runs in which catalyst charge was used: Run 35

State of catalyst at beginning of run: activated (State-2)

Reactor pressure: 94 to 96 kPa

Feed composition: 0.965% CH<sub>4</sub>, 3.96% O<sub>2</sub>, in He

Data Set	Catalyst Time-in-Stream, h	Oven Temp, °C	Reactor Temp., °C	Reactant Feed Rate, mL/min	Reactant Feed Rate, µmol/s	Methane Fractional Conversion, %
970731A	12.25	200	196.6	128.31	83.6	0
970731B	12.32	200	196.6	128.31	83.6	0
970731C	12.69	225	223.54	129.17	84.1	0
970731D	12.77	225	223	129.17	84.1	0
970731E	13.62	248	246.28	129.6	84.4	0
970731F	13.74	248	246.28	129.6	84.4	0
970731G	14.02	273	270.76	128.05	83.4	2.38
970731H	14.15	274	271.73	128.05	83.4	2.5
970731HH	14.25	275	272	128.05	83.4	2.14
970731I	14.85	301	298.85	128.73	83.8	6.17
970731J	14.95	301	298.85	128.73	83.8	6.09
970731K	15.29	324	321.48	128.85	83.9	12.44
970731L	15.4	325	322	128.85	83.9	12.32
970731M	15.97	351	348.29	129.4	84.3	21.57
970731N	12.34	350	347.8	129.4	84.3	19.56
970731O	16.69	401	400.12	128.59	83.7	52.61
970731P	16.79	401	399.64	128.59	83.7	50.71
970731Q	17.17	448	446.76	128.59	83.7	82.1
970731R	17.25	449	446.76	128.59	83.7	81.48
970731S	17.67	449	499	128.59	83.7	97.51
970731T	17.77	449	499	128.59	83.7	97.52
970731U	18.24	524	526	127.13	82.8	100
970731V	18.35	524	526	127.13	82.8	100

Table A-37. Results for Run 37 (970813)

Catalyst: RF34 (5 mass % Pd supported on Al<sub>2</sub>O<sub>3</sub>)

Catalyst charge: 96.2 mg

State of catalyst at beginning of run: freshly reduced (State-1)

Reactor pressure: 94 to 96 kPa

Feed composition: 0.965% CH<sub>4</sub>, 3.96% O<sub>2</sub>, in He

Data Set	Catalyst Time-in-Stream, h	Oven Temp, °C	Reactor Temp., °C	Reactant Feed Rate, mL/min	Reactant Feed Rate, µmol/s	Methane Fractional Conversion, %
970813A	0.08	400	398.69	127.51	83.0	12.81
970813B	0.18	400	398.93	127.24	82.9	14.08
970813C	0.62	400	400.12	127.59	83.1	23.41
970813D	0.72	401	400.12	127.59	83.1	25.58
970813E	1.27	401	400.12	127.59	83.1	37.34
970813F	1.42	400	400.12	127.59	83.1	40.68
970813G	1.68	400	400.58	127.59	83.1	47.72
970813H	2.17	400	400.58	126.92	82.6	61.22
970813I	2.28	400	401	126.92	82.6	62.95
970813J	3.25	400	401.52	126.71	82.5	76.9
970813K	3.35	400	401.52	126.71	82.5	78.04
970813L	4.08	400	402.48	127.11	82.8	84.67
970813M	4.2	401	402.48	127.11	82.8	85.58
970813N	4.7	400	402.48	126.76	82.5	88.32
970813O	4.8	400	402.48	126.76	82.5	88.9
970813P	5.28	400	402.48	127.16	82.8	90.61
970813Q	5.38	400	402.48	127.16	82.8	91.44
970813R	7.08	400	402.48	126.12	82.1	94.96
970813S	7.2	400	402.48	126.12	82.1	95.25
970813T	7.55	400	402.48	126.12	82.1	95.53
970813U	8.03	400	402.48	126.54	82.3	96.05
970813V	8.28	400	402.48	126.54	82.4	95.96
970813W	10	400	402.48	126.68	82.5	96.86
970813X	10.08	400	402.48	126.68	82.5	97.08
970813Y	10.85	400	402.48	126.68	82.5	97.36
970813Z	10.93	400	402.48	126.68	82.5	97.05
970813A1	17.18	400	401.52	127.36	82.9	96.88
970813A2	17.28	400	401.52	127.36	82.9	97
970813A3	17.63	400	399.17	58.58	38.1	100
970813A4	17.72	400	400.12	58.58	38.1	100
970813A5	18.18	400	401.52	127.08	82.7	96.55
970813A6	18.3	400	399.17	127.08	82.7	100

Table A-38. Results for Run 38 (970814)

Catalyst: RF34 (5 mass % Pd supported on Al<sub>2</sub>O<sub>3</sub>)

Catalyst charge: 96.2 mg

Previous runs in which catalyst charge was used: Run 37

State of catalyst at beginning of run: activated (State-2)

Reactor pressure: 94 to 96 kPa

Feed composition: 0.965% CH<sub>4</sub>, 3.96% O<sub>2</sub> in He

Data Set	Catalyst Time-in-Stream, h	Oven Temp, °C	Reactor Temp., °C	Reactant Feed Rate, mL/min	Reactant Feed Rate, μmol/s	Methane Fractional Conversion, %
970814A	18.38	200	196.58	127.96	83.3	0
970814B	18.65	224	223	128.26	83.5	0.71
970814C	18.77	225	223	128.26	83.5	0
970814D	19.05	251	250.22	127.9	83.3	2.71
970814E	19.17	251	250.22	127.9	83.3	2.87
970814F	19.78	276	275.61	128.27	83.5	7.2
970814G	19.88	276	275.61	128.27	83.5	7.45
970814H	20.18	299	298.85	128.23	83.5	15.61
970814I	20.28	300	299.34	128.23	83.5	16
970814J	20.5	324	323.39	127.8	83.2	31.52
970814K	20.6	325	323.88	127.8	8.32	32.21
970814L	21.17	351	350.67	126.98	82.7	58.76
970814M	21.28	351	350.67	126.98	82.7	58.92
970814N	21.6	399	400	126.38	82.3	96.45
970814O	21.7	399	400	126.38	82.3	96.65

Table A-39. Results for Run 39 (970827)

Catalyst: RF34 (5 mass % Pd supported on Al<sub>2</sub>O<sub>3</sub>)

Catalyst charge: 96.2 mg

State of catalyst at beginning of run: freshly reduced (State-1)

Reactor pressure: 94 to 96 kPa

Feed composition: 0.965% CH<sub>4</sub>, 3.96% O<sub>2</sub>, in He

Data Set	Catalyst Time-in-Stream, h	Oven Temp, °C	Reactor Temp., °C	Reactant Feed Rate, mL/min	Reactant Feed Rate, μmol/s	Methane Fractional Conversion, %
970827A	0.1	373	370.19	127.44	83.0	2.14
970827B	0.2	373	370.19	126.2	82.2	2.6
970827C	0.5	374	371.62	126.94	82.7	3.22
970827D	0.6	375	371.62	126.94	82.7	3.2
970827E	1.4	375	371.1	126.88	82.6	4.35
970827F	1.5	375	371.1	126.88	82.6	4.38
970827G	13.68	375	371.1	126.2	82.2	58.54
970827H	13.85	375	371.1	126.2	82.2	59.7
970827I	15.67	375	371.1	127.52	83.0	65.53
970827J	16.12	375	371.1	127.52	83.0	66.77
970827K	16.57	376	374.1	126.72	82.5	68.28
970827L	16.75	376	374.1	126.72	82.5	67.68
970827M	17.17	375	372.57	127.29	82.9	69.55
970827N	17.27	375	372.57	127.29	82.9	69.87
970827O	20.43	375	373.52	126.67	82.5	76.4
970827P	20.7	375	373.52	126.67	82.5	76.39
970827Q	23.57	375	373.52	125.7	81.9	79.56
970827R	23.67	375	373.52	125.7	81.9	79.77
970827S	24.7	375	374	125.64	81.8	80.63
970827T	24.8	375	373.52	125.64	81.8	80.59
970827U	25.2	375	374	125.64	81.8	80.87
970827V	25.3	375	374	125.64	81.8	80.99
970827W	26.42	375	373.52	125.98	82.0	81.96
970827X	26.5	375	373.52	125.98	82.0	81.64
970827Y	27.3	375	373.52	125.3	81.6	82.01
970827Z	27.4	375	373.52	125.3	81.6	82.23
970827A1	35.93	375	373.52	125.05	81.4	83.99
970827A2	38.78	375	373.52	127.15	82.8	83.58
970827A3	38.87	375	373.52	127.15	82.8	83.75

Table A-40. Results for Run 40 (970904)

Catalyst: RF34 (5 mass % Pd supported on Al<sub>2</sub>O<sub>3</sub>)

Catalyst charge: 96.2 mg

Previous runs in which catalyst charge was used: Run 39

State of catalyst at beginning of run: activated (State-2)

Reactor pressure: 94 to 96 kPa

Feed composition: 0.965% CH<sub>4</sub>, 3.96% O<sub>2</sub> in He

Data Set	Catalyst Time-in-Stream, h	Oven Temp, °C	Reactor Temp., °C	Reactant Feed Rate, mL/min	Reactant Feed Rate, μmol/s	Methane Fractional Conversion, %
970904A	38.95	200	197.83	127.68	83.1	0
970904B	39.34	224	224	127.58	83.1	0.71
970904C	39.44	224	223.54	127.58	83.1	0
970904D	40.19	252	251.2	127.75	83.2	3.12
970904E	40.27	251	251.2	127.75	83.2	3.22
970904F	40.5	274	273.17	127.43	83.0	7.32
970904G	40.59	274	273.17	127.43	83.0	7.52
970904H	40.79	300	300.31	126.85	82.6	17.09
970904I	40.95	300	299.83	126.85	82.6	16.87
970904J	41.27	326	325	127.04	82.7	34.47
970904K	41.37	326	325	127.04	82.7	34.18
970904L	41.67	349	347.8	125.56	81.8	57.44
970904M	41.75	349	347.8	125.56	81.8	57.75
970904N	42.07	375	374	125.76	81.9	82.94
970904O	42.15	375	374	125.76	81.9	82.87



Table A-41. Results for Run 41 (961112)

Catalyst: RF30 (5 mass % Pd supported on Al<sub>2</sub>O<sub>3</sub>)

Catalyst charge: 96.2 mg

State of catalyst at beginning of run: freshly reduced (State-1)

Reactor pressure: 94 to 96 kPa

Feed composition: 0.965% CH<sub>4</sub>, 3.96% O<sub>2</sub> in He

Data Set	Catalyst Time-in-Stream, h	Oven Temp., °C	Reactor Temp., °C	Reactant Feed Rate, mL/min	Reactant Feed Rate, μmol/s	Methane Fractional Conversion, %
961112-A	0.5	275	273.17	125.75	81.9	0
961112-B	0.65	275	273.17	97.66	63.6	0
961112-C	0.8	275	273.66	58.11	37.8	0
961112-D	1	275	273.66	36.7	23.9	0
961112-E	1.17	325	322.9	126.49	82.4	1.71
961112-F	1.3	325	322.9	96.36	62.7	2.16
961112-G	1.45	325	322.9	57.94	37.7	3.41
961112-H	1.62	325	322.9	36.88	24.0	4.27
961112-I	1.78	351	348.76	127.51	83.0	4.56
961112-J	1.93	351	348.76	96.51	62.8	5.5
961112-K	2.12	351	348.76	57.8	37.6	7.9
961112-L	2.28	351	348.76	36.93	24.0	9.64
961112-M	2.45	375	372.57	126.88	82.6	9.59
961112-N	2.6	375	372.57	97.05	63.2	11.46
961112-O	2.93	375	372.57	58.13	37.9	15.16
961112-P	3.2	375	372.57	37	24.1	18.88
961112-Q	3.37	400	397.74	126.18	82.2	18.95
961112-R	3.75	400	398.21	97.06	63.2	23.06
961112-S	3.92	400	397.74	58.63	38.2	29.55
961112-T	4.08	400	397.74	37.06	24.1	35.62
961112-U	4.25	425/426	423.76	125.75	81.9	33.92
961112-V	4.38	425/426	423.76	97.61	63.6	38.91
961112-W	4.83	425/426	423.76	58.77	38.3	52.42
961112-X	4.98	425/426	423.76	37.24	24.2	63.2
961112-Y	5.15	450/449	449.7	126.67	82.5	61.24
961112-Z	5.28	450/449	449.7	97.5	63.5	69.14
961112-A1	5.62	450/450	449.7	58.65	38.2	82.99
961112-B1	5.78	450/450	449.7	36.9	24.0	90.31
961112-C1	5.95	475/474	475.57	125.71	81.9	90.31
961112-D1	6.08	475/474	474.4	97.89	63.7	94.97
961112-E1	6.45	475/475	473.23	58.18	37.9	99.51
961112-F1	6.58	475	473.23	36.84	24.0	100

Table A-42. Results for Run 42 (961120)

Catalyst: RF30 (5 mass % Pd supported on Al<sub>2</sub>O<sub>3</sub>)

Catalyst charge: 96.2 mg

Previous runs in which catalyst charge was used: Run 41

State of catalyst at beginning of run: activated (State-2)

Reactor pressure: 94 to 96 kPa

Feed composition: 0.965% CH<sub>4</sub>, 3.96% O<sub>2</sub> in He

Data Set	Catalyst Time-in-Stream, h	Oven Temp, °C	Reactor Temp., °C	Reactant Feed Rate, mL/min	Reactant Feed Rate, µmol/s	Methane Fractional Conversion, %
961120-A	16.8	230	230.48	127.61	83.1	0
961120-B	16.97	230	230	97.02	63.2	0
961120-C	17.08	230	230	58.58	38.1	0
961120-D	17.3	230	230	36.78	23.9	1.19
961120-E	17.47	275	275.61	127.21	82.8	3.32
961120-F	17.55	275	275.61	96.35	62.7	4.44
961120-G	17.72	275	275.61	58.73	38.2	5.81
961120-H	17.88	275	275.61	36.72	23.9	6.81
961120-I	18.05	325	326.26	126.26	82.2	16.04
961120-J	18.23	325	326.26	98.55	64.2	17.79
961120-K	18.35	325	325.79	58.32	38.0	22.74
961120-L	18.53	325	325.31	36.99	24.1	26.85
961120-M	18.7	375	377.81	125.59	81.8	47.57
961120-N	18.83	375	377.33	97.69	63.6	52.22
961120-O	19.3	375	376.86	58.01	37.7	61.57
961120-P	19.75	375	376.38	36.7	23.9	69.41
961120-Q	19.92	425	429.67	125.39	81.6	87.04
961120-R	20	425	429.43	97.13	63.2	91.32
961120-S	20.42	425	427.53	57.88	37.7	96.18
961120-T	20.82	425	426.6	36.98	24.1	98.69
961120-U	20.98	454	460.29	126.33	82.3	98.28
961120-V	21.1	454	459.12	97.46	63.5	100
961120-W	21.47	455	455.58	58.09	37.8	100
961120-X	21.6	455	455.58	58.09	37.8	100

Table A-43. Results for Run 43 (961125)

Catalyst: RF30 (5 mass % Pd supported on Al<sub>2</sub>O<sub>3</sub>)

Catalyst charge: 96.2 mg

Previous runs in which catalyst charge was used: Runs 41 and 42

State of catalyst at beginning of run: activated (State-2)

Feed composition: 0.965% CH<sub>4</sub>, 3.96% O<sub>2</sub> in He

Data Set	Catalyst Time-on-Stream, h	Reactor Pressure, psia	Oven Temp., °C	Reactor Temp., °C	Reactant Feed Rate, mL/min	Reactant Feed Rate, $\mu$ mol/s	Methane Fractional Conversion, %
961125-A	91.35	13.59	275	275.61	126.86	82.6	3.71
961125-B	91.52	13.59	275	275.61	98.18	63.9	4.37
961125-C	91.68	13.59	275	275.12	58.26	37.9	5.75
961125-D	91.85	13.59	275	275.12	36.87	24.0	6.97
961125-E	93.52	56.59	275	274.63	527.83	343.7	1.81
961125-EE	93.6	56.59	275	274.63	527.83	343.7	1.57
961125-F	94.55	56.59	275	274.63	409.63	266.7	2.53
961125-G	94.68	56.59	275	274.63	409.63	266.7	1.99
961125-H	95.05	56.59	275	274.63	241.89	157.5	3.26
961125-I	95.18	56.59	275	274.63	241.9	157.5	3.11
961125-J	96.27	56.59	275	275.61	154.04	100.3	3.99
961125-K	96.4	56.59	275	275.61	154.04	100.3	3.94
961125-L	96.57	56.59	325	325.79	152.96	99.6	16.98
961125-M	96.68	56.59	325	325.79	153.58	100.0	17
961125-N	96.82	56.59	325	326.74	241.89	157.5	13.57
961125-O	96.97	56.59	325	326.74	241.97	157.5	13.84
961125-P	97.35	56.59	325	327.22	409.95	266.9	11.3
961125-Q	97.47	56.59	325	327.22	409.95	266.9	11.41
961125-R	97.67	56.59	325	327.22	528.01	343.8	10.45
961125-S	97.82	56.59	325	327.22	528.01	343.8	10.4
961125-T	97.98	13.59	325	326.26	126.84	82.6	18.89
961125-U	98.18	13.59	325	325.79	97.72	63.6	21.47
961125-V	98.35	13.59	325	325.31	58.04	37.8	27.09
961125-W	98.82	13.59	325	325	36.67	23.9	32.32
961125-X	98.98	13.59	376	378.76	127.58	83.1	52.33
961125-Y	99.12	13.59	376	378.29	127.21	82.8	52.46
961125-Z	99.5	56.59	375	383.5	528.23	344.0	40.51
961125-A1	99.58	56.59	375	383	528.23	344.0	40.58
961125-B1	99.75	56.59	424	442.63	526.32	342.7	81.75
961125-C1	99.88	56.59	424	442.63	526.32	342.7	81.73
961125-D1	100.23	13.59	424	429.67	126.1	82.1	89.8
961125-E1	100.4	13.59	457	461.47	126.38	82.3	98.67
961125-F1	100.53	13.59	456	460.29	96.18	62.6	100

Table A-44. Results for Run 44 (961031)

Catalyst: RF16 (5 mass % Pd supported on MgO)

Catalyst charge: 96.2 mg

State of catalyst at beginning of run: freshly reduced (State-1)

Reactor pressure: 94 to 96 kPa

Feed composition: 0.965% CH<sub>4</sub>, 3.96% O<sub>2</sub> in He

Data Set	Catalyst Time-in- Stream, h	Oven Temp, °C	Reactor Temp., °C	Reactant Feed Rate, mL/min	Reactant Feed Rate, µmol/s	Methane Fractional Conversion, %
961031-A	0.33	150	145.6	37.1	24.2	0
961031-B	0.41	200	196.58	37.36	24.3	0
961031-C	0.5	300	298.85	37.23	24.2	0
961031-D	0.58	300	348.76	36.82	24.0	0
961031-E	0.66	375	370.67	37.24	24.2	0
961031-F	0.75	401	396.55	37.11	24.2	2.06
961031-G	0.88	401	396.55	58.01	37.8	1.75
961031-H	1	401	397.74	98.6	64.2	1.39
961031-I	1.08	401	397.74	126.88	82.6	1
961031-J	1.16	424	420.21	36.8	24.0	4.21
961031-K	1.31	425	420.21	58.46	38.1	3.45
961031-L	1.41	425	420.21	98.25	64.0	2.06
961031-M	1.56	425	420.21	127.65	83.1	1.64
961031-N	1.66	425	420.21	127.65	83.1	1.91
961031-O	1.75	475	469.7	37.21	24.2	9.14
961031-P	1.86	475	469.7	58.4	38.0	6.27
961031-Q	2.03	475	469.7	50	32.6	4.31
961031-R	2.2	475	469.7	127.51	83.1	3.39
961031-S	2.28	540	537.76	127.61	83.1	10.42
961031-T	2.38	540	537.76	98.56	64.2	13.93
961031-U	2.5	540	537.76	57.87	37.7	20.6
961031-V	2.61	540	537.76	37.12	24.2	27.33
961104A	16.5	200	197.58	36.79	24.0	0

Table A-45. Results for Run 45 (961104)

Catalyst: RF16 (5 mass % Pd supported on MgO)

Catalyst charge: 96.2 mg

Previous runs in which catalyst charge was used: Run 44

State of catalyst at beginning of run: activated (State-2)

Reactor pressure: 94 to 96 kPa

Feed composition: 0.965% CH<sub>4</sub>, 3.96% O<sub>2</sub> in He

Data Set	Catalyst Time-in-Stream, h	Oven Temp, °C	Reactor Temp., °C	Reactant Feed Rate, mL/min	Reactant Feed Rate, μmol/s	Methane Fractional Conversion, %
961104B	16.58	230	227.75	36.79	24.0	0
961104C	16.67	275	273.66	36.79	24.0	0
961104D	16.75	350	348.76	37.43	24.4	0
961104E	16.83	350	348.76	37.43	24.4	0
961104F	17.58	425	422.33	37.25	24.3	2.72
961104G	17.83	425	422.33	58.42	38.0	2.11
961104H	17.95	425	422.33	99.14	64.6	1.26
961104I	18.07	425	422.33	128.45	83.6	0.84
961104J	18.18	425	422.33	128.45	83.6	1.04
961104K	18.27	400	397.74	37.41	24.4	1.5
961104L	18.38	400	397.74	58.59	38.2	0.92
961104M	18.52	400	397.74	99.35	64.7	0
961104N	18.65	400	397.74	128.19	83.5	0
961104O	18.73	475	470.29	37.12	24.2	9.92
961104P	18.88	475	471	58.59	38.2	7.4
961104Q	19.02	475	471	99.4	64.7	4.87
961104R	19.13	475	471	128.38	83.6	4.02
961104S	19.25	475	471	128.38	83.6	4.16
961104T	19.67	540	534.24	37.12	24.2	33.97
961104U	19.82	540	534.24	58.61	38.2	26.7
961104V	19.93	540	536.58	99.33	64.7	19.39
961104W	20.1	540	535.42	128	83.3	16.23

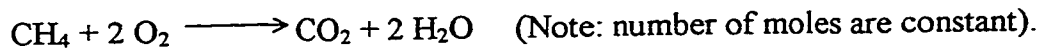
## Appendix B: Sample Calculation for Methane Conversion

Methane conversions were calculated from the gas chromatographic analyses.

The fractional conversion of methane,  $X$ , is defined as

$$X_{CH_4} \equiv X = \frac{F_{CH_4,o} - F_{CH_4,E}}{F_{CH_4,o}} ; \quad \text{where } F_i = \text{molar flow rate of } i$$

The molar flow rates of all the reactants and products can be expressed in terms of  $X$  and the feed molar flow rates using the stoichiometry of the methane combustion reaction, i.e.



The exit molar flow rates of reactants and products as a function of  $X$  and molar feed rates are:

$$F_{CH_4,E} = F_{CH_4,o} (1-X) \quad X = X_{CH_4} \quad (1)$$

$$F_{O_2,E} = F_{O_2,o} - 2 (F_{CH_4,o} - F_{CH_4,E}) \quad (2)$$

$$\begin{aligned} F_{CO_2,E} &= F_{CO_2,o} + (F_{CH_4,o} - F_{CH_4,E}) \\ &= F_{CO_2,o} + F_{CH_4,o} X \end{aligned}$$

for all runs  $F_{CO_2,o} = 0$

$$\text{So, } F_{CO_2,E} = F_{CH_4,o} X \quad (3)$$

Ratio of Eq (1) to (2) is

$$\frac{F_{CH_4,E}}{F_{O_2,E}} = \frac{F_{CH_4,o} (1-X)}{F_{O_2,o} - 2 F_{CH_4,o} X} \quad (4)$$

Solving Eq. 4 for  $X$  yields

$$X = \frac{(F_{O_2,E} / F_{CH_4,E}) - (F_{O_2,o} / F_{CH_4,o})}{(F_{O_2,E} / F_{CH_4,E}) - 2} \quad (5)$$

but

$$\frac{F_{O_2,E}}{F_{CH_4,E}} = \frac{F_T Y_{O_2,E}}{F_T Y_{CH_4,E}} = \frac{Y_{O_2,E}}{Y_{CH_4,E}}$$

where  $F_T$  = total molar feed rate = total product flow rate

$Y_{i,E}$  = mole fraction of  $i$  in product stream

$Y_{i,o}$  = mole fraction of  $i$  in feed stream

but  $(Y_{O_2,E}/Y_{CH_4,E}) = (A_{O_2,E}/R_{O_2})(R_{CH_4}/A_{CH_4,E}) = (A_{O_2,E}/A_{CH_4,E}) (R_{CH_4}/R_{O_2})$

where  $A_{i,E}$  = gas chromatographic area of component  $i$  in product stream

$R_i$  = response factor for component  $i$

The response factors are defined as

$$\frac{R_i}{R_j} = \frac{(A_i) (Y_j)}{(A_j) (Y_i)}$$

Substituting above into Eq 5 yields

$$X = \frac{(A_{O_2,E}/A_{CH_4,E})(R_{CH_4}/R_{O_2}) - (Y_{O_2,o}/Y_{CH_4,o})}{(A_{O_2,E}/A_{CH_4,E})(R_{CH_4}/R_{O_2}) - 2} = X_1 \quad (6)$$

Similarly, taking ratios of Eq (1) to (3) yields

$$\frac{F_{CH_4,E}}{F_{CO_2,E}} = \frac{F_{CH_4,o}(1-X)}{F_{CH_4,o}X} \quad (7)$$

Solving for  $X$  yields

$$X = \frac{1}{1 + (F_{CH_4,E}/F_{CO_2,E})} = \frac{1}{1 + (Y_{CH_4,E}/Y_{CO_2,E})}$$

$$X = \frac{1}{1 + (A_{CH_4,E}/A_{CO_2,E})(R_{CO_2}/R_{CH_4})} = X_2 \quad (8)$$

Taking the ratio of Equations 2 and 1 yields

$$\frac{F_{O_2,E}}{F_{CO_2,E}} = \frac{F_{O_2,o} - 2 F_{CH_4,o}X}{F_{CH_4,o}X} = \frac{(F_{O_2,o}/F_{CH_4,o}) - 2X}{X}$$

Solving for X yields

$$X = \frac{(F_{O_2}/F_{CH_4,o})}{(F_{O_2}/F_{CO_2,E}) + 2} = \frac{(Y_{O_2}/Y_{CH_4,o})}{2 + (A_{O_2}/A_{CO_2,E})(R_{CO_2}/R_{O_2})} = X_3 \quad (9)$$

Following are examples for calculating the methane conversion values of Run 2 using the above three equations (Equations 6, 8 and 9) for Run 2.

Catalyst: RF34 (5 mass % Pd supported on  $Al_2O_3$ )

Catalyst charge: 96.2 mg

Reactor pressure: 93 kPa

Feed composition: 0.965%  $CH_4$ , 3.96%  $O_2$  in helium (values used for  $Y_{I,o}$ )

#### Calculating GC response factors:

The GC response factors were determined before and after each run by analyzing premixed feed of known compositions at zero and 100 % conversion, i.e.,

$$R_{CH_4}/R_{O_2} = (A_{CH_4}/A_{O_2}) \times (Y_{O_2}/Y_{CH_4,o}) = (A_{CH_4}/A_{O_2}) \times (9.96/0.965)$$

$$\begin{aligned} R_{CO_2}/R_{O_2} &= (A_{CO_2}/A_{O_2}) \times (Y_{O_2} @ 100\% \text{ methane conversion} / Y_{CO_2} @ 100\% \text{ methane conversion}) \\ &= (A_{CO_2}/A_{O_2}) \times (2.03/0.965) \end{aligned}$$

$$R_{CH_4}/R_{CO_2} = (R_{CH_4}/R_{O_2}) / (R_{CO_2}/R_{O_2})$$

The measured GC areas are given in the table below.

$O_2$ Area	$CH_4$ Area	$CO_2$ Area	$R_{CH_4}/R_{O_2}$	$R_{CO_2}/R_{O_2}$
19300	4353	0	0.9256	
10270	0	6313		1.2931

The measured GC areas and the methane conversions  $X_1$ ,  $X_2$ ,  $X_3$ , using Equations 6, 8 and 9, and converting to % are shown in the table below.

Data Set	$O_2$ Area	$CH_4$ Area	$CO_2$ Area	$X_1\%$	$X_2\%$	$X_3\%$
960820A	19350	4355	0	0.42	0	0
960820B	19230	4308	83	1.32	1.36	1.36
960820D	19780	4438	30	1.02	0.48	0.48
960820E	19680	4413	0	1.13	0	100
960820F	19620	4402	51	1.02	0.82	0.83
960820G	19540	4376	69	1.38	1.12	1.12



Data Set	O <sub>2</sub> Area	CH <sub>4</sub> Area	CO <sub>2</sub> Area	X <sub>1</sub> %	X <sub>2</sub> %	X <sub>3</sub> %
960820H	19780	4438	56	1.02	0.90	0.90
960820I	19530	4349	100	2.46	1.62	1.62
960820J	19730	4394	97	2.44	1.56	1.55
960820K	19570	4330	134	3.65	2.17	2.16
960820L	18090	3833	680	11.17	11.29	11.30
960820M	18350	3915	548	10.04	9.13	9.08
960820N	18790	4053	454	8.18	7.44	7.41
960820O	18650	4016	438	8.47	7.26	7.21
960820OO1	18840	4050	434	8.77	7.14	7.07
960820P	18760	4028	410	8.97	6.81	6.72
960820Q	18940	4075	409	8.62	6.72	6.65
960820R	16940	3235	1565	26.11	25.77	25.70
960820S	17660	3475	1265	22.20	20.71	20.51
960820T	18030	3655	1043	18.02	16.99	16.89
960820U	18180	3668	1037	18.70	16.86	16.67
960820V	18250	3743	939	16.29	15.25	15.16
960820W	18440	3782	981	16.29	15.69	15.63
960820X	12650	1123	4686	75.04	74.96	74.84
960820Y	13800	1611	3980	64.52	63.93	63.39
960820Z	14710	2057	3356	54.46	53.93	53.61
960820A1	14860	2061	3405	54.99	54.24	53.78
960820B1	15240	2216	3198	51.81	50.87	50.36
960820C1	15120	2196	3203	51.89	51.14	50.72
960820D1	10510	0	6422	100	100	99.81
960820-E1	10600	44	6336	99.05	99.04	98.68
960820F1	10990	179	6170	96.16	96.11	95.48
960820G1	10840	169	6144	96.33	96.31	95.97
960820H1	11130	261	6081	94.39	94.36	94.09
960820I1	11020	230	6119	95.03	95.02	94.92
960820J1	10200	0	6283	100	100	100.23
960820K1	10270	0	6313	100	100	100.12
960820L1	10220	0	6254	100	100	99.89
960820M1	10320	0	6324	100	100	99.96

Equation 8, i.e.  $X_2$ , was used to calculate the fractional conversions reported in the body of the thesis because it does not require knowledge of the feed composition.

### **Accuracy of Fractional Conversion Calculated Using Equation 8**

Repeat analysis showed that the standard deviation of the GC areas was  $\pm 50$ , and the magnitude to methane area range was 0 to 4500 and the range of the carbon dioxide areas was 0 to 6400. The ratio of carbon monoxide to methane to response factors was  $1.39 \pm 0.02$ . Substituting these ranges of values into Equations 8 shows that error in  $X_2$  is less than  $\pm 1.5\%$ .

## Appendix C: Sample Calculation for Pd Dispersion from H<sub>2</sub> Chemisorption Data

Catalysts: RF34 (5 mass % Pd supported on Al<sub>2</sub>O<sub>3</sub>)

Powder size: <210 μm

Amount of catalyst sample loaded: 90.4 mg

Data Name: YW101

$$\text{Amount of Pd in Sample} = \frac{0.0964 \text{ (g)} \times 0.05}{106.4} \times 10^6 = 42.48 \text{ } \mu\text{moles}$$

Integrated Areas of eluted H<sub>2</sub> peaks for the at injections (arbitrary units):

86, 602, 1410, 1792, 1801, 1794, 1787, 1797, 1798, 1799, 1809, 1804, 1797, 1811, 1812

Area corresponding to a completely eluted pulse is take as the average of the areas after the area ha become relatively constant (the last 11 peaks in the above case).

$$\text{Area per peak} = (1801+1794+1787+1797+1799+1809+1797+1811+1812)/11 = 1801$$

Number of pulses adsorbed by catalyst Pd is equal to the sum of the parts of pulses adsorbed. In the above case parts of pulses 1 to 4 were adsorbed. Hence, the number of pulses of hydrogen adsorbed is

$$((1801-86)+(1801-602)+(1801-1410) + (1801-1792))/1800 = 1.80$$

The size of each pulse is equal to 2.33 μmol of H<sub>2</sub> .

Hence, the amount of H<sub>2</sub> adsorbed on the Pd is: 1.84×2.33μmol = 4.29 μmol.

It is assumed that one surface Pd atom adsorbs on hydrogen atom; hence the Pd dispersion, D, which is defined as the ratio of suface Pd atoms to total Pd atoms, is

$$\text{Pd dispersion} = \frac{2 \times 1.80}{42.48} = 0.202 = 20.2\%$$

## Appendix D: Summary of XRD Runs and XRD Data Analysis

### Listing of XRD Patterns Measured

The XRD patterns listed in the table below were used in the analysis of Pd and PdO crystal sizes. the scans done for the 35 to 55°(2 $\theta$ ) range were done at a step size of 0.02°/step and counting for 100 s at each step; the scans done for the 10 to 90°(2 $\theta$ ) range were done at a step size of 0.1°/step and counting for 40 s at each step. All the angle versus intensity data for these XRD patterns are stored on the hard drive of the XRD PC in Room CME 835, with back-up storage on floppy discs.

Table D-1. Desxcription of XRD data files.

Data File XR.....	Sample	State of Catalyst (At beginning of run)	Previous Run	Others
AD953	RF34	Fresh	H <sub>2</sub> -Adsorption (YW103,104)	35-55°(2 $\theta$ ), before Run 29,30
AD954	RF34	Fresh	H <sub>2</sub> -Adsorption (YW103,104)	10-90°(2 $\theta$ ), before Run 29,30
AD962	RF34	Fresh	H <sub>2</sub> -Adsorption (YW106,107)	35-55°(2 $\theta$ ), before Run 31,32
AD961	RF34	Fresh	H <sub>2</sub> -Adsorption (YW106,107)	10-90°(2 $\theta$ ), before Run 31,32
AD972	RF34	Fresh	H <sub>2</sub> -Adsorption (YW108,109)	10-90°(2 $\theta$ ), before Run 33,34
AD973	RF34	Fresh	H <sub>2</sub> -Adsorption (YW108,109)	35-55°(2 $\theta$ ), before Run 33,34
AD979	RF34	Fresh	H <sub>2</sub> -Adsorption (YW112,113)	35-55°(2 $\theta$ ), before Run 35,36
AD980	RF34	Fresh	H <sub>2</sub> -Adsorption (YW112,113)	10-90°(2 $\theta$ ), before Run 35,36
AD1003	RF34	Fresh	H <sub>2</sub> -Adsorption (YW117,118)	35-55°(2 $\theta$ ), before Run 37,38
AD1004	RF34	Fresh	H <sub>2</sub> -Adsorption (YW117,118)	10-90°(2 $\theta$ ), before Run 37,38
AD1030	RF34	Fresh	H <sub>2</sub> -Adsorption (YW123,124)	35-55°(2 $\theta$ ), before Run 39,40
AD1031	RF34	Fresh	H <sub>2</sub> -Adsorption (YW123,124)	10-90°(2 $\theta$ ), before Run 39,40
AD964	RF34	Aged at 350°C	Run 29,30	35-55°(2 $\theta$ ), after Run 29,30
AD969	RF34	Aged at 350°C	Run 29,30	10-90°(2 $\theta$ ), after Run 29,30
AD974	RF34	Aged at 400°C	Run 31,32	35-55°(2 $\theta$ ), after Run 31,32

Data File XR.....	Sample	State of Catalyst (At beginning of run)	Previous Run	Others
AD975	RF34	Aged at 400°C	Run 31,32	10-90°(2θ), after Run 31,32
AD986	RF34	Aged at 450°C	Run 33,34	35-55°(2θ), after Run 33,34
AD987	RF34	Aged at 525°C	Run 35,36	35-55°(2θ), after Run 35,36
AD988	RF34	Aged at 525°C	Run 35,36	10-90°(2θ), after Run 35,36
AD1027	RF34	Aged at 400°C	Run 37,38	35-55°(2θ), after Run 37,38
AD1026	RF34	Aged at 400°C	Run 37,38	10-90°(2θ), after Run 37,38
AD1029	RF34	Aged at 400°C	Run 37,38	35-55°(2θ), after Run 37,38
AD1028	RF34	Aged at 400°C	Run 37,38	10-90°(2θ), after Run 37,38
AD1037	RF34	Aged at 375°C	Run 39,40	35-55°(2θ), after Run 39,40
AD1036	RF34	Aged at 375°C	Run 39,40	10-90°(2θ), after Run 39,40
AD1063	RF34	Aged at 375°C	-	35-55°(2θ)
AD1064	RF34	Aged at 375°C	-	10-90°(2θ)
AD981	RF34	Reduced(after aging at 350°C)	H <sub>2</sub> -Adsorption (YW110,111)	35-55°(2θ)
AD982	RF34	Reduced(after aging at 350°C)	H <sub>2</sub> -Adsorption (YW110,111)	10-90°(2θ)
AD989	RF34	Reduced(after aging at 400°C)	H <sub>2</sub> -Adsorption (YW114,116)	35-55°(2θ)
AD990	RF34	Reduced(after aging at 400°C)	H <sub>2</sub> -Adsorption (YW114,116)	10-90°(2θ)
AD1009	RF34	Reduced(after aging at 450°C)	H <sub>2</sub> -Adsorption (YW119,120)	35-55°(2θ)
AD1008	RF34	Reduced(after aging at 450°C)	H <sub>2</sub> -Adsorption (YW119,120)	10-90°(2θ)
AD1013	RF34	Reduced(after aging at 525°C)	H <sub>2</sub> -Adsorption (YW121,122)	35-55°(2θ)
AD1014	RF34	Reduced(after aging at 525°C)	H <sub>2</sub> -Adsorption (YW121,122)	10-90°(2θ)
AD1032	RF34	Reduced(after aging at 400°C)	H <sub>2</sub> -Adsorption (YW125,126)	35-55°(2θ)
AD1033	RF34	Reduced(after aging at 400°C)	H <sub>2</sub> -Adsorption (YW125,126)	10-90°(2θ)
AD1054	RF34	Reduced(after aging at 375°C)	H <sub>2</sub> -Adsorption (YW127,128)	35-55°(2θ)
AD1055	RF34	Reduced(after aging at 375°C)	H <sub>2</sub> -Adsorption (YW127,128)	10-90°(2θ)
AD1127	Al <sub>2</sub> O <sub>3</sub> Support	Aged, in air at 500°C for 4 hours.	Calcined in air at 500°C, 4 hrs.	10-90°(2θ)
AD1128 & 1129	Al <sub>2</sub> O <sub>3</sub> Support	Aged, in air at 500°C for 4 hours.	Calcined in air at 500°C, 4 hrs	35-55°(2θ)
AD1198	Silica	Prepared, no further treatment	No	10-90°(2θ)

Data File XR.....	Sample	State of Catalyst (At beginning of run)	Previous Run	Others
AD1199	5.11%SiO <sub>2</sub> +Al <sub>2</sub> O <sub>3</sub> (w/w)	Al <sub>2</sub> O <sub>3</sub> (aged, in air at 500°C, 4 hrs.) SiO <sub>2</sub> (prepared, no further treatment)	Al <sub>2</sub> O <sub>3</sub> (aged, in air at 500°C, 4 hrs.) SiO <sub>2</sub> (prepared, no further treatment)	10-90°(2θ)
AD1158	YW114	Fresh	No	10-90°(2θ)
AD947	YW114	Aged	Run 7	10-90°(2θ)
AD948	YW114	Aged	Run 7	35-55°(2θ)
AD966	YW114	Reduced	After Run 7 and BET	10-90°(2θ)
AD965	YW114	Reduced	After Run 7 and BET	35-55°(2θ)
AD945	YW113	Aged	Run 28	10-90°(2θ)
AD946	YW113	Aged	Run 28	35-55°(2θ)
AD952	RF36	Aged	-	35-55°(2θ)
AD951	RF36	Aged	-	10-90°(2θ)
AD968	RF36	Aged	Run 11	10-90°(2θ)
AD967	RF36	Aged	Run 11	35-55°(2θ)
AD823	RF16	Fresh	No	10-90°(2θ)
AD822	RF16	Aged	Run 44	10-90°(2θ)
AD1328	quartz wool (possible contaminant of used catalysts)			10-60°(2θ) at 0.1°/step with 40 s/step
AD1329	fresh RF34 mixed with quartz wool (about 20 to 30% quartz wool by volume)			10-60°(2θ) at 0.1°/step with 40 s/step
AD1330	empty shallow stainless steel sample holder (may contribute to XRD pattern in some cases)			10-60°(2θ) at 0.1°/step with 40 s/step

The XRD patterns listed in the table below were exploratory runs scanned at a more rapid rate of 4 s/step with a step size of 0.1°.

Table D-2. Description of exploratory XRD data files.

XRD Run	Sample	State of Catalyst (At beginning of run)	Previous Run	Others
AD821	RF30	Reduce	Run 5 and then BET	10-90°(2θ)
AD905	RF106	Fresh	No	10-90°(2θ)
AD904	RF105	Fresh	No	10-90°(2θ)
AD885	RF104	Fresh	No	10-90°(2θ)
AD902	RF104	Reduced	Run 13 and then BET	10-90°(2θ)
AD903	YW103	Reduced	Run 17 and then BET	10-90°(2θ)
AD884	YW103	Fresh	No	10-90°(2θ)
AD848	YW102	Aged	-	10-90°(2θ)

AD847	YW102	Fresh	No	10-90°(2θ)
AD883	YW102	Fresh	No	10-90°(2θ)
AD888	YW102	Reduced	Run 14 and then BET	10-90°(2θ)
AD884	YW103	Fresh	No	10-90°(2θ)
AD885	YW104	Fresh	No	10-90°(2θ)
AD886	RF30	Reduced	Run 42 and then BET	10-90°(2θ)
AD887	RF34	Reduced	Run 21 and then BET	10-90°(2θ)
AD824	RF102	Fresh/Reduced	BET	10-90°(2θ)
AD795	RF34	reduced	Run xx and then BET	10-90°(2θ)
AD794	RF34	Fresh/Reduced	BET	10-90°(2θ)
AD793	RF30	Fresh/Reduced	BET	10-90°(2θ)

### Plots of Representative XRD Patterns

Representative XRD patterns (as measured) are shown in Figures D-1 to D-6?. Repeat measurements, each starting with a different freshly reduced sample of RF34, are shown in Figure D-1. This plot shows that the XRD measurements were very reproducible. XRD patterns of RF34 activated at different temperatures are shown in Figure D-2 and the patterns for the catalysts reduced after the activation are shown in Figures D-3 and D-4 for the two ranges of angles; the diffraction pattern for the alumina support is included in Figures D-3 and D-4. The patterns for the 5% Pd/SiO<sub>2</sub> catalysts (YW114 and RF36) are shown in Figures D-5 and D-6.

### Analysis of XRD Patterns

It is apparent from the patterns that the support pattern interferes with the lines for the Pd and PdO; hence, corrections for the support were applied by subtracting the support patterns from the catalyst patterns. Scaling and baseline corrections have to be applied in the support subtraction. The general equation used for obtaining the diffracted intensity due to the Pd and PdO, i.e. 'support-free' patterns, was

$$I_{\text{subtracted},i} = I_{\text{Catalyst},i} - (\text{SF}) \times (I_{\text{Support},i}) + A \times [^\circ(2\theta)]_i + B \quad (\text{D-1})$$

where  $I_{\text{subtracted},i}$  = diffracted intensity due at Pd and PdO at diffraction angle  $[\theta(2\theta)]_i$

$I_{\text{Catalyst},i}$  = diffracted intensity of catalyst diffraction angle  $[\theta(2\theta)]_i$

$I_{\text{Support},i}$  = diffracted intensity of support at diffraction angle  $[\theta(2\theta)]_i$

(SF), A and B are constants.

Values of SF, the scaling factor, A and B used in the various support subtractions are listed in Table D-3. Additional corrections for the samples contaminated with quartz wool were required; these are also listed in Table D-3.

Plots of subtracted XRD patterns are given in Figures D-7 and D-8. Other subtracted patterns have already been shown Chapter 4 (Figures 4-20 and 4-21).

The Scherrer equation, Equation D-2, (see Anderson, J.R. and Praatt, K.C., "*Introduction to Characterization and Testing of Catalysts*", Academic Press, Sidney, p. 65, 1985) was used to estimate Pd and PdO crystal sizes,  $d_{\text{crystal}}$ .

$$d_{\text{crystal}} = [1.05 \lambda] / [B_{1/2} \cos (\theta)] \quad (\text{D-2})$$

where  $d_{\text{crystal}}$  = the 'diameter' of the crystal

$\lambda$  = wavelength of x-rays

= 0.1541 nm for the Cu  $K\alpha_1$  radiation used in the current work

$\theta$  = the diffraction angle of the line on which the size is based

$B_{1/2}$  = the integrated half-width of the diffraction line in radians.

The value of  $B_{1/2}$  was determined by determining the area under the various subtracted patterns and dividing this area by the maximum intensity of the line. No correction for machine broadening since all the values of  $B_{1/2}$  were more than an order of magnitude greater than the machine broadening. The reported Pd size are based on the 111 line since this is the most



intense Pd line (see Figure D-7). The 112 line of PdO was used for the PdO sizes. This is not the most intense PdO line, but the 002 PdO line overlaps with the most intense PdO line, the 101 line.

Table D-3. Parameters used for subtraction of x-ray profiles.

Catalyst	Angle Range	State of Catalyst	Kinetic Run	X-Ray Files		Constants on Equation D-2			
				Support	Catalyst	SF	A	B	
RF34	35 - 55	fresh	none	1128 + 1129	953	0.70	0.15	-15.25	
					962	0.70	0.15	-15.25	
					973	0.70	0.20	-17.00	
					979	0.70	0.05	-9.25	
					1003	0.70	0.15	-15.25	
					1030	0.70	0.15	-15.25	
					981	0.7	0.10	-11.5	
		reduced	30		989	0.7	-0.05	-4.25	
			32		1009	0.7	0.05	-7.75	
			34		1013	0.7	-0.40	14.0	
			36		1032	0.7	-0.25	4.75	
			38		1054	0.7	-0.30	10.5	
	75 - 90	fresh	none	1127	1031	0.7	0	0	
					30	982	0.7	0.06	-12.4
					32	990	0.7	0.18	-21.2
					34	1008	0.7	0.12	-15.8
					36	1014	0.7	0.29	-32.1
					38	1033	0.7	0.23	-26.7
					40	1055	0.7	0.06	-11.4
		10 - 90	oxidized		30	969*	0.55	0.10	-20.0
					32	975*	0.55	0.0	-13.0
					36	988*	0.55	0	-15.0
					38	1028*	0.41	0.06	-25.4
					40	1036*	0.46	0.15	-23.0
YW114	10 - 90	fresh	none	1198	1158	0.8097	0	0	
		reduced	7		966	0.97	0	0	
		oxidized	7		947	1.00	0	0	
RF36	10 - 90	oxidized	11	1198	968	0.95	0	0	

\* Additional baseline corrections required due to presence of quartz wool in samples

The following additional baseline corrections were applied:

Run 969 in range of 10 to 38 °2θ:  $+0.56 \times (^\circ 2\theta) - 21.2$  followed by an additional correction in the range of 10 to 30 °2θ:  $-0.25 \times (^\circ 2\theta) - 2.5$

Run 975 in range of 10 to 40 °2θ:  $+1.8 \times (^\circ 2\theta) - 72$

Run 988 in range of 10 to 38 °2θ:  $+2.2 \times (^\circ 2\theta) - 83.6$

Run 1028 in range of 10 to 40 °2θ:  $+2.2 \times (^\circ 2\theta) - 88$

Run 1036 a shift of -0.1 °2θ followed by a correction in range of 10 to 40 °2θ:  $+1.5 \times (^\circ 2\theta) - 60$

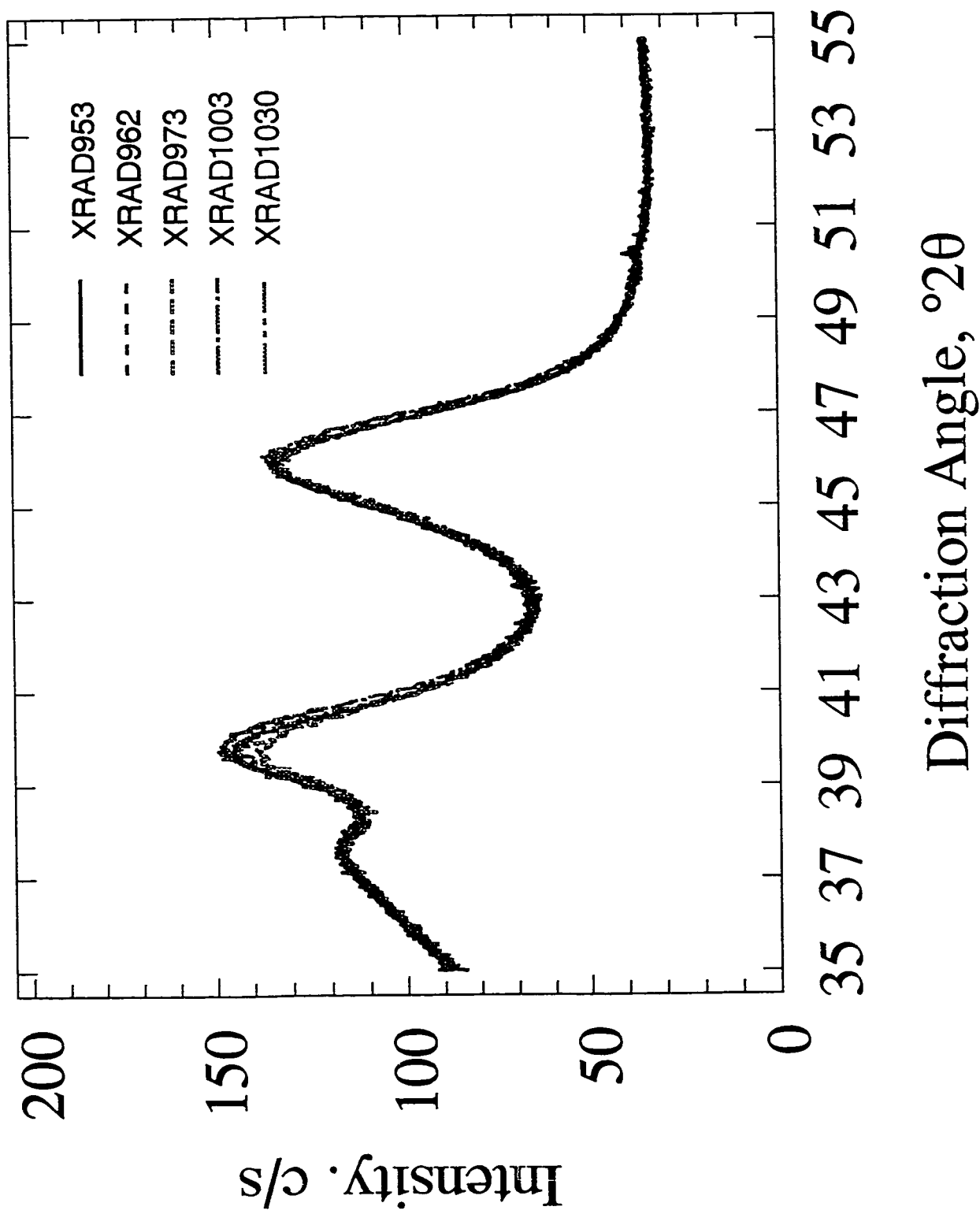


Figure D-1. XRD patterns for freshly reduced RF34 before various catalytic runs.

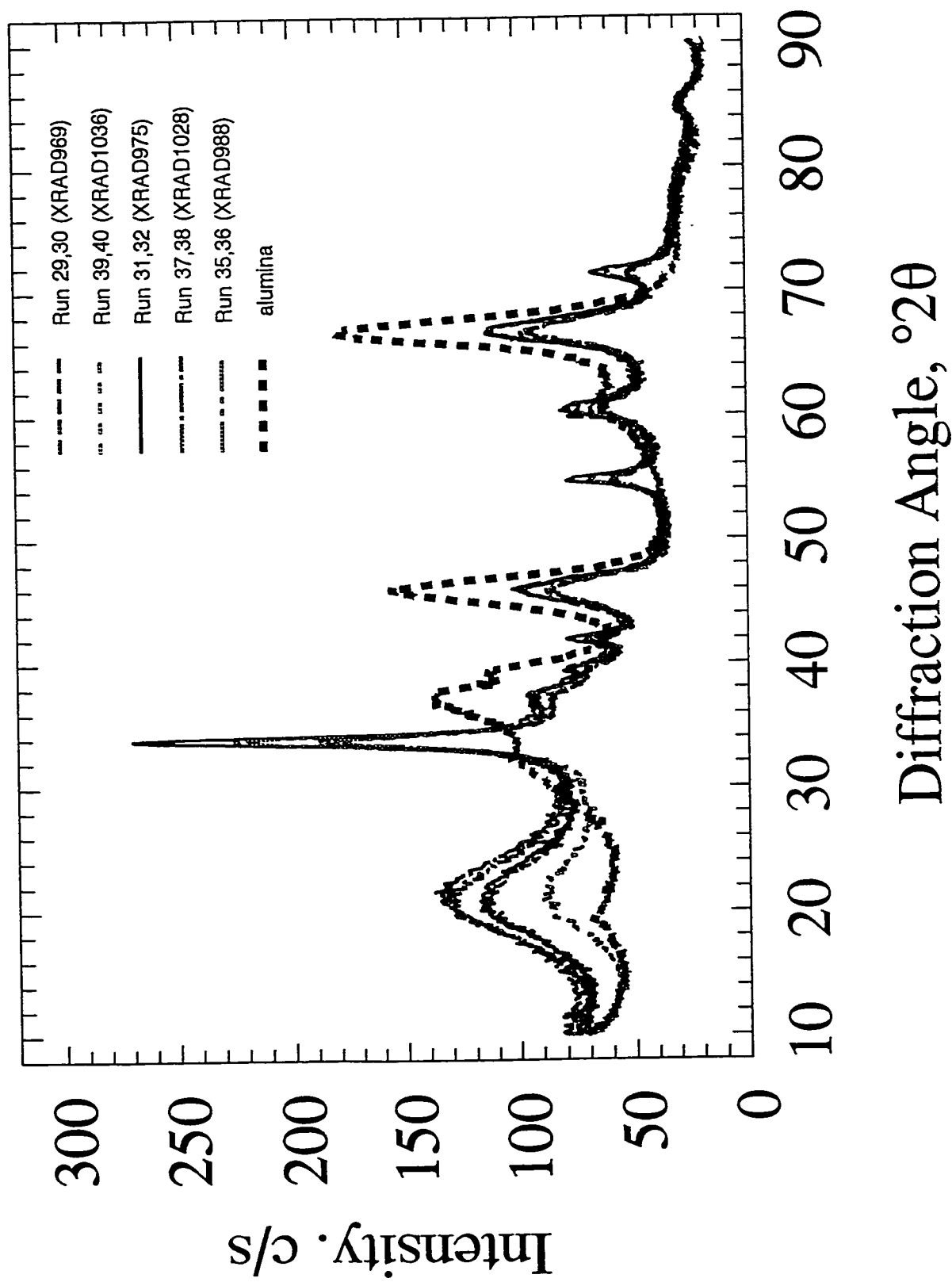


Figure D-2. XRD patterns for unreduced RF34 after various runs (alumina support pattern included).

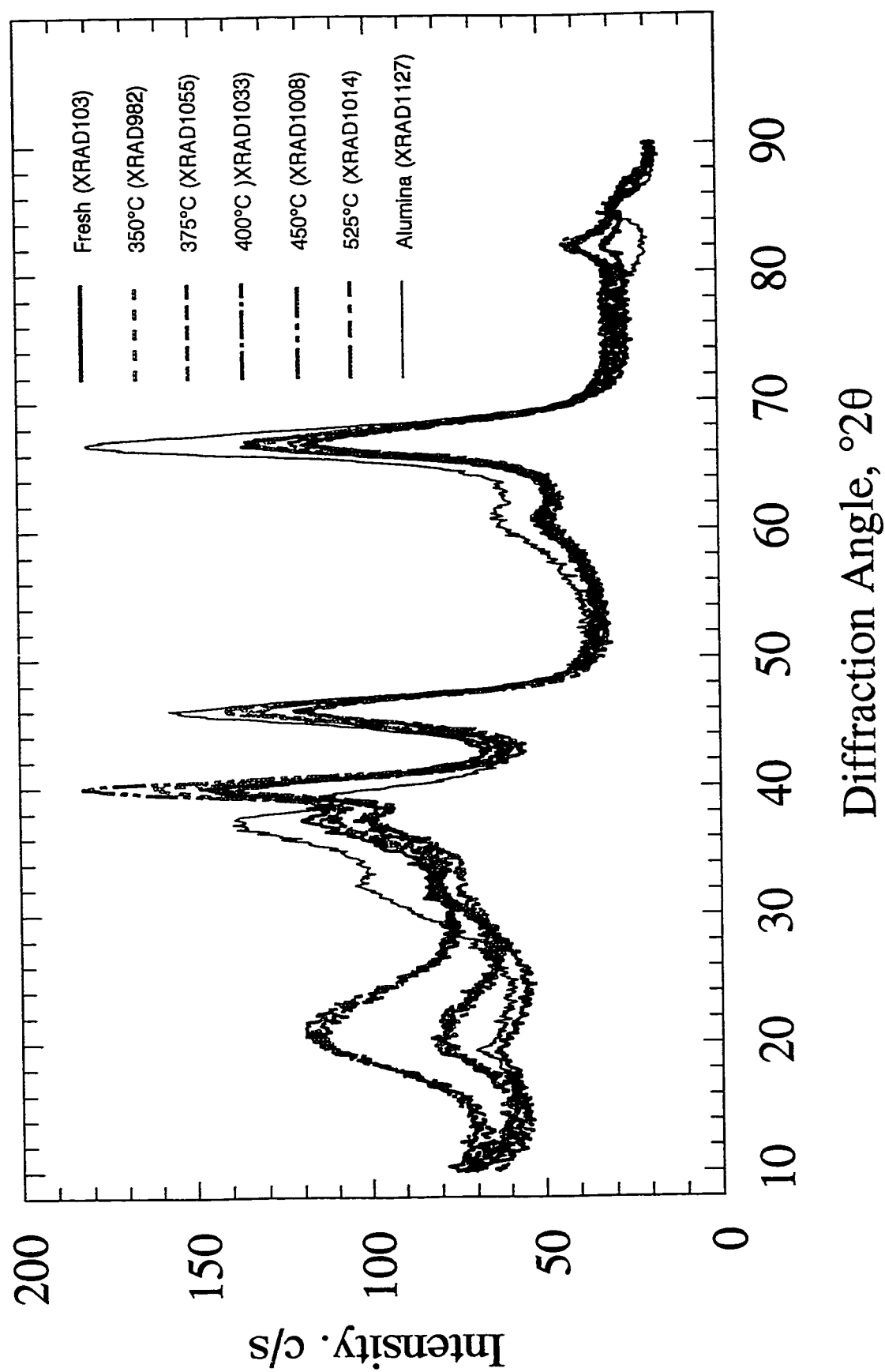


Figure D-3. XRD patterns for alumina support and reduced RF34 after treatment at various temperatures.

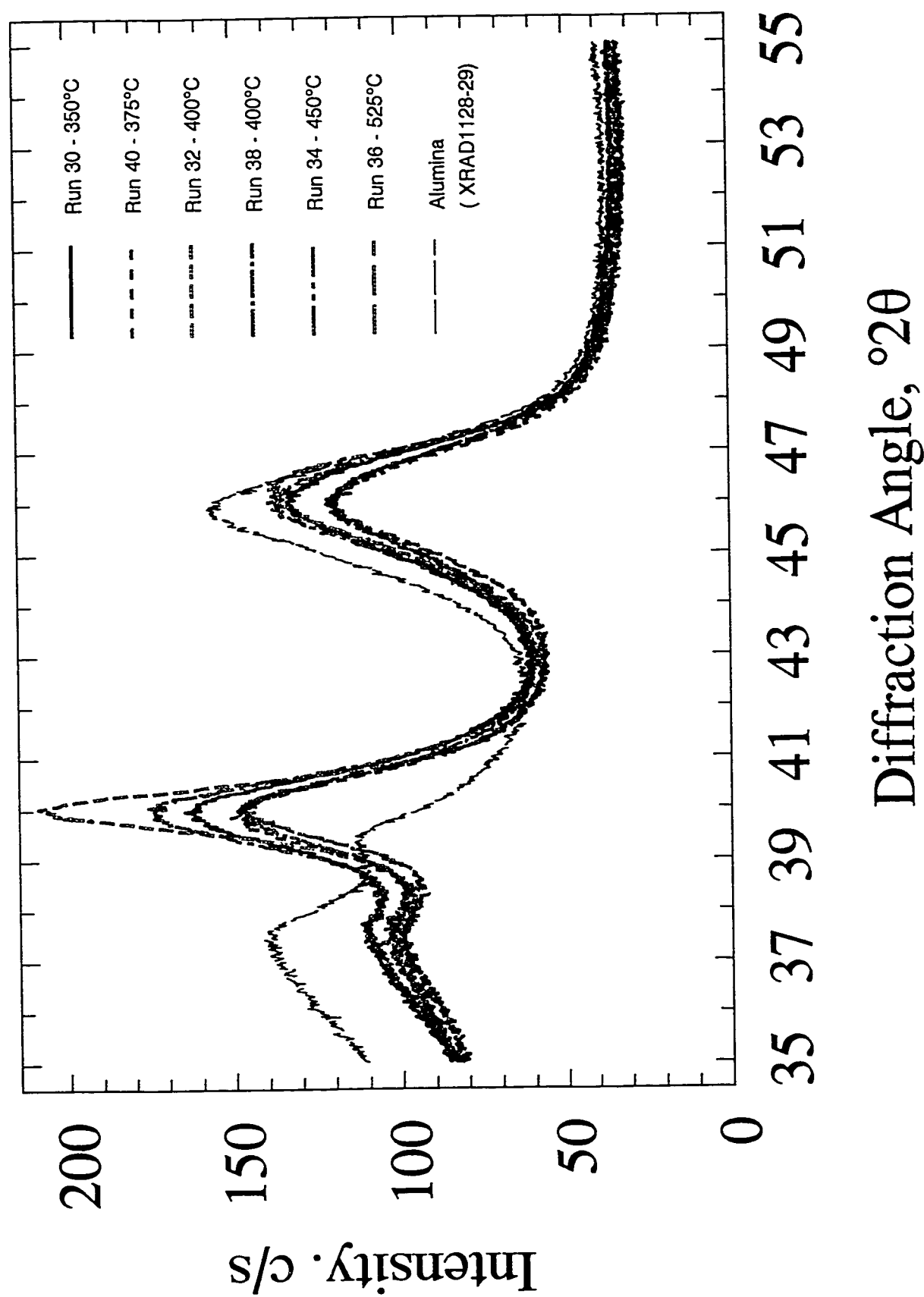


Figure D-4. terns for reduced RF34 after activation at different temperatures an use in various catalytic runs.

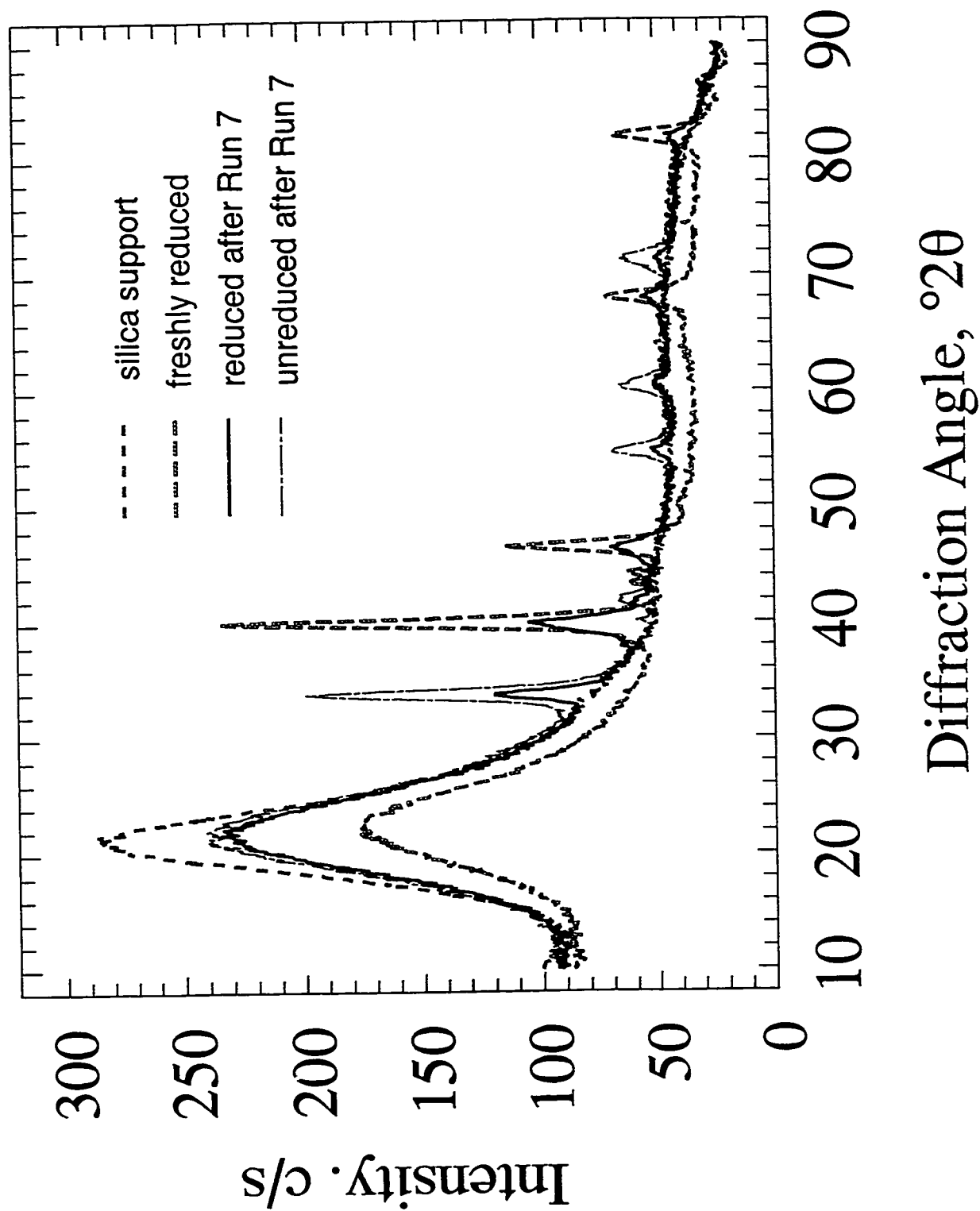
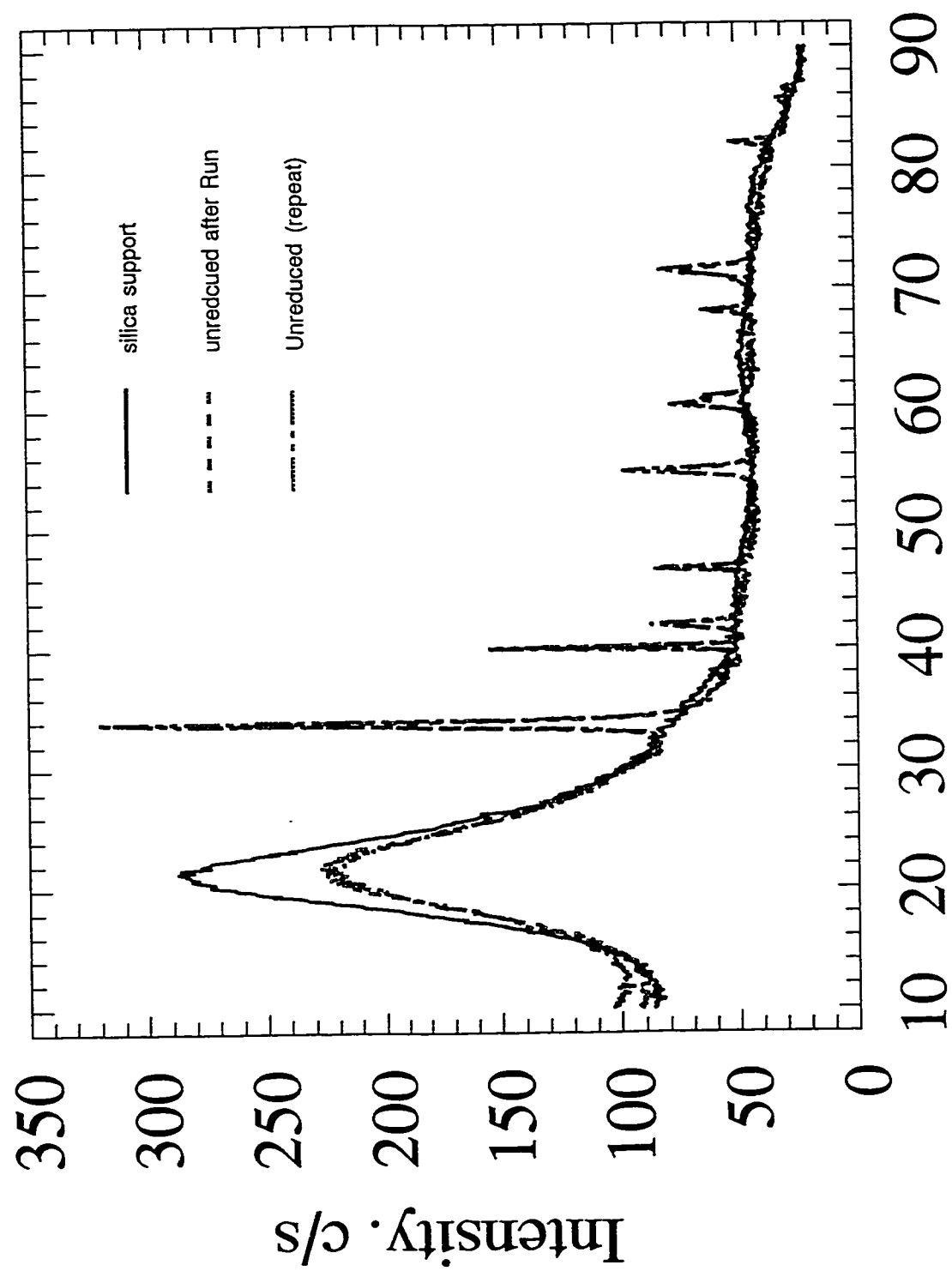


Figure D-5. XRD Patterns for silica, and reduced and unreduced YW114.



## Diffraction Angle, °2θ

Figure D-6. XRD Patterns for silica and unreduced RF36.

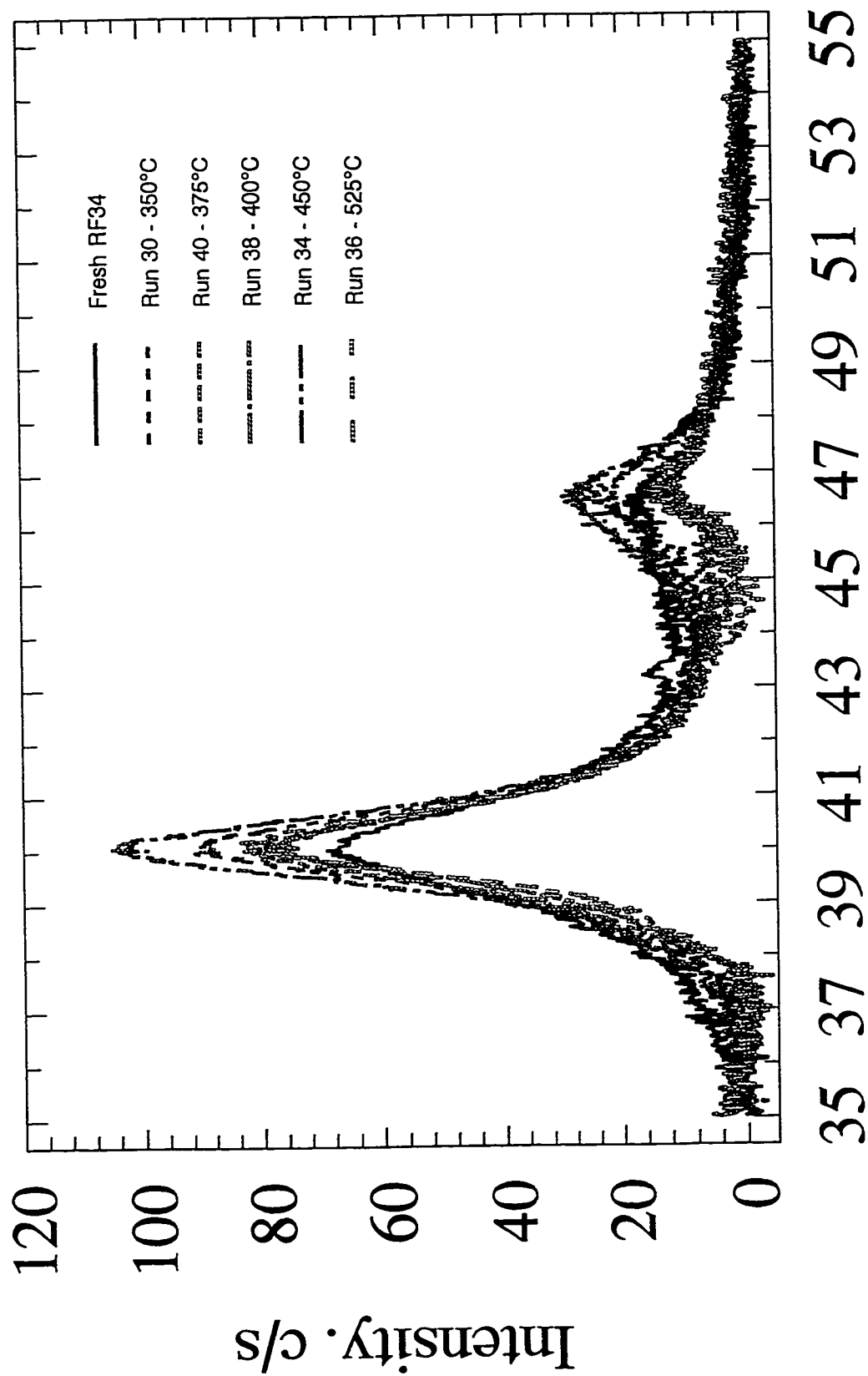


Figure D-7. Subtracted XRD patterns for reduced RF34 after various treatments and use.



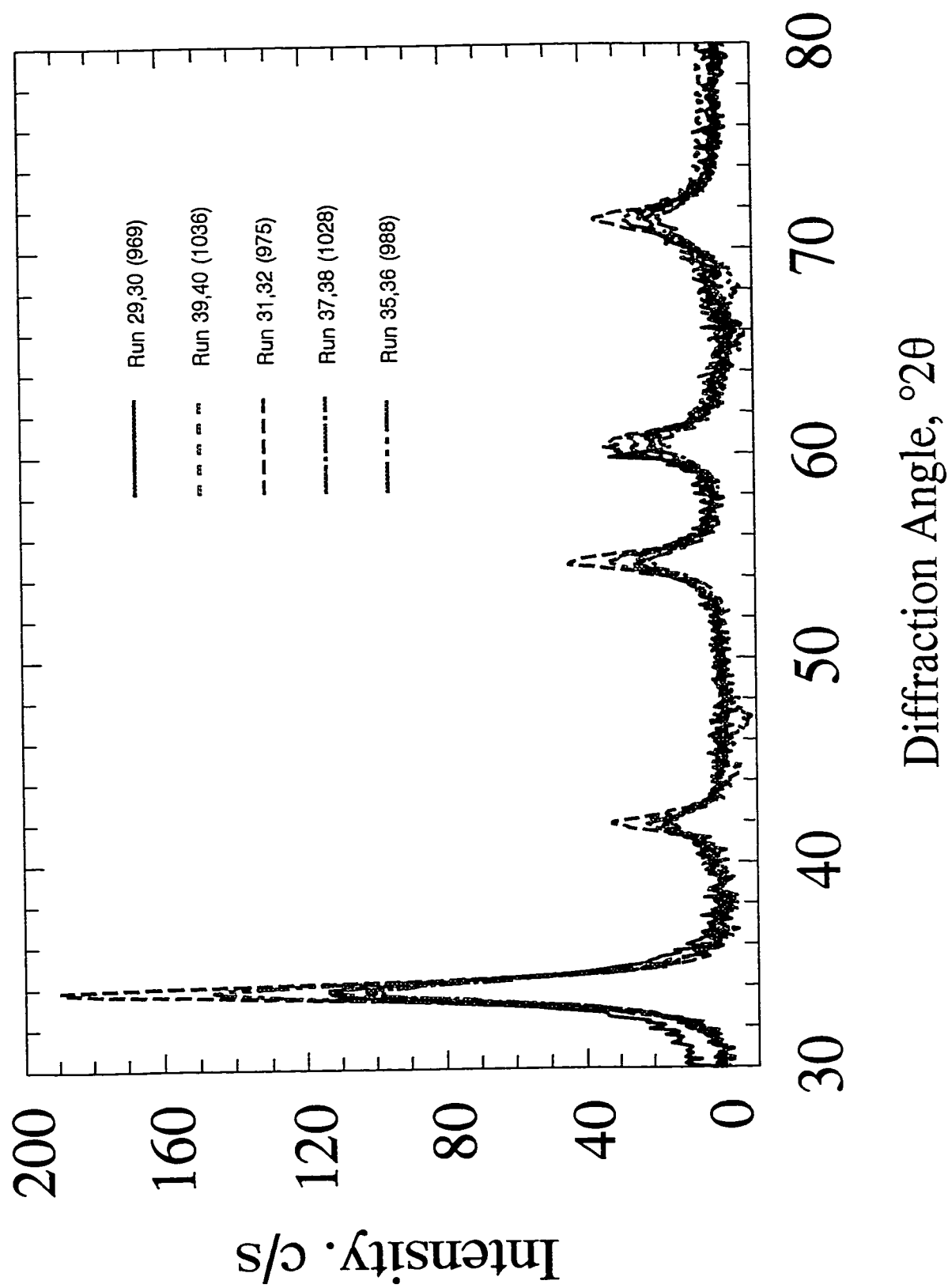


Figure D-8. Subtracted XRD Patterns for unreduced RF34.